Evaluation of Tsunami Design Codes and Recommendations for Bridges Susceptible to Tsunami Inundation

Spencer Nathaniel Livermore

A thesis

submitted in partial fulfillment of the

requirements for the degree of

Masters of Science in Civil Engineering

University of Washington

2014

Committee:

Michael Motley

Marc Eberhard

Pedro Arduino

Program Authorized to Offer Degree

Civil & Environmental Engineering

University of Washington

Abstract

Evaluation of Tsunami Design Codes and Recommendations

for Bridges Susceptible to Tsunami Inundation

Spencer Nathaniel Livermore

Co-chairs of Supervisory Committee:

Michael Motley

Marc O. Eberhard

Department of Civil and Environmental Engineering

Much of the past tsunami research has focused on inundation modeling, evacuation strategies and to a lesser extent, building design. Although many of the bridges that lie within possible tsunami inundation zones provide critical lifelines to coastal communities, the effects of tsunamis on transportation systems have not been evaluated. The high fluid velocities, wave heights, long period waves and inundation speeds of tsunamis are not typically seen for storm surges or flooding, and result in large fluid forces on structures. As a result, design codes that consider storm surges and flooding do not reflect the extreme nature of tsunami loads.

In this thesis the bridge types most susceptible to a large tsunami event along the west coast of the United States, as well as Alaska and Hawaii, are identified. Current tsunami loading methodologies are then summarized and compared. The extension of these methodologies to

bridges is discussed, including research recommendations for fluid loading on bridge superstructures.

The tsunami force equations were applied to two case studies. These studies provided the opportunity to evaluate the adequacy and varying approaches in estimating tsunami forces on bridge superstructures. In some cases the same tsunami force estimated by each of the codes and recommendations resulted in vastly differing forces. The influence of the estimate of flow parameters in some cases dominated the estimates. The discrepancies among the methods for estimating tsunami forces make the need for a unified tsunami design code apparent.

Acknowledgments

I would like to thank my advisors: Michael Motley and Marc Eberhard for giving me the opportunity to conduct this research. I would also like to thank Pedro Arduino for taking the time to be one my defense committee. And a special thanks is also due for Gary Chock and Catherine Petroff for taking the time to give me feedback and providing me with a draft version of the ASCE 7-16 tsunami loading chapter. Finally, I would also like to thank my family and friends for their support.

Table of Contents:

List of Figures:

List of Tables:

List of Equations:

Chapter 1 Introduction

Tsunamis occur due to the large vertical displacement of water volume typically caused by a large earthquake, or less commonly, by a landslide (Rabinovich et al. 1999) or asteroid impact. Once enough stress builds up between two tectonic plates, the plates will either slip relative to each other or fracture, causing a rapid vertical movement of the ocean floor displacing water upwards, creating a tsunami (www.tsunami.noaa.gov).

In the last decade, tsunamis in Indonesia (2004), Samoa (2009), Chile (2010), and Japan (2011) have caused hundreds of thousands of deaths and hundreds of billions of dollars in damage to coastal communities (Kajitani et al. 2013). The pacific region of the United States, including the states of Alaska, Washington, Oregon, California and Hawaii, as well as several U.S. territories (e.g., Guam), are also susceptible to being struck by major tsunamis. Along the west coast of the United States, the Cascadia Subduction zone spans from Vancouver Island in Canada to northern California, where the thinner Juan de Fuca Tectonic Plate is subducting beneath the thicker North American Tectonic Plate. Geological records along the coastlines near the Cascadia Subduction Zone show that major tsunami events have occurred many times in the past with approximate return periods of 500 years (Atwater et al. 2005).

The failure of critical bridges during large hurricane and tsunami events has become a major issue in tsunami and hurricane prone areas. Recent events in the U.S., such as Hurricane Katrina, have shown how susceptible the transportation systems can be, not only to tsunami events but also to storm surges caused by hurricanes or tropical storms. The loss of critical transportation infrastructure in coastal areas has delayed emergency services, evacuation, and recovery efforts for extended periods of time. As the transportation infrastructure ages, the likelihood of failure of the transportation system during an earthquake and subsequent tsunami will continue to increase.

The bridge damage caused by tsunamis is typically caused by fluid and debris forces, which are the focus of this thesis. Although not discussed here, it should be noted that bridges can also experience substructure scour, which can also lead to serious structural damage (Chock et al. 2013).

1.1 Bridge Superstructure Uplift

Typically, bridge superstructures in seismic regions are restrained well in the horizontal direction to resist the horizontal shaking caused by an earthquake, but the vertical restraints can be limited. Once a tsunami reaches a bridge, it can lift the superstructure off of its supports and transport it large distances if the resistance to uplift is insufficient. Field surveys following tsunami events have repeatedly found this type of failures to be common (Aglipay et al. 2011, Akiyama et al. 2012, Kosa 2012, and Murakami et al. 2012). For example, throughout the hardest hit areas in

Japan during the Great East Japanese Earthquake and the accompanying Tōhoku Tsunami (2011), bridges were constructed with shear keys and other structural components meant to resist horizontal movement. Figure 1-1 shows an example of a bridge in which the superstructure's horizontal restraints are inadequate to resist vertical uplift forces due to a tsunami.

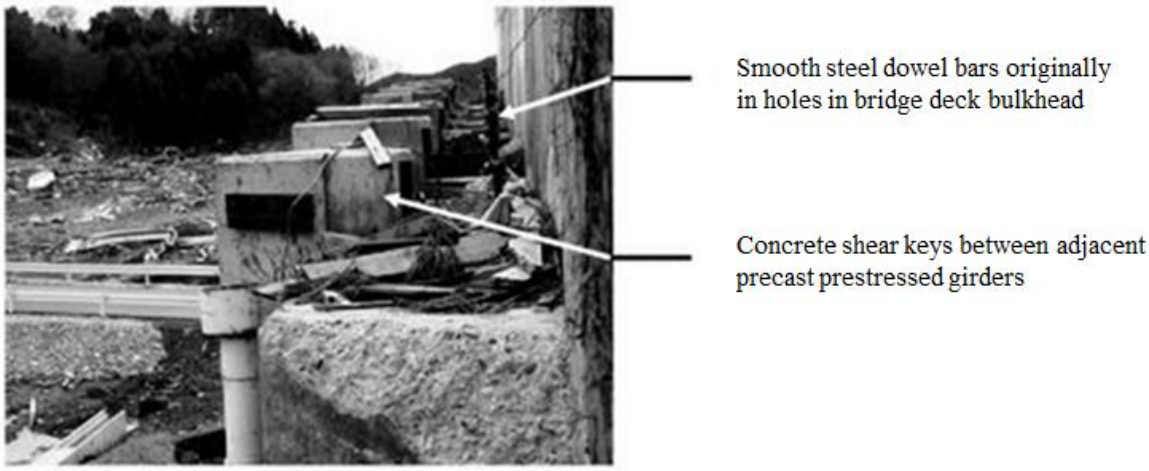

Figure 1-1: Abutment Shear Keys and Dowel Bars Revealed after Superstructure is removed by the 2011 Great East Japanese Earthquake and Tōhoku Tsunami (Robertson, with permission from ASCE)

The substructures of these bridges tended to have low or little damage, but the superstructures were often lifted and transported, more than 500 meters in some cases (Akiyama et al. 2012). These structural components did supply adequate horizontal restraint during the earthquake, but they were not designed to supply vertical restraint. Thus when the bridges were submerged by the tsunami, the superstructures were lifted from their substructures by vertical hydrodynamic and buoyancy forces and transported away from the substructure. These uplift forces can be amplified when air is trapped under the superstructure, leading to larger buoyancy effects (Aglipay et al. 2011). Figures 1-2 to 1-5 show a selection of bridges for which the superstructures failed through uplift and scour during the 2011 Great East Japanese Earthquake and Tōhoku Tsunami.

Figure 1-2: Deck Sections Displaced from the Piers and Abutments (left); Severe Scour behind Abutment (right) (2011 Great East Japanese Earthquake and Tōhoku Tsunami, Robertson, with permission from ASCE)

Figure 1-3: Deck Section Displaced from Original Location due to the Uplift (2011 Great East Japanese Earthquake and Tōhoku Tsunami, Robertson, with permission from ASCE)

Figure 1-4: Steel-Truss Road Bridge Swept up to 800m Inland from its Original Location due to the 2011 Great East Japanese Earthquake and Tōhoku Tsunami (2011) (Robertson, with permission from ASCE)

Figure 1-5: Flipped Bridge Superstructures due to the 2011 Great East Japanese Earthquake and Tōhoku Tsunami (Chock (left) & Robertson (right), with permission from ASCE)

Similar superstructure uplift has also been observed during storm surges, during which offshore rises in water level are caused by the high winds. Hurricanes are usually preceded by storm surges due to their high winds "pushing" the water ahead of them and causing a rise in the static water line. This rise in the static water line allows for waves to impact low laying structures otherwise unaffected by wave action. Most of the damage caused by storm surges is due to wave action or large areas of land being flooded due to the increasing water level, where the increasing water level leads to uplift forces on structures. Storm surges can cause loss of life and property damage, but unlike tsunamis, they can typically be forecast (NOAA: "Floods the Awesome Power", March 2005).

During Hurricane Katrina the spans of a number of bridges were lifted and displaced from their substructures (Douglass et al. 2006, Robertson et al. 2007, and Robertson et al. 2011). It was noted that many, if not all, of the bridges that experienced failure had limited horizontal and vertical restraints. Typically the superstructure was attached to the substructure only by thick angles which could not withstand the horizontal and vertical forces brought on by the storm surge and wave action (Robertson et al. 2007). In addition these bridges were typically close to the static water line and therefore they were particularly vulnerable to even small storm surges (Cuomo et al. 2009). This sort of storm surge uplift can be seen in Figure 1-6 for U.S. 90 after Hurricane Katrina.

Figure 1-6: The Biloxi Bay Bridge after Hurricane Katrina (Douglass et al. 2006)

1.2 Debris Impact and Damning

In addition to forces caused by the fluid alone, structures that experience tsunamis can also be susceptible to debris impact forces. As a tsunami moves inland it can pick up large amounts of debris of varying size and mass. This debris can then impact both the substructure and superstructure of bridges and lead to superficial or even critical damage (Chock et al., 2013). Impact alone might not lead to heavy damage, but the debris can become entangled in the bridge and create damming effects, which will lead to much higher hydrodynamic forces resulting from the increased surface area normal to the direction of the flow. Numerous ships, cars and other floating debris impacted bridges during the 2011 Great East Japanese Earthquake and Tōhoku Tsunami, an example of which can be seen in Figure 1-7 (Chock et al., 2013).

Figure 1-7: Fishing Boat Trapped Below Steel-Box-Girder Bridge (left) (Kriebel), Causing only Superficial Damage (right) (Robertson) (with permission from ASCE)

1.3 Thesis Objectives and Scope

Much of past tsunami research has focused on inundation modeling, evacuation strategies and to a lesser extent, building design. Although many of the bridges that lie within possible tsunami inundation zones provide critical lifelines to coastal communities, the effects of tsunamis on transportation systems have not been evaluated. Recommendations are needed for evaluating and designing bridges in regions susceptible to tsunamis.

Along the West Coast of the United States, tsunamis are of the most interest near the Cascadia Subduction Zone, which has a high possibility of a large seismic event and subsequent tsunami. Hawaii can experience Central Pacific hurricanes, but the waves and storm surges they would produce would typically lead to smaller forces than those produced by a large tsunami. The high fluid velocities, wave heights, long period waves and inundation speeds of tsunamis are not typically seen for storm surges or flooding, and result in large fluid forces on structures. As a result, design codes that consider storm surges and flooding do not reflect the extreme nature of tsunami loads. These large fluid forces have led to catastrophic failures of structural systems that were not properly designed to resist them.

The objective of this thesis is to evaluate the forces on typical bridge superstructures determined from available tsunami force prediction equations. Tsunami force prediction equations are provided by the following, building-focused, codes and recommendations:

1. Honolulu Building Code: Chapter 16 Article 11 "Regulations Within Flood Districts and Development Adjacent to Drainage Facilities"

2. FEMA P646: "Guidelines for Design of Structures for Vertical Evacuation from Tsunamis"

3. ASCE 7 Standards Committee Proposals No. I to XI to Revise the 2010 Edition of ASCE/SEI 7 (ASCE 7-16 draft proposal): "Chapter 6: Tsunami Loads and Effects"

From these findings, recommendations will be introduced for possible improvements to the current design procedures, as they might be applied to bridges in the future.

This thesis investigates the vulnerability of bridges to tsunamis by:

- Identifying the most common types of bridges (e.g., material and geometry) that are located in regions likely to be affected by tsunamis (Chapter 2)
- Summarizing and comparing differences among tsunami loading procedures from the available codes and recommendations (Chapter 3)
- Discussing the extension of these codes and recommendations to bridges in addition to current research advances in fluid loading on bridge superstructures (Chapter 4)
- Applying these tsunami force equations from the codes and recommendations to two case studies (Chapter 5).

Chapter 2 Bridges Susceptible to Tsunami Inundation

It is important that research on the effects of tsunamis on bridges focus on bridge geometries and materials that are typical of regions susceptible to tsunamis. Using the National Bridge Inventory, the bridge inventory was identified for a nominal inundation zone corresponding to a region extending one mile from the Pacific Ocean. In the future, once standard inundation maps have been established, the inventory can be evaluated again.

2.1 National Bridge Inventory

The National Bridge Inventory (NBI, 2012) documents key properties for approximately 600,000 bridges located throughout the United States. This inventory includes bridges located on public roads, including interstate highways, U.S. highways, state and county roads, and publicly accessible bridges on Federal lands. The full database was downloaded from the Federal Highway Administration website (www.fhwa.dot.gov).

The NBI supplies the longitude and latitude coordinates for each bridge in the database. The NBI also provides many other bridge attributes, including a description of the bridge condition, key dimensions, traffic flow, and design methods. Particularly relevant to this research, the NBI also provides the structure and material types for each bridge, which was important for determining what types of bridges are within regions susceptible to tsunamis. It should be noted that a small fraction of the bridges in the database do not have longitudinal or latitudinal coordinates (or other bridge data).

2.2 Bridges within Nominal Tsunami Inundation Zone

The bridge information for each state (Alaska, Washington, Oregon, California and Hawaii) was sorted based on state and county (or "borough", Alaska does not use the term "county") codes provided for each bridge in the NBI. Any bridge that was not within a county or borough bordered by the Pacific Ocean was discarded. Figure 2-1 shows the counties that border the Pacific Ocean in Washington State. For each state, the numbers of bridges within coastal counties or boroughs bordered by the Pacific Ocean are reported in Table 2-1. Overall, nearly one-half (46%) of all of the bridges within these five states are located within regions that share a border with the Pacific Ocean.

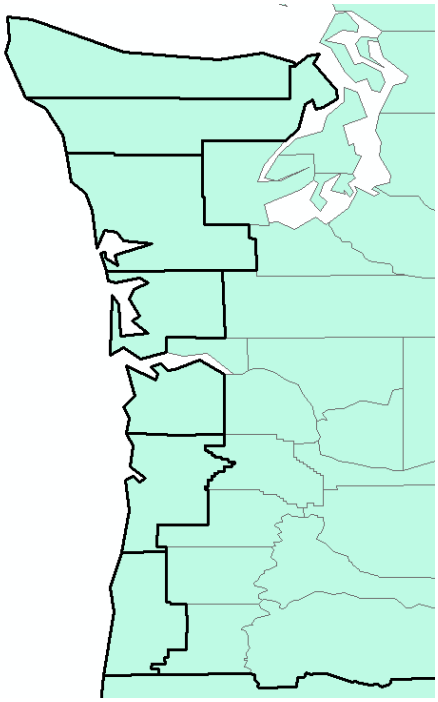

Figure 2-1: Washington Coastal Counties

Table 2-1: NBI Bridge Count by Location

State	Total Number of Bridges	Number of Bridges in Coastal Regions	Percentage in Coastal Regions	Number of Bridges Within 1 mile of Coastline	Percentage Within 1 Mile
Alaska	1,286	1,286	100%	368	28.6%
Washington	9,049	633	7.0%	88	1.0%
Oregon	8,869	2,539	28.6%	323	3.6%
California	34,062	19,527	57.3%	2,745	8.0%
Hawaii	1,212	1,212	100%	695	57.3%
Total	**54,478**	**25,197**	**46.3%**	**4,219**	**7.7%**

The bridge data was imported into the geospatial processing program ArcMap™. Within ArcMap™, the bridge data was manipulated to identify the bridges that were within 1 mile of the Pacific Ocean coastline (Table 2-1). As an example, the eighty-eight bridges within the nominal one-mile inundation zone are shown for Washington State in Figure 2-2, and the results of the analysis are reported in Table 2-1. The details of this analysis are provided in Appendix A.

The bridges within the nominal inundation zone were then sorted based on their material and superstructure geometry codes to determine the typical type of bridge susceptible to tsunami inundation in the nominal inundation zone. The definitions of the material and geometry codes are listed in Table 2-2.

Figure 2-2: Nominal Inundation Zone for Washington State

Table 2-2: NBI Superstructure and Material Types

Bridge Material and Superstructure Types			
NBI Code	**Material Type**	**NBI Code**	**Structure Type**
1	Concrete	1	Slab
2	Concrete Continuous	2	Stringer/Multi-beam or Girder
3	Steel	3	Girder and Floor beam System
4	Steel Continuous	4	Tee beam
5	Prestressed Concrete	5	Box Beam or Girders - Multiple
6	Prestressed Concrete Continuous	6	Box Beam or Girders - Single or Spread
7	Wood or Timber	7	Frame (except frame culverts)
8	Masonry	8	Orthotropic
9	Aluminum, Wrought Iron, or Cast iron	9	Truss - Deck
0	Other	10	Truss - Thru
		11	Arch - Deck
		12	Arch - Thru
		13	Suspension
		14	Stayed girder
		15	Movable - Lift
		16	Movable - Bascule
		17	Movable - Swing
		18	Tunnel
		19	Culvert (includes frame culverts)
		20	Mixed types (only approach spans)
		21	Segmental Box Girder
		22	Channel beam
		0	Other

2.3 Bridge Types within Nominal Inundation Zones

This section discusses the typical bridge types that were found to be within the nominal inundation zone for the states of Alaska, Washington, Oregon, California and Hawaii. A total of 4,219 bridges are located within the nominal inundation zone of one mile from the Pacific Ocean coastline (Table 2-1). The following tables contain the bridge materials and structural geometry types for the five considered states nominal inundation zones, determined from the ArcMap™ analysis (Appendix A).

Table 2-3 lists the number of bridges with the most common bridge materials and corresponding structural geometry found within the nominal inundation zone for the Alaskan coastline. A total of 368 bridges are located within the nominal inundation zone. The first row of the table should be interpreted as follows: the most common material type designation was "Steel", which applied to 137 bridges, which in turn, applied to 37% of the bridges within the nominal inundation zone (137/368). The most common structural geometry designation for this material type was Stringer/Multi-beam, a designation that applied to 53% of these bridges (72/137).

Table 2-3: Alaskan Bridges within Nominal Inundation Zone

Material Type	Count	Percent of Coastal Bridges	Most Common Structural Geometry for given Material Type	Count of Structural Type	Percent of Structural Geometry for given Material Type
Steel	137	37.2%	Stringer/Multi-beam or Girder	72	52.6%
Prestressed Concrete	134	36.4%	Tee beam	111	82.8%
Wood or Timber	48	13.0%	Stringer/Multi-beam or Girder	46	95.8%
Steel Continuous	28	7.6%	Stringer/Multi-beam or Girder	24	85.7%
Concrete	15	4.1%	Tee beam	4	26.7%
Concrete Continuous	3	0.8%	Stringer/Multi-beam or Girder	2	66.7%
Other	2	0.5%	Tunnel	2	100.0%
Aluminum, Wrought Iron, or Cast iron	1	0.3%	Culvert (includes frame culverts)	1	100.0%

For Washington State, Table 2-4 indicates the most common bridge materials and corresponding structural geometry found within the nominal inundation zone. A total of 88 bridges along the Washington coastline are within this zone. The most common material types are Prestressed Concrete (of which 54% are slab bridges) and Wood (of which 74% are girder bridges).

Table 2-4: Washington Bridges within Nominal Inundation Zone

Material Type	Count	Percent of Coastal Bridges	Most Common Structural Geometry for given Material Type	Count of Structural Type	Percent of Structural Geometry for given Material Type
Prestressed Concrete	24	27.3%	Slab	13	54.2%
Wood or Timber	23	26.1%	Stringer/Multi-beam or Girder	17	73.9%
Concrete Continuous	17	19.3%	Slab	12	70.6%
Concrete	8	9.1%	Channel beam	3	37.5%
Prestressed Concrete Continuous	8	9.1%	Stringer/Multi-beam or Girder	4	50.0%
Steel	7	8.0%	Stringer/Multi-beam or Girder	2	28.6%
Steel Continuous	1	1.1%	Stringer/Multi-beam or Girder	1	100.0%

Table 2-5 provides similar information for bridges within the nominal inundation zone along the Oregon coastline. The most common bridge material type was prestressed concrete (138 of 323 bridges), and for these bridges, approximately one quarter were slab bridges.

Table 2-5: Oregon Bridges within Nominal Inundation Zone

Material Type	Count	Percent of Coastal Bridges	Most Common Structural Geometry for given Material Type	Count of Structural Type	Percent of Structural Geometry for given Material Type
Prestressed Concrete	138	42.7%	Slab	35	25.4%
Concrete Continuous	63	19.5%	Stringer/Multi-beam or Girder	28	44.4%
Concrete	39	12.1%	Stringer/Multi-beam or Girder	20	51.3%
Steel	25	7.7%	Stringer/Multi-beam or Girder	4	16.0%
Prestressed Concrete Continuous	23	7.1%	Stringer/Multi-beam or Girder	12	52.2%
Wood or Timber	21	6.5%	Stringer/Multi-beam or Girder	11	52.4%
Steel Continuous	14	4.3%	Truss - Thru	0	0.0%

For the State of California, Table 2-6 indicates the most common bridge material and corresponding structural geometry found along the nominal inundation zone. A total of 2,745 bridges are located within the nominal inundation zone along the Californian coastline.

Table 2-6: Californian Bridges within Nominal Inundation Zone

Material Type	Count	Percent of Coastal Bridges	Most Common Structural Geometry for given Material Type	Count of Structural Type	Percent of Structural Geometry for given Material Type
Concrete Continuous	1,078	39.3%	Box Beam or Girders - Multiple	568	52.7%
Concrete	462	16.8%	Culvert (includes frame culverts)	125	27.1%
Prestressed Concrete Continuous	432	15.7%	Box Beam or Girders - Multiple	351	81.3%
Prestressed Concrete	415	15.1%	Box Beam or Girders - Multiple	209	50.4%
Steel	254	9.3%	Stringer/Multi-beam or Girder	166	65.4%
Steel Continuous	65	2.4%	Stringer/Multi-beam or Girder	55	84.6%
Wood or Timber	28	1.0%	Stringer/Multi-beam or Girder	27	96.4%
Masonry	6	0.2%	Arch - Deck	6	100.0%
Other	5	0.2%	Tunnel	4	80.0%

Table 2-7 indicates the most common bridge material and corresponding structural geometry found along the nominal inundation zone for the State of Hawaii. A total of 695 bridges along the Hawaiian coastline are within the nominal inundation zone.

Table 2-7: Hawaiian Bridges within Nominal Inundation Zone

Material Type	Count	Percent of Coastal Bridges	Most Common Structural Geometry for given Material Type	Count of Structural Type	Percent of Structural Geometry for given Material Type
Concrete Continuous	248	35.7%	Tee beam	82	33.1%
Concrete	193	27.8%	Tee beam	73	37.8%
Prestressed Concrete	139	20.0%	Stringer/Multi-beam or Girder	90	64.7%
Steel	55	7.9%	Culvert (includes frame culverts)	23	41.8%
Prestressed Concrete Continuous	42	6.0%	Stringer/Multi-beam or Girder	15	35.7%
Wood or Timber	10	1.4%	Stringer/Multi-beam or Girder	7	70.0%
Masonry	6	0.9%	Arch - Deck	4	66.7%
Steel Continuous	2	0.3%	Stringer/Multi-beam or Girder	2	100.0%

Figure 2-3 shows the percentage of the bridge material types within the nominal inundation zone for each of the five states. Concrete bridges (continuous or not and prestressed) make up the largest number of the bridges within the nominal inundation zones for each state, whereas steel bridges make up less than 10% of the bridges in the nominal inundation zone for each state besides Alaska State (37.2%). Wood or timber construction makes up the second largest material type in the nominal inundation zone for Washington State (26.1%). With concrete, steel and wood having the highest percentage of use in the nominal inundation zone in the five considered states the other material types are not of interest (masonry, other, aluminum, wrought iron, and cast iron).

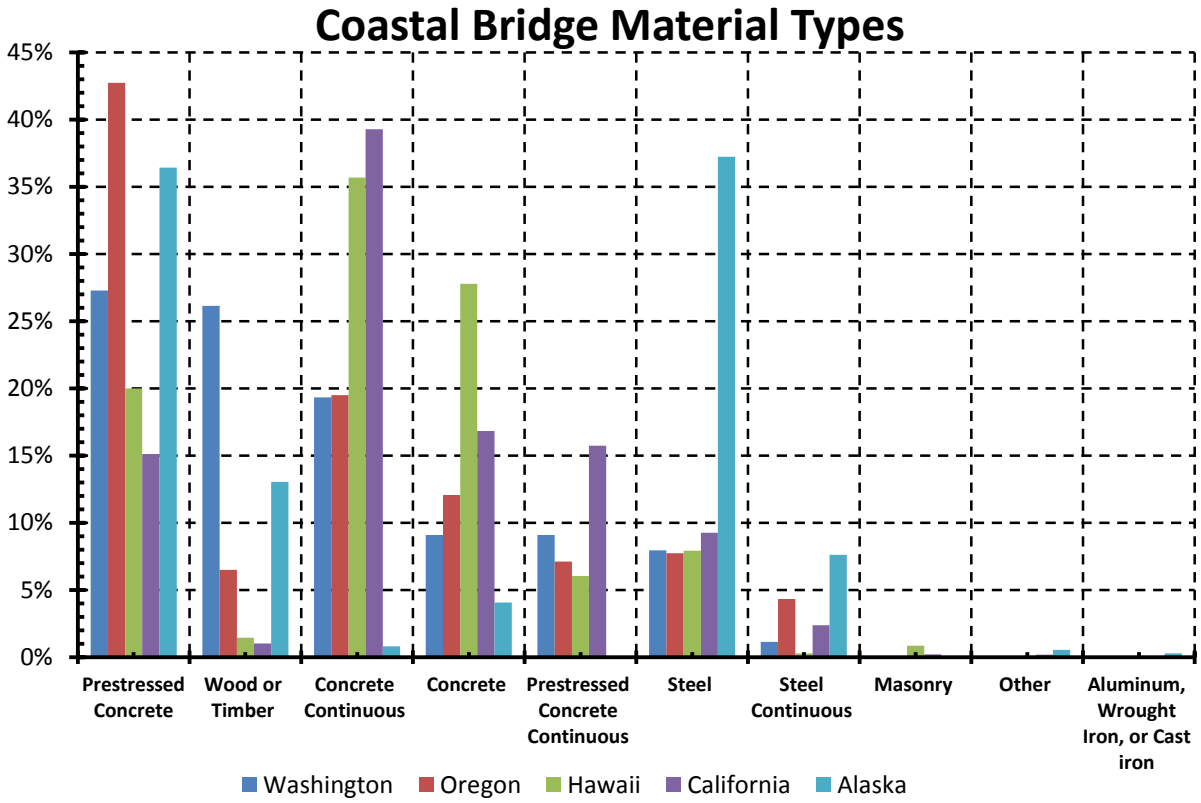

Figure 2-3: Coastal Bridge Material Types

Concrete is by far the most widely used material type in the nominal inundation zone between the five considered states. Therefore concrete bridges were selected to be examined in the case studies in Chapter 5. There are many types of geometries used in concrete bridge construction, but the three most widely used geometries in the five considered states are tee-beam, deck-girder and slab type geometries (Tables 2-3 to 2-7). From these considerations both a concrete slab and deck-girder type bridge was selected along the Pacific Ocean coastline to be examined in the case studies in Chapter 5.

Chapter 3 Tsunami Loading Guidelines

Bridge codes in the United States provide little guidance for designing bridges to resist tsunamis. The California Department of Transportation (Caltrans) did issue a memo entitled "Tsunami Hazard Guidelines" (2010), which notifies designers that tsunami hazards need to be considered on a project-specific basis. Some other design guidelines, such as AASHTO (AASHTO LRFD Bridge Design Specifications: Water Loads, Section 3.8), have hydraulic loading cases that apply to riverine and storm surge flooding conditions, but these guidelines cannot be applied to tsunami events. None of these bridge-focused documents provide specific recommendations for estimating forces caused by tsunamis.

More information is available for buildings. In the United States, two sets of design codes and recommendations specify tsunami forces for buildings: the Federal Emergency Management Agency's "Guidelines for Design of Structures for Vertical Evacuation from Tsunamis", FEMA P646 (2008); and the Honolulu Building Code (Chapter 16 Article 11) (Yim 2005, Yim et al. 2011). In addition, a new set of mandatory tsunami design requirements for buildings will be included in ASCE 7-16 (Minimum Design Loads for Buildings and Other Structures). It should be noted that this chapter is only in the draft stage and is subject to change.

This chapter discusses the draft ASCE 7-16 draft proposal (ASCE 2014), along with both the FEMA P646 recommendations and Honolulu Building Code. Specifically, the following sections discuss the types of forces that are considered (Section 3.1), the force equations contained in each of the three codes (Section 3.2), the details of each code (Sections 3.3-3.5) and the differences among them (Section 3.6).

Figure 3-1 shows the nomenclature used for tsunami depths and inundation distances by the ASCE 7-16 draft. This nomenclature will be adopted throughout this chapter.

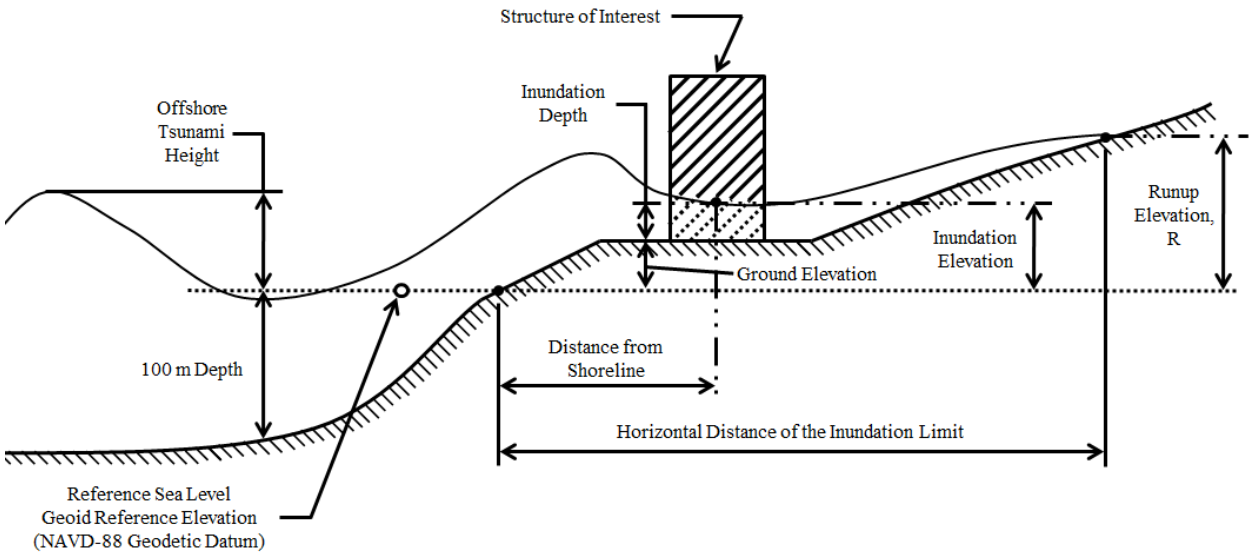

Figure 3-1: Typical Tsunami Depth and Inundation Nomenclature (Modified from ASCE 7-16 draft proposal)

3.1 Types of Forces Considered

3.1.1 Hydrostatic Forces

Hydrostatic forces are generated when static water comes in contact with a structure and causes an imbalance in pressures due to uneven water depths in or around the structure. These forces act perpendicularly to the face of the structure and increase linearly with depth. Hydrostatic forces are usually important for long structures, such as sea walls, as opposed to structures where the water can flow around the structure quickly.

If there are areas on the structure that are watertight, hydrostatic forces need to be considered. A typical hydrostatic pressure distribution along a submerged wall is illustrated schematically in Figure 3-2, with the resultant force (F_h) being applied at the area centroid of the distributed load. Hydrostatic forces are usually a function of the depth of water around the structure, the area of the structure submerged, the fluid density, and the gravitational constant. Hydrostatic forces can be quite large and depend on how deep the structure is submerged and the magnitude in pressure differences the structure is experiencing.

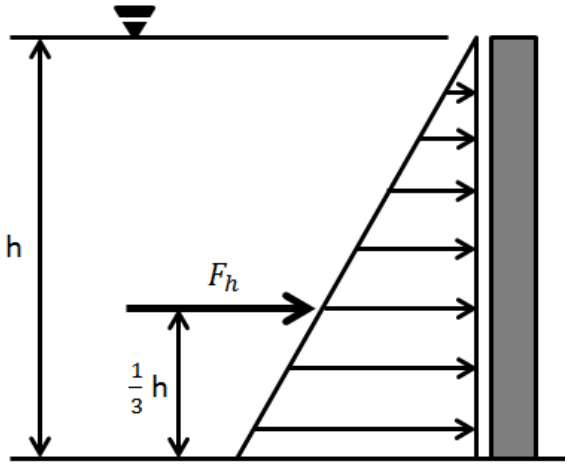

Figure 3-2: Hydrostatic force distribution along a wall

3.1.2 **Buoyancy Force**

Buoyancy forces, also known as vertical hydrostatic forces, act vertically through the centroid of the displaced fluid volume caused by the partial or total submergence of a structure or structural component. As the fluid depth increases, the pressure increases due to the weight of the overlaying fluid. Therefore an object submerged in the fluid will feel an upward force equal to the weight of the fluid it displaces (Archimedes Principle). Figure 3-3 depicts the force distribution on a partially submerged slab due to buoyancy, with the resultant force (F_b) acting through the centroid of the displaced fluid volume.

The buoyancy force varies with the volume of fluid displaced, the density of the fluid, and the gravitational constant. The buoyancy force will be resisted by the weight of the structure and any vertical restraints.

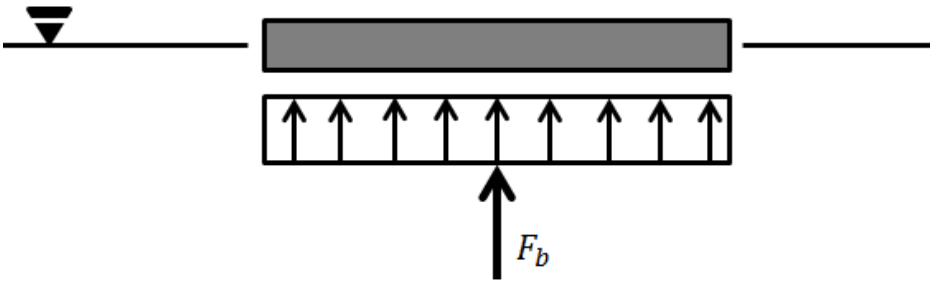

Figure 3-3: Force distribution due to buoyancy

3.1.3 **Hydrodynamic Drag Forces**

Hydrodynamic forces are induced on a structure by the flow of water moving at moderate to high velocities, and are a function of the fluid density, the flow velocity and the structural geometry. This force is also known as the drag force, which is a combination of lateral forces caused by the pressure forces from the moving mass of water and the friction of the water flowing around the structure.

The drag coefficient is used to quantify the drag a structure will experience when it is placed in a fluid flow. To estimate the drag coefficient for an object two behaviors need to be taken into account: skin friction and form drag. The skin friction arises from the friction of the fluid against the wetted surface of the object it is flowing around. The form drag is influenced largely by the size and shape of the object in the flow.

The flow type, denoted by the value of the Reynolds number, will define what component of the drag (skin friction or form drag) dominates for incompressible flow. The Reynolds number is a parameter that describes the ratio of the inertial forces to the viscous forces, based on a characteristic length, with laminar flow corresponding to low Reynolds numbers (viscous forces dominate) and turbulent flow corresponding to high Reynolds numbers (inertial forces dominate). Therefore if the flow is laminar the viscous forces will dominate, and the drag coefficient will largely depend on its skin friction component. On the other hand, if the flow is turbulent and the inertial forces dominate, the drag coefficient will largely depend on its form drag component (Anderson, 76).

Figure 3-4 depicts a hydrodynamic induced force distribution on a submerged wall with a uniform flow velocity, where the resultant force (F_d) acts through the centroid of the wetted surface of the walls cross-section perpendicular to the flow.

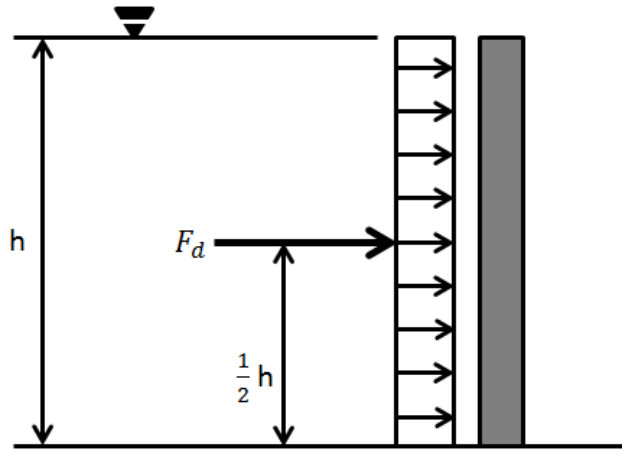

Figure 3-4: Hydrodynamic force distribution

3.1.4 **Hydrodynamic Uplift Forces**

During rapid inundation vertical hydrodynamic forces can cause uplift on the underside of structural components. Such forces can also develop as the result of differential fluid velocities above and below a structural component.

At horizontal structural components extending out from columns or walls, there is the possibility of generating a particularly large uplift force. As the flow tries to move around the object it also tries to move over it and encounters the horizontal structural components. The vertical component of the flow velocity will also be influenced by the topography/bathymetry near the structure.

To determine the hydrodynamic uplift force, the structural geometry will need to be known along with the gravitational constant and the density of the fluid. The uplift force should be distributed over the bottom wetted surface of the structure.

3.1.5 **Hydrodynamic Impulsive Forces (Surge)**

As the tsunami wave approaches a coastline and is influenced by the local bathymetry the tsunamis wave height will increase due to shoaling. When a tsunami enters the shoaling region of a coastline, the water depth will begin to decrease and, correspondingly, the tsunamis speed will decrease (decrease in kinetic energy). To conserve the energy lost by the decrease in speed, the tsunamis height will increase (increase in potential energy) (www.tsunami.noaa.gov).

Impulsive forces are caused by the surge of the tsunami bore impacting the structure's surface. From past research it has been shown that the initial dry-bed surge (first tsunami wave) transmit little to no impulsive force, but the subsequent waves moving over an already flooded area form bores and do cause a substantial impulsive force on the structure (Ramsden 1993). A tsunami does not always appear as a turbulent bore. Instead, it could also appear as a rapidly rising tide or a series of breaking waves. The local bathymetry, topography and the characteristics of the tsunami wave itself will dictate its final form.

An impulsive force will only be created if a bore or wave is formed and impacts a structural component and not after it has moved past the structural component. Impulsive forces typically depend on the velocity of the bore and the depth of the bore. These forces are important to consider when designing for tsunamis, because they can act on the structure simultaneously with other hydrodynamic forces (as the surge moves through the structure components downstream will also be experiencing hydrodynamic forces). Impulsive forces are typically applied uniformly over the structural component they are impacting, as shown in Figure 3-4 for the hydrodynamic drag force.

3.1.6 **Debris Impact and Damming Forces**

As the tsunami moves inland, large amounts of debris can accumulate in the flow, which can then impact structures in the path of the flow. These impact forces can be large, depending on the flow velocity, as well as the mass and effective stiffness of the debris. It is important for the engineer to determine what types of objects, in the considered structures area, may become debris.

Debris can also build up around the structure and increase the surface area that will experience hydrodynamic forces from the flow trying to move around it. Figure 3-5 shows the force distribution for a debris dam between two columns. In practice, the resultant force for the debris dam (F_{dm}) is applied to the centroid of the dam's area perpendicular to the flow direction.

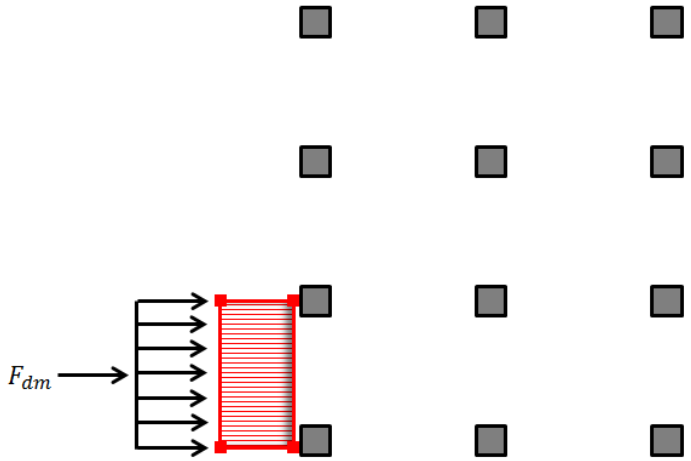

Figure 3-5: Debris dam force distribution

3.1.7 **Retained Water**

The FEMA P646 recommendations and the ASCE 7-16 draft proposal also consider the possibility of added gravitational forces due to static water. As the tsunami recedes there is the possibility for water to be retained inside structural components. This retained water will increase the gravity loads on the structure and is typically considered as a uniformly distributed gravity load over the areas that are expected to retain water.

3.2 Force Equations

This section will introduce the equations and relevant nomenclature introduced by the three codes and recommendations. Sections 3.3 to 3.5 will then discuss each of the three codes and recommendations, and Section 3.6 discusses similarities and differences among the three codes and recommendations.

Table 3-1 provides the tsunami force equations for the three design codes and recommendations. The definitions of the terms and variables used in Table 3-1 are provided in Table 3-2.

Table 3-1: Tsunami Design Force Equations

Force	Honolulu Building Code	FEMA P646	ASCE 7-16 Draft Proposal
Hydrostatic	$F_h = \frac{1}{2}\rho b g \left\{h + \frac{u^2}{2g}\right\}^2$	$F_h = p_c A_w = \frac{1}{2}\rho_s g b h_{max}^2$	$F_h = \frac{1}{2}\gamma_s b h_{max}^2 = \frac{1}{2}\rho_s g b h_{max}^2$
Buoyancy	$F_b = \rho g V$	$F_b = \rho_s g V$	$F_b = \gamma_s V_w = \rho_s g V$
Hydrodynamic	$F_d = \frac{1}{2}\rho C_d A_n u^2$	$F_d = \frac{1}{2}\rho_s C_d b (hu^2)_{max}$	$F_d = F_{dx} = \frac{1}{2}\rho_s I_{tsu} C_d C_{cx} b (hu^2)$
Uplift	Not considered	$F_u = \frac{1}{2} C_u \rho_s A_f u_v^2$	$P_u = 1.5 I_{tsu} \rho_s A_f u_v^2$
Surge	$F_{bore} = 4.5\rho g h_b^2$	$F_{bore} = 1.5 * F_d$	$F_{bore} = F_w = \frac{3}{4}\rho_s I_{tsu} C_d b (h_e u^2)$
Debris Impact	$F_i = \frac{m_f d U_b}{dt}$ or $F_i = \frac{31 * U_b}{\Delta t}$	$F_i = C_m u_{max}\sqrt{km}$	$F_i = 400 I_{tsu}\ (kips) = 1780 I_{tsu}\ (kN)^*$
Debris Damming	Not considered	$F_{dm} = \frac{1}{2}\rho_s C_d B_d (hu^2)_{max}$	Affects Minimum Closure Ratio
Additional Forces	Not considered	$f_r = \rho_s g h_r$	$P_r = \gamma_s h_r = \rho_s g h_r$

* This force represents the conservative simplified debris impact force provided by the ASCE 7-16 draft, it should be noted that multiple equations are provided for varying debris scenarios.

Table 3-2: Nomenclature

Symbol	Dimension	Definition
A_f	L^2	Horizontal projected area
A_n	L^2	Projected area normal to flow (vertical projected area)
A_w	L^2	Wetted area of component
B	L	Breadth (width) of component
B_d	L	Breadth (width) of debris dam
C_{cx}	--	Proportion of closure coefficient
C_d	--	Coefficient of drag
C_m	--	Added mass coefficient
C_u	--	uplift pressure coefficient (FEMA = 3.0)
$dt, \Delta t$	T	Change in time
f_r	$MLT^{-2} * L^{-2}$	Additional gravity force per unit area
F_b	MLT^{-2}	Buoyancy force
F_{bore}	MLT^{-2}	Bore impact force
F_d	MLT^{-2}	Hydrodynamic force
F_{dm}	MLT^{-2}	Debris damming force
F_h	MLT^{-2}	Hydrostatic force
F_i	MLT^{-2}	Debris impact force
F_u	MLT^{-2}	Uplift force
F_w	MLT^{-2}	Load on wall or pier
g	LT^{-2}	Gravitational constant ($9.81\ m/s^2$)
h	L	Tsunami depth above base of structure
h_b	L	Bore depth
h_e	L	Inundated height of an individual element
h_{max}	L	Maximum inundation depth above ground elevation
h_r	L	Depth of captured fluid
$(hu^2)_{max}$	L^3T^{-2}	Maximum momentum flux
I_{tsu}	--	Importance factor
k	$MLT^{-2} * L^{-1}$	Effective stiffness of debris
m	M	Mass of debris
m_f	M	Mass of fluid displaced by debris
p_c	$MLT^{-2} * L^{-2}$	Hydrostatic pressure
u	LT^{-1}	Flow velocity at structure location
u_{max}	LT^{-1}	Maximum flow velocity carrying debris
u_v	LT^{-1}	Vertical component of flow velocity at structure location
U_b	LT^{-1}	Velocity of debris
V	L^3	Volume of water displaced by structure
V_w	L^3	Displaced water volume
γ_s	$ML*L^{-3}T^{-2}$	Specific weight including sediment
ρ	ML^{-3}	Fluid density
ρ_s	ML^{-3}	Fluid density including sediment

3.3 Honolulu Building Code

Chapter 16 in the Revised Ordinances of Honolulu (originally created in the early 1980's) contains the Honolulu Building Code, which in turn, contains force provisions in Article 11 "Regulations Within Flood Districts and Development Adjacent to Drainage Facilities" Section 16-11.5 Subsection f, entitled "Coastal Flood Water Design". These provisions apply mainly to coastal zones subject to inundation by a storm with a 1-percent annual chance of exceedance. This code does not contain any tsunami inundation maps. However, the code specifies that the provisions can also be used to determine tsunami-induced forces.

The following excerpt from the code summarizes five key considerations for buildings:

1) Buildings or structures shall be designed to resist the effects of coastal floodwaters due to tsunamis. The regulatory flood elevation due to tsunamis is considered to result from a non-bore condition, except where a bore condition is shown on the flood insurance maps or in the flood study adopted for the county.

2) Habitable space in building structures must be elevated above the regulatory flood elevation by such means as posts, piles, piers or shear walls parallel to the expected direction of flow of the tsunami wave. The forces and effects of floodwaters on the structure shall be fully considered in the design.

3) Allowable stresses (or load factors in the case of ultimate strength or limit design) for the building materials used shall be the same as the building code provides for wind or earthquake loads combined with gravity loads, i.e., treat loads and stresses due to tsunamis in the same fashion as for earthquake loadings.

4) The main building structure shall be adequately anchored and connected to the elevated substructure system to resist all lateral, uplift and downward forces. In wood construction, toenailing is not allowed.

5) Scour of soil from around individual piles and piers shall be provided for in the design in the coastal flood hazard district. Shallow foundation types are not permitted unless the natural supporting soils are protected on all sides against scour by a shore protection structure, preferably a bulkhead. Shallow foundations may be permitted beyond 300 feet from the shoreline, provided they are founded on natural soil and at least two feet below the anticipated depth of scour, and provided not more than three feet of scour is expected at the structure.

The Honolulu Building Code requires knowledge of the structure geometry, tsunami flow velocity, and debris characteristics. The structure geometry and local debris possibilities need to be considered by the design engineer. The flow velocity can be obtained from a detailed

numerical model (no description provided), tsunami inundation limit maps (no tsunami design zone maps are provided), or it may be estimated to be equal to the depth of the flow at the structure (i.e., if the depth of tsunami flow at a particular location is 3m then the velocity may be estimated as 3m/s).

The Honolulu Building Code also recommends three drag coefficients for calculating the hydrodynamic forces on the structure. The code recommends the use of drag coefficients of 1.0 for circular piles, 2.0 for square piles, and 1.5 for wall sections.

The Honolulu Building Code employs the impulse-momentum concept for the impact of debris. Additionally, the impact of debris is assumed to occur over a finite time interval (0.1 seconds for reinforced concrete and 0.5 seconds for steel).

These assumptions should be applied to the equations listed in Table 3-1 for the Honolulu Building Code to determine tsunami-induced forces on a structure. A discussion is also provided on load and force combinations and will be discussed in more detail in Subsection 3.6.7. It should be noted that this subsection also references Dames & Moore (1980) for a more detailed study and analysis of tsunami forces.

3.4 FEMA P646 (2008 Edition)

The Federal Emergency Management Agency (FEMA) recommends tsunami force equations in a manual titled "Guidelines for Design of Structures for Vertical Evacuation from Tsunamis". This manual, FEMA P646, was first published in 2008 with the goal of addressing the need for guidance on building structures that would be capable of resisting the extreme forces of both a tsunami and earthquake. This manual also contains tsunami force combinations and load combinations along with other tsunami considerations. These guidelines have been developed by FEMA specifically for tsunami evacuation structures. This section does not reflect updates to the FEMA P646 recommendations introduced in 2012 (FEMA 2012)

3.4.1 **Key Assumptions**

Based on past research and eyewitness accounts, a number of assumptions and recommendations were used to formulate the equations for determining tsunami forces. Specifically,

- The density of the sea water is assumed to be multiplied by a factor of 1.2 to account for sediment accumulation.
- Because of the uncertainty in the tsunami runup elevation and inundation depth at the structure, the estimation of the runup elevation is multiplied by a factor of 1.3.

- Due to the uncertainties in the numerical modeling of tsunami flow, predicted velocities and maximum momentum fluxes from any numerical solution are not taken to be any less than 80% of the values determined from the analytical solutions provided in the document. These equations are provided for estimating flow and debris characteristics so that the designer can determine forces on the structure in the absence of detailed computer models.
- The design engineer needs to know the structure's elevation and the structural geometry.
- FEMA P646 makes assumptions regarding the general characteristics of the tsunami wave including, but not limited to, the observation that the first wave may not be the largest and that the tsunami wave typically breaks off shore.
- The flow parameters that are required for calculating tsunami-induced forces for the FEMA P646 recommendations are the flow velocity, flow depth, and the maximum momentum flux at the structure.
- The document recommends using a detailed numerical model for determining flow parameters, but equations are provided, with some simplifications and assumptions, and are useful for checking the reasonableness of results or as an estimate of approximate values if no numerical model data can be obtained.
- The provided analytical solutions for flow parameters are based on one-dimensional, fully nonlinear shallow-water-wave theory for the condition with a uniformly sloping beach and no friction. According to Chock (2014), "this uniformly sloping frictionless solution does not agree with actual tsunami observations and video analysis, and leads to unconservative design flow parameters."

3.4.2 **Flow Velocity**

For estimating the flow velocity, two methods are provided, one for debris impact and the other for fluid forces. For debris impacts there are two maximum flow velocity estimates, depending on the draft of the debris, where the draft refers to how deep the debris needs to be submerged to become buoyant. Flow velocities carrying lumber or wooden logs (with essentially no draft) may be estimated as:

$$u_{max} = \sqrt{2gR\left(1 - \frac{z}{R}\right)} \quad \textbf{(3-1)}$$

where z is the ground elevation at the base of the structure, R is the design runup elevation (Fig. 3-1) at the structure and g is the gravitational constant. Equation 3-1 represents the exact solution for the maximum fluid velocity at the leading runup tip for an incident bore given by Shen and Meyer (1963), presented as a function of ground elevation. Additionally, Equation 3-1

is based on the tsunami bores height "collapsing" to zero at the shoreline before the initial inundation occurs.

For larger debris (e.g., shipping containers) a graphical procedure is employed with the use of Figure 3-6. A graphical procedure is needed due to larger debris not having a small enough draft to become buoyant in a flow depth with a velocity represented by Equation 3-1. Therefore, Figure 3-6 allows for the designer to determine a flow velocity more representative of the velocity for a flow that is deep enough to allow for the debris to become buoyant.

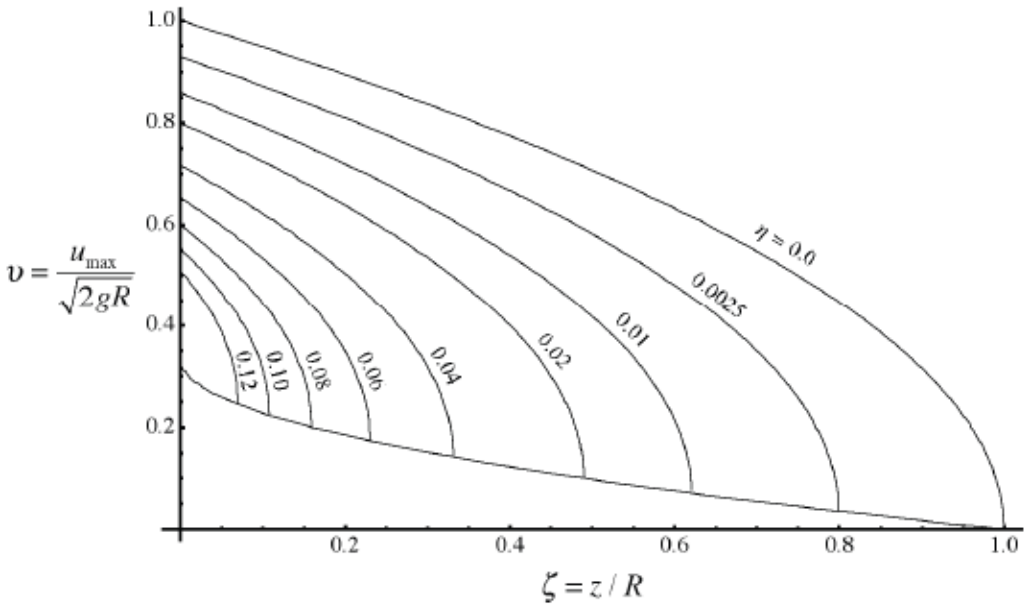

Figure 3-6: Maximum Flow Velocity (FEMA P646 pg. 77)

To determine the maximum flow velocity one needs to calculate the value of ζ and then draw a vertical line until it intersects one of the lines representing η (the lower curve represents a lower bound for determining flow velocity) corresponding to the specific design situation. The value of η can be determined as:

$$\eta = \frac{d}{R} \quad \textbf{(3-2)}$$

with the draft, d, defined as follows:

$$d = \frac{W}{\rho_s g A_f} \quad \textbf{(3-3)}$$

where W is the weight of the debris, ρ_s is the fluid density considering sediment, and A_f is the cross-sectional area parallel to the water surface such that the product of the draft and cross-sectional area represents the volume of water displaced by the debris. Figure 3-6 was introduced by Yeh (2007) based on previous work done by both Shen and Meyer (1963), and Peregrine and Williams (2001). Because beaches are not typically uniformly sloped, the above equations are introduced as a function of the ground elevation.

The two maximum flow velocity approximations mentioned above are only applicable for determining debris impact forces.

For determining uplift forces in FEMA P646, the vertical flow velocity can be estimated by first using Figure 3-6 to estimate the horizontal flow velocity, but with a slight modification to the η term. The value of η needs to be modified to represent the flow velocity at the structural component; this is because the use of the maximum estimated flow velocity would be unnecessarily conservative. The modified η can be seen below, where h_s is the elevation of the structural component.

$$\eta = \frac{h_s}{R} \quad \textbf{(3-4)}$$

Once the new η term is determined, the horizontal flow velocity can be estimated. Equation 3-5 then can be used to estimate the vertical flow velocity, where α is the average slope or grade at the site and u is the estimated horizontal flow velocity from Figure 3-6.

$$u_v = u * \tan(\alpha) \quad \textbf{(3-5)}$$

3.4.3 **Maximum Momentum Flux**

Another flow parameter that is needed is the maximum momentum flux per unit mass at the structure. This quantity is used to determine the tsunami induced hydrodynamic and debris damming forces. Equation 3-6 is provided for estimating the maximum momentum flux at the structure location and was developed based on work done by Yeh (2006) who expanded on previous work done by Carrier et al. (2003).

$$(hu^2)_{max} = gR^2\left(0.125 - 0.235\left(\frac{z}{R}\right) + 0.11\left(\frac{z}{R}\right)^2\right) \quad \textbf{(3-6)}$$

Equation 3-6, like the velocity equations, is based on the one-dimensional nonlinear shallow-water theory for a uniformly sloping beach, with no lateral topographical variation or friction,

similar to the maximum flow equations. Because typical beaches are not uniformly sloped, Equation 3-6 is also expressed as a function of ground elevation instead of distance.

FEMA P646 also recommends that the approximation of the maximum momentum flux be used only for preliminary design, approximate design in the absence of numerical modeling results, or to evaluate the reasonableness of numerical modeling results. It should be noted that the maximum momentum flux will not necessarily occur at the time corresponding with the maximum inundation depth and or maximum velocity at the structure. This is why a numerical model or Equation 3-6 is required for determining its value.

3.4.4 **Debris Characteristics**

For determining the debris characteristics, Table 3-3 is provided for estimating the mass and effective stiffness of a select number of possible debris that might impact the structure. Table 3-3 should be expanded if there are other possible debris sources in the proximity of the structure, and engineering judgment should be used.

Table 3-3: Possible Mass and Stiffness of Debris (FEMA P646)

Location of Source	Mass (m) in kg	Effective Stiffness (k) in N/m
Lumber or Wood Log	450	2.4×10^6
40-ft Standard Shipping Container	3800 (empty)	6.5×10^8
20-ft Standard Shipping Container	2200 (empty)	1.5×10^9
20-ft Heavy Shipping Container	2400 (empty)	1.7×10^9

Once this required information is known it can be used to determine the forces induced on a structure due to a debris impact with the FEMA P646 equation that was introduced in Table 3-1.

3.5 ASCE 7-16 Draft Proposal

A new chapter, in draft stage, will be included in ASCE 7-16, titled “Chapter 6: Tsunami Loads and Effects”. If this chapter is adopted into ASCE 7-16, it will be the first national design standard for tsunami resilience, and it will be required for the use in the states of Alaska, Washington, Oregon, California, and Hawaii (only states with a tsunami risk). Currently probabilistic tsunami hazard analysis is lacking for other US territories and therefore these territories will not be covered by the ASCE 7-16 draft proposal. It should be noted that the following information is still in the draft stage and may not represent its final form in the ASCE 7-16 Minimum Design Loads for Buildings and Other Structures.

3.5.1 **General Design Considerations**

The draft forces and design considerations were developed for Tsunami Risk Category II (denoted from this point forward as "Risk Category") buildings and Other Structures with a height greater than 65-ft, and Risk Category III and IV Buildings and Other Structures. The types of buildings that fall within these Risk Categories are identical to those found in ASCE 7- 10 Table 1.5-1 with the following revisions. Critical facilities designated by state and local governments are permitted to be designated as Risk Category III structures (unless already designated as Risk Category IV). Additionally, tsunami vertical evacuation refuge structures are designated as Risk Category IV structures, whereas fire stations, ambulance facilities, emergency vehicle garages, earthquake or hurricane shelters, and emergency aircraft hangers do not need to be considered Risk Category IV structures. These "susceptible" structures are within the Tsunami Design Zone, which is an area that is deemed vulnerable to tsunami inundation during a Maximum Considered Tsunami event (2% probability of being exceeded in 50-years).

Even with the inclusion of "Other Structures" in the scope of the provisions, the main focus of the draft chapter is on buildings, including tsunami vertical evacuation refuge structures, which is the focus of FEMA P646. The draft chapter has a general organized as follows:

- Determining flow parameters
- Discussing the structural design procedures
- Determining tsunami induced forces and effects

The design flow parameters that are required for determining the design tsunami forces are the runup elevation, inundation limit, inundation depth, flow velocity, and momentum flux. In addition to these design flow parameters, debris characteristics, site specific information and structural characteristics and geometry are also needed to determine the tsunami induced forces. In the design procedures section of the draft chapter, a number of load cases, load combinations, assumptions, and recommendations are introduced. Three load cases are provided that represent the critical stages of structural loading during the Maximum Considered Tsunami event. These load cases and combinations will be discussed further in the following section (Subsection 3.6.7).

Like the previous two documents, a number of key assumptions and recommendations are made to both introduce conservatism into the determination of the tsunami forces and to aid the designer in applying the tsunami forces. The density of the sea water is assumed to be increased by a factor of 1.1 to account for the accumulation of sediment. Also, the rise in the mean sea level during the design life of the structure needs to be taken into account along with the possibility of the ground elevation changing due to seismic subsidence. These represent only a few of many requirements included in the ASCE 7-16 draft.

There are a number of methods that are introduced for determining the design flow parameters based on the Risk Category of the structure. The design flow parameters for Risk Category II and III structures are determined by using the Energy Grade Line (EGL) Analysis method. A Site-Specific Probabilistic Tsunami Hazard Analysis (PTHA) may be used in lieu of the EGL Analysis. Additionally, if inundation depths are determined to be less than 3-ft (0.914 m) at the structure's location, tsunami forces do not need to be considered for Risk Category II and III structures. For Risk Category IV structures, both an EGL Analysis and a PTHA need to be performed; however the PTHA need not be performed if the inundation depth determined from the EGL Analysis is less than 12-ft (3.66 m). These two procedures are discussed in the following paragraphs.

3.5.2 **Energy Grade Line Analysis**

To perform the EGL analysis, the inundation limit and runup elevation for the maximum considered tsunami can be determined from detailed inundation limit maps. These maps should be available from the authority having jurisdiction for the location of the structure. Additionally the National Oceanic and Atmospheric Administration (NOAA) is in the process of constructing inundation maps for the coastlines to be supplied in the new ASCE 7-16 chapter. The modeling used for creating these detailed maps must take into account sea level change and the possibility of ground elevation change due to seismic subsidence.

If inundation limit maps are not available, an alternate method may be used for Risk Category II and III structures, but only if the structure's location is not in an area where wave focusing may take place (e.g., headlands, v-shaped bays). This alternate method is based on the ratio of the tsunami runup elevation above mean high water level to offshore tsunami amplitude (R/H_T), and the mean slope of the near shore profile from a depth of 100 m to the mean high water elevation along the axis of the topographic transect (profile of vertical elevation data versus horizontal distance along a cross-section of the terrain) for the site. The value of the offshore tsunami amplitude (H_T) can be determined from provided maps for the region where the structure is located. Figure 3-7 represents this alternative method for determining runup elevation, where ϕ represents the mean slope angle of the nearshore profile. Additionally, peer-reviewed literature may be used to refine the prediction of runup in certain cases.

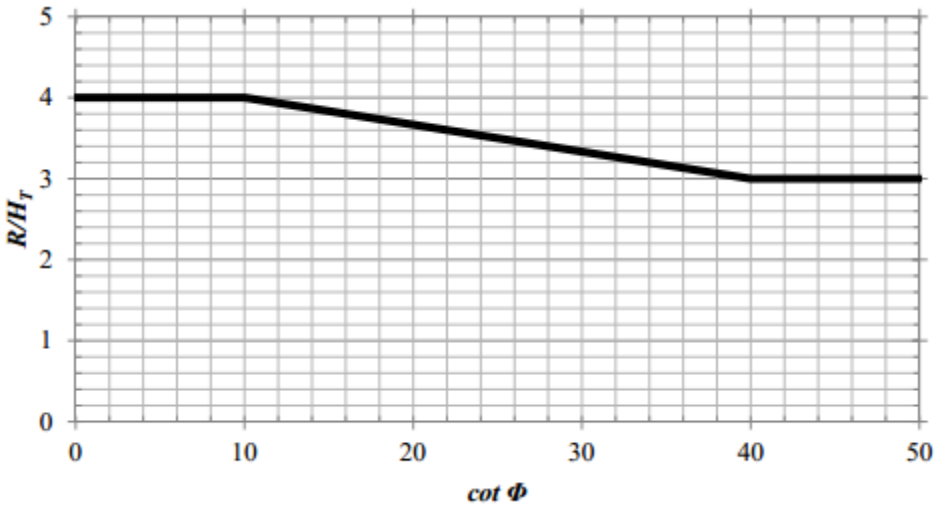

Figure 3-7: Run-up Ratio as a Function of the Mean Slope of the Nearshore Profile, where no Mapped Inundation Limit Exists (obtained from ASCE 7-16 draft)

Once the design run-up elevation and inundation limit are determined by either an inundation limit map or the above alternate procedure, the EGL method may be applied. The EGL method is not as accurate as a precise computer simulation for determining flow parameters at the structure's location, but it does account for uncertainties. Therefore, because uncertainties are accounted for, the EGL method provides a lower limit that numerical models should not fall below. Thousands of numerical code simulations were compared against the EGL method to verify its conservatism and statistical allowance. Equations 3-7 to 3-9 represent the EGL method along with Figure 3-8, reproduced from the ASCE 7-16 draft Chapter 6, depicting the meaning of the variables.

$$E_{g,i+1} = E_{g,i} + (\varphi_i + s_i)\Delta x_i \quad \textbf{(3-7)}$$

$$E_{g,i} = Hydraulic\ Head\ at\ point\ i = h_i + \frac{u_i^2}{2g} = h_i(1 + 0.5F_{ri}^2) \quad \textbf{(3-8)}$$

$$F_{ri} = Froude\ Number = \frac{u}{\sqrt{gh}}, \quad at\ point\ i \quad \textbf{(3-9)}$$

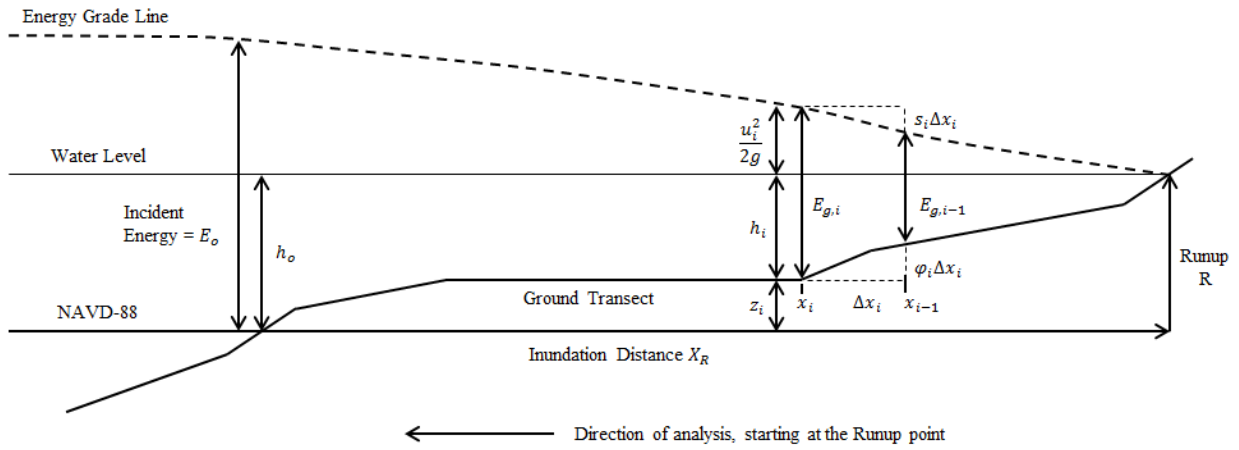

Figure 3-8: EGL Method (Adapted from ASCE 7-16 Chapter 6 Draft)

The EGL method is a step-by-step method for determining the flow parameters at vertical cuts of the topographic transect. In Figure 3-8, φ_i represents the average ground slope between points i and $i+1$ and s_i represents the friction slope of the energy grade line between points i and $i+1$, which is calculated by Equation 3-10.

$$s_i = \frac{u_i^2}{\left(\frac{1.49}{n}\right)^2 h_i^{4/3}} = \frac{gF_{ri}^2}{\left(\frac{1.49}{n}\right)^2 h_i^{1/3}} \quad U.S.inch-pound\ units$$

$$= \frac{gF_{ri}^2}{\left(\frac{1.00}{n}\right)^2 h_i^{1/3}} \quad metric\ units \qquad \textbf{(3-10)}$$

In Equation 3-10, the variable n represents Manning's roughness coefficient of the terrain segment being analyzed based on the frictional surface, as shown in Table 3-4.

Table 3-4: Manning's Roughness Coefficients Provided by ASCE 7-16 Draft Proposal

Description of Frictional Surface	n
Coastal water nearshore bottom friction	0.025 to 0.030
Open land / field	0.025
All other cases	0.03
Commercial/industrial buildings of at least urban density	0.04

The velocity can then be determined at the structure's location as a function of the inundation depth, in accordance with the prescribed value of the Froude number calculated according to Equation 3-11.

$$F_r = \alpha \left(1 - \frac{x}{x_R}\right)^{0.5} \quad \textbf{(3-11)}$$

The maximum value of the Froude number cannot exceed 1.0 at any of the step locations for the EGL method.

3.5.3 **Probabilistic Tsunami Hazard Analysis**

In lieu of the EGL method, a more in-depth site-specific PTHA method can be used for Risk Category II and III structures, and it must be used with the EGL method for Risk Category IV structures, as long as the determined inundation depth by the EGL is greater than 12 ft. This type of analysis is discussed in detail in the draft chapter, but it is outside of the scope of this research and will not be discussed here.

If the site-specific analysis is used, the design flow velocity predicted for urban environments may not be less than 100% of that predicted from the EGL method, while the design flow velocity predicted for other terrain may not be less than 80% of that predicted from the EGL method. These limitations should be applied prior to any velocity adjustments due to flow amplification. Additionally these limitations help ensure that the flow parameters determined by the PTHA method are conservative, and in line with the conservatism of the EGL method discussed above.

3.5.4 **Other Characteristics**

In addition to the above flow parameters, debris, structure, and site characteristics are also needed to be able to determine tsunami-induced forces on the structure. The type of structure being designed needs to be considered for determining the Risk Category of the structure and whether tsunami loads need to be considered. Based on the Risk Category of the structure, importance factors (I_{tsu}) must be applied to force equations to amplify the loads the structure will experience. These importance factors are provided in Table 3-5.

Table 3-5: Importance Factors (Adapted from ASCE 7-16 Draft)

Risk Category	I_{tsu}
II	1.0
III	1.2
IV, Vertical Evacuation Structures, and Risk Category III Critical Structures	1.3

The site where the structure will be located also needs to be considered for determining flow direction, if the flow velocity needs to be amplified, and what debris are around the area and need to be considered as potential debris impact hazards. The possibility of debris impact is high

during a tsunami and the types of debris can be vast, therefore engineering judgment should be used in determining what types of objects need to be considered for debris impact.

Additionally, the ASCE 7-16 draft also provides a selection of drag coefficients based on the ratio of the width of the structure to inundation depth and can be seen in Table 3-6.

Table 3-6: Drag Coefficients Provided in ASCE 7-16 Draft

Width to Inundation Depth	Drag Coefficient (C_d)
< 12	1.25
≥ 12 and < 20	1.3
≥ 20 and < 32	1.4
≥ 32 and < 40	1.5
≥ 40 and < 80	1.75
≥ 80 and < 120	1.8
≥ 120	2.0

Additional drag coefficients are also supplied based on specific structural elements.

3.6 Differences among Codes and Recommendations

As shown in tables 3-1 and 3-2 the tsunami force equations and their respective variables vary among the three documents. These variations in the fluid and debris induced forces are discussed here along with variations in the variables. Additionally, the section discusses the load combinations provided by both FEMA P646 and the ASCE 7-16 draft, along with the load cases provided by the ASCE 7-16 draft. Separate discussions are provided for each of the force types that were introduced in Section 3.1, and also for the recommended load combinations and cases.

3.6.1 **Hydrostatic Equations**

For hydrostatic forces the Honolulu Building Code includes the velocity head of the fluid along with the hydrostatic force solely due to gravity. Both the FEMA P646 recommendations and ASCE 7-16 draft proposal only consider the hydrostatic force due to gravity. A potential reason for the exclusion of the velocity head in these two codes and recommendations is that the fluid-velocity induced forces are best considered as part of in hydrodynamic force calculations.

The hydrostatic force, if applicable, should be calculated at the maximum inundation depth experienced by a component. In the FEMA P646 recommendation and the ASCE 7-16 draft proposal, the maximum fluid depth (h_{max}) is assumed for these calculations, whereas in the Honolulu Code, this assumption is not specified

Additionally, the FEMA P646 recommendations also require a 30% increase in the estimated design runup elevation. This increase in the runup elevation will lead to higher fluid-induced forces. In the ASCE 7-16 draft, the inundation maps are based on a probabilistic analysis, which takes into account uncertainties explicitly. Further conservatism is added based on the Risk Category (application of importance factors) of the structure being designed.

3.6.2 **Buoyancy Force Equations**

Buoyancy forces are calculated identically in all three of the documents. Nonetheless, there are differences in the selection of both the fluid density and specific weight to be used. Both the FEMA P646 and ASCE 7-16 draft documents consider an increase due to sediment (20% and 10% respectively) while the Honolulu Building Code does not. Additionally, FEMA P646 applies this 20% increase to the density of fresh water, whereas the ASCE 7-16 draft increases both the density and specific weight of sea water by 10%. The use of different fluid densities, as seen in Table 3-7, leads to varying buoyancies.

Table 3-7: Varying Fluid Densities

Code or Recommendation	Density
Honolulu Building Code	1,030 kg/m^3
FEMA P646 Recommendations	1,200 kg/m^3
ASCE 7-16 Draft	1,128 kg/m^3

3.6.3 **Hydrodynamic Force Equations**

The FEMA P646 document and ASCE 7-16 draft both consider the maximum momentum flux in the calculation of hydrodynamic forces. For FEMA P646 this consideration can be seen in Table 3-1 ($(hu^2)_{max}$) and for the ASCE 7-16 draft the maximum momentum flux is considered through the use of the provided load cases (Subsection 3.6.7). The Honolulu Building Code's equation for the hydrodynamic force does not explicitly use the momentum flux but rather uses the area normal to the tsunami flow. FEMA P646 also supplies Equation 3-6 for estimating the maximum momentum flux, and while the ASCE 7-16 draft also supplies methods for determining flow parameters (EGL, PTHA), the Honolulu Building Code only supplies a single method for estimating the flow velocity (flow depth equal to flow velocity).

Another difference between the hydrodynamic force equations is the addition of an importance factor (Table 3-5) introduced by the ASCE 7-16 draft. This importance factor amplifies the hydrodynamic forces based on the Risk Category of the structure being designed. Also, again the 30% increase in runup elevation by FEMA P646 will also influence the calculation of the hydrodynamic force.

Additionally there are variations in the selections of the drag coefficients used in the hydrodynamic force equations, which also leads to varying hydrodynamic forces. Both the Honolulu Building Code and the ASCE 7-16 draft (Table 3-6) provide situation-dependent drag coefficients, whereas the FEMA P646 document recommends only one value. A flat plate perpendicular to the flow direction in a laminar flow leads to a drag coefficient of 2.0 (Anderson, 76), identical to the one supplied by the FEMA P646 document. This value of 2.0 may not be adequate for bridges due to their multiple geometries and their extended width that will contribute to the effect of the skin friction component of the drag. Additionally flow regimes (laminar, transitional, and turbulent) during tsunami inundation will vary and therefore the drag coefficient will also vary. Fluid density and inundation depth are also used in the calculation of the hydrodynamic forces and therefore also contributes to the variations in the results of the hydrodynamic force calculations.

Finally, in addition to the hydrodynamic force equation in Table 3-1, the ASCE 7-16 draft also introduces a hydrodynamic force equation for components. This component equation is identical to the hydrodynamic force equation in Table 3-1 but with a different depth variable representing the component depth. Additionally, the ASCE 7-16 draft also supplies a simplified equation to represent the hydrostatic and hydrodynamic forces together. This equation is conservative and requires a 30% increase in the inundation depth at the site. The purpose of this simplified equation is to help the designer determine if hydrostatic and hydrodynamic forces will be larger than the earthquake forces that the structure must also be designed to resist.

3.6.4 **Impulsive Force Equations**

There are large differences in the calculation of the surge or impulsive forces in the three codes and recommendations. FEMA P646 simply amplifies the hydrodynamic force (by a factor of 1.5) for the calculation of the impulsive force. According to Yeh (2007), the Honolulu Building Code amplifies the pressure the fluid applies statically, depending on the structure's height (derived by the summing the hydrostatic force and the change in linear momentum). If the structure's height is less than three times the bore height, the Honolulu Code recommends an "appropriate" combination of the hydrostatic and hydrodynamic forces for determining the impulsive force. The amplification of the hydrodynamic force by FEMA P646 allows for its momentum flux to also influence the impulsive force calculation. The ASCE 7-16 draft introduces a surge force equation that is also an amplification of the hydrodynamic force equation and is dependent on the width to inundation depth of the structure (amplified by either ½ for width to inundation depth less than 3 or ¾, as seen in Table 3-1). Additionally, the ASCE 7-16 draft also includes surge forces for perforated and slanted walls.

3.6.5 **Uplift Force Equations**

The Honolulu Building Code does not consider uplift forces (besides buoyancy), whereas FEMA P646 considers uplift as the vertical hydrodynamic force. The ASCE 7-16 draft considers a number of uplift scenarios, where the equation in Table 3-1 represents the uplift force equation for a slab over a grade that exceeds 10 degrees. In addition to this force equation a minimum uplift force of 20 psf is required (in addition to the buoyancy force) and another equation for uplift is presented for the scenario of a tsunami bore being trapped between a slab and a wall as depicted in Figure 3-9.

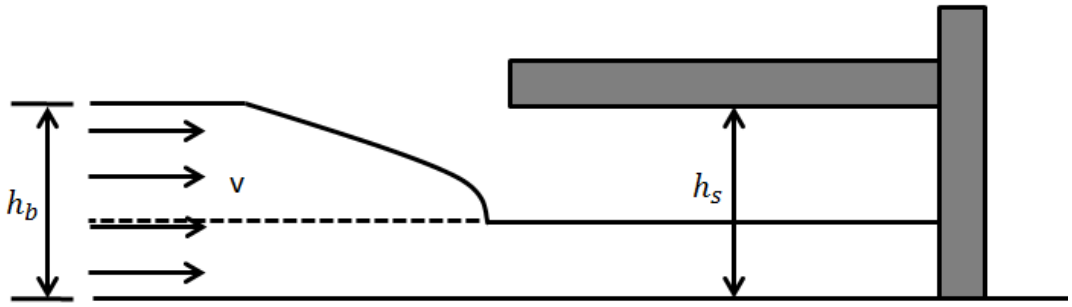

Figure 3-9: ASCE 7-16 Draft Uplift Experimental Setup for Wall/Slab (Adapted from Chock et al. 2013)

The ASCE 7-16 draft also allows for reductions in the predicted uplift force based on openings in the structure, and the inundation depth at the structure. For the case studies in Chapter 5 the minimum uplift force of 20 psf will be used due to the site location and the structural geometry of a bridge superstructure.

3.6.6 **Debris Impact and Damming Force Equations**

The formulation of the debris impact equations varied significantly among the documents. The Honolulu Building Code introduces a debris impact equation based on the impulse-momentum concept. The debris impact equation provided for the ASCE 7-16 draft in Table 3-1 represents the simplified equation provided by the draft, and is therefore conservative. Additionally, the ASCE 7-16 draft also supplies equations for multiple debris types including logs, vehicles, boulders, concrete, shipping containers, and ships. The Honolulu Building Code also supplies varying impact duration times depending on the structural material.

On the other hand, FEMA P646 formulated a debris impact equation based on past experimental research (Haehnel and Daly, 2002) and a linear dynamic model (neglecting damping effects). In addition, the FEMA P646 recommendation also includes an added mass coefficient (C_m) to take into account the momentum of the water surrounding the debris also contributing to the impact force.

Both the FEMA P646 recommendations and the ASCE 7-16 draft take into account debris damming, but in different ways. FEMA P646 accounts for debris damming as a force that should be applied at the most detrimental location on the structure. On the other hand, the ASCE 7-16 draft accounts for debris damming by modifying the coefficient called "closure ratio" (how "closed" the structure is to allowing water to flow through it) of the structure to account for the debris building up around the structure and increasing tsunami induced fluid forces.

3.6.7 **Force and Load Combinations**

It is very unlikely that all of the possible tsunami forces will occur simultaneously or on the same structural components during a tsunami event. The Honolulu Building Code supplies a number of force and load combinations such that the combined effect will result in the maximum probable loads on the structural members. FEMA P646 provides suggestions of what forces should be considered together and when they should be applied to the structure. It is noted that engineering judgment should be used in determining other possible combinations depending on the situation and structural system being considered. Once the controlling tsunami force is determined, it can be applied to the structure along with the load factor and the other applicable forces. The ASCE 7-16 draft also contains load cases and combinations that will be discussed following both the Honolulu Building Code and the FEMA P646 documents force and load combinations.

Honolulu Building Code

The Honolulu Building Code requires multiple force combinations for certain load types. The full intensity of the dead load must be applied to the structure. This is also true for the wind loads that may apply to the structure above the water depth at the structure. The possibility of storage structures being filled during a tsunami event must also be considered for live loads and the reduction of live loads on certain structural components is permitted. Finally, earthquake and tsunami loads do not need to be considered together.

The Honolulu Building Code also states that the required load combinations should be identical to those provided by the locally adopted building code. Additionally, the load factors applied to tsunami loads should be identical to those applied to earthquake loads.

FEMA P646

FEMA P646 breaks the tsunami force combinations into three sets, one for the overall structure, a second for individual structural components, and a third for slab-type components.

For the overall structure the buoyancy and hydrodynamic uplift forces should be combined to adequately estimate the vertical forces on the structure for a given design runup elevation and inundation depth. Hydrodynamic drag effects and surge (impulsive) forces should be considered

together as the tsunami moves across the structure. Typically the worst combination of impulsive and hydrodynamic forces occurs when the bore impacts the last structural components while the other components, downstream of the bore, are experiencing hydrodynamic forces. Every part of the structure needs to be designed to resist debris impacts in combination with all other loads (excluding surge forces). Additionally debris damming forces should be applied to the most detrimental location on the structure in combination with hydrodynamic drag forces acting on all other components of the structure. Finally, breakaway wall segments cannot be considered as structural components.

There are a number of situations where it is recommended that the force equations be evaluated for the maximum momentum flux ($(hu^2)_{max}$). Surge forces should be applied to individual components of the structure, hydrodynamic drag forces should be combined with debris impact forces at the most critical location, and a minimum 40-foot wide debris dam should be applied at the worst possible loading location. Additionally, hydrostatic forces for the maximum possible water depth should be applied to any structural component that is watertight.

Finally, force combinations for slab components are considered in the FEMA P646 document. Buoyancy forces need to be considered with the additional consideration of trapped air and or other structural components (i.e. girders). In addition to buoyancy, vertical hydrodynamic uplift forces need to be considered. The maximum uplift case will be the largest of the previous mentioned (buoyancy and vertical hydrodynamic) combined with 90% of the dead load and zero live load. Additionally, during drawdown, downward forces due to retained water need to be combined with 100% of the dead load.

FEMA P646 introduces two strength design load combinations that are to be considered with the current building code being used by the designer:

Load Combination 1: $1.2D + 1.0T_s + 1.0L_{REF} + 0.25L$

Load Combination 2: $0.9D + 1.0T_s$

where: D = dead load

T_s = tsunami load

L_{REF} = live load inside refuge area (areas designed to act as a tsunami evacuation assembly point)

L = live load outside of refuge area

Earthquake loads are not considered to act in combination with tsunami loads because the main earthquake event generally precedes the tsunami, and the aftershocks are typically smaller than the initial earthquake. A load factor of 1.0 is used for tsunamis for three main reasons. First it is anticipated that the tsunami hazard level corresponding to the Maximum Considered Tsunami will be consistent with the 2500-year return period associated with the Maximum Considered Earthquake used in seismic design. Additionally during the tsunami force calculations a number of conservative assumptions have already been made. For example, during the determination of the tsunami forces, the runup elevation is increased by 30%, the fluid density is increased by 20%, and any of the numerical solutions used must not be less than 80% of those determined from the provided equations.

Finally the design for tsunami forces considers only the elastic response of the structural components, unlike the consideration of inelastic responses for seismic forces and therefore the corresponding load factor is less than 1.0.

ASCE 7-16 Draft

The ASCE 7-16 draft contains both load cases and combinations. Three load cases are provided that represent the three critical times during a tsunami inundation. Each of the load cases needs to be considered when determining the controlling forces on the structure.

- The first load case represents the minimum condition of combined hydrodynamic force and buoyant force, where the inundation depth is equal to one story but not exceeding the maximum inundation depth at the structure's location. The exception to this load case is that the structure is considered an open Structure as defined in the ASCE 7-16 draft.
- The second load case occurs at an inundation depth of two-thirds the maximum inundation depth and is when it is assumed that the maximum flow velocity and momentum flux occur for either the incoming or receding directions of the tsunami.
- The third load case represents the maximum inundation depth at the structure where the flow velocity is assumed to be one-third of the maximum flow velocity in either the incoming or receding directions. Figure 3-10 is reproduced from the ASCE 7-16 draft, and shows the second and third load cases.

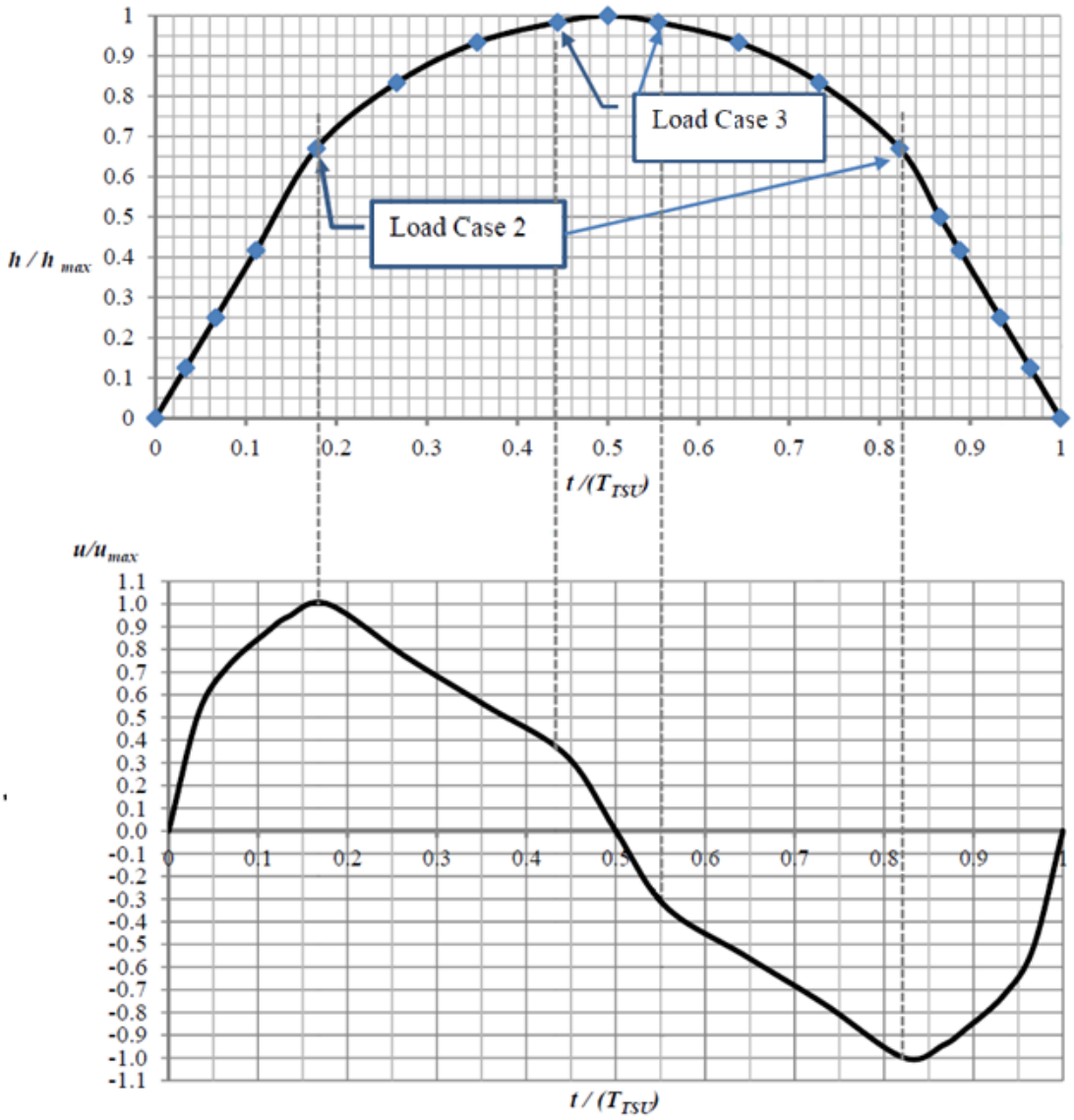

Figure 3-10: Load Cases 2 and 3 (Obtained from ASCE 7-16 Drafts)

The vertical axis in Figure 3-10 above represents either the flow depth (h) normalized by the maximum flow depth (h_{max}) at the structure's location or the flow velocity (u) normalized by the maximum flow velocity (u_{max}) at the structure's location. The horizontal axis in Figure 3-10 above both represent the time (t) normalized by the tsunami's period (T_{TSU}).

In addition to these load cases, the ASCE 7-16 draft also supplies a set of two load combinations:

Load Combination 1: $0.9D + F_{TSU} + 1.2H$

Load Combination 2: $1.2D + F_{TSU} + 0.5L + 0.2S + 1.2H$

where: D = dead load

F_{TSU} = tsunami load or effect

L = live load

S = snow load

H = load due to lateral earth pressure or ground water pressure

These load combinations are different from those provided by the FEMA P646 recommendations. Unlike the FEMA P646 recommendations the ASCE 7-16 draft also includes a consideration for snow loads and lateral earth pressures. During the case studies in Chapter 5 these load combinations and cases will not be applied. They are supplied here for completeness.

Chapter 4 Extensions of Methodologies to Bridges

The three design codes and recommendations that were introduced in Chapter 3 were specifically developed to apply to building structures. Tsunami guidelines for buildings and bridges, though similar, will vary from one another due to the differences between the two structure types. This chapter discusses how the calculation of forces on a bridge superstructure might differ substantially from that for a building.

Differences between bridges and buildings would affect the application of the tsunami force equations (Table 3-1). Three key differences would be the elevation of the base of the structure (Section 4.1), the structural geometry (Section 4.2) and the likelihood of channeling (Section 4.3).

4.1 Elevated Superstructures

Buildings are, typically, in contact with the ground across their entire foundation, whereas bridge superstructures are elevated over most of their length, and typically, they are only in contact with the ground at the ends of the bridge. For this reason, bridge superstructures can be subjected to large hydrodynamic uplift forces due to differing velocities above and below the superstructure. This effect is not considered in any of the building-focused documents, because they assume that no water flows below the building.

In addition, the definition of the water depth (h and h_{max}) at the structure where the tsunami forces are being determined will differ between buildings and bridge superstructures. The fluid depth used for determining the hydrostatic, hydrodynamic, impulsive, and debris damming forces will need to be based on the elevation of the bridge superstructure instead of the reference ground elevation as it would for a building. Figure 4-1 shows the effect of the reference elevation on the hydrostatic pressure distribution, in which a wall is shown on the left while a bridge superstructure is shown on the right.

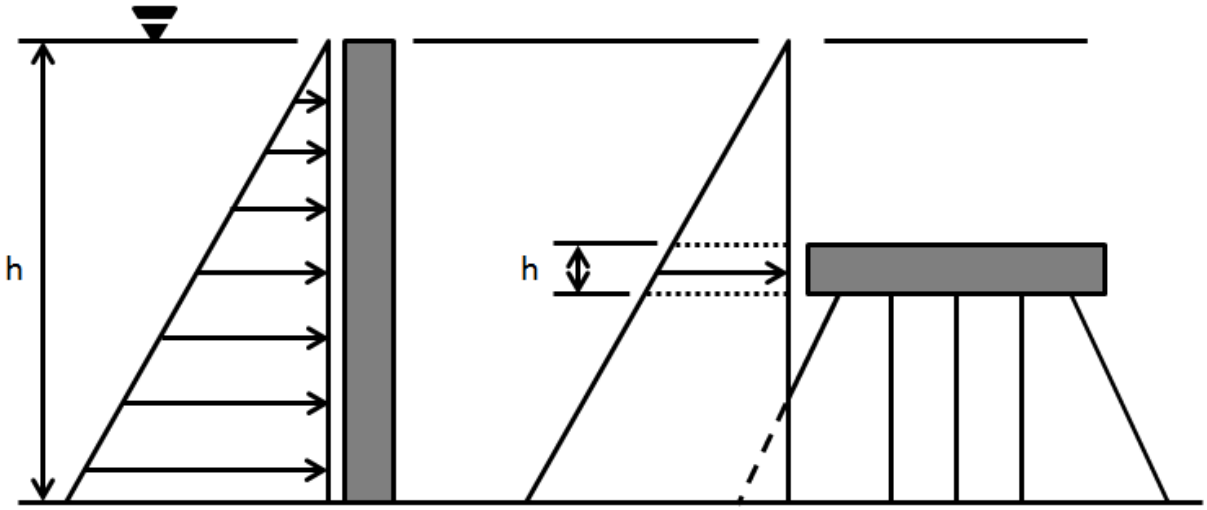

Figure 4-1: Effect of Structural Orientation on Hydrostatic Force

Additionally, when determining the momentum flux for bridge superstructures, the water height will also depend on how deep the bridge is submerged. While for a building the entire water column's momentum flux will attempt to move "through" the building area perpendicular to the flow (building not completely submerged), a bridge superstructure will only experience the momentum flux over its depth perpendicular to the flow. The vast majority of the momentum flux in the area under the bridge superstructure does not contribute to the hydrodynamic force. Figure 4-2 shows the effect of the height difference between the two structure types in the calculation of hydrodynamic tsunami forces. This figure also shows how large the skin friction component of the drag can be with most of the bridge superstructure surface area being parallel to the flow direction. Because most of the superstructure's area is parallel to the flow direction viscous forces (skin friction) will have a large effect on the drag, while only a small portion of the superstructure's area is perpendicular to the flow representing the inertial forces (form drag) of the drag. Again the contributions from each of these drag components is dependent on the flow type (laminar, transitional, or turbulent) determined by the Reynolds number.

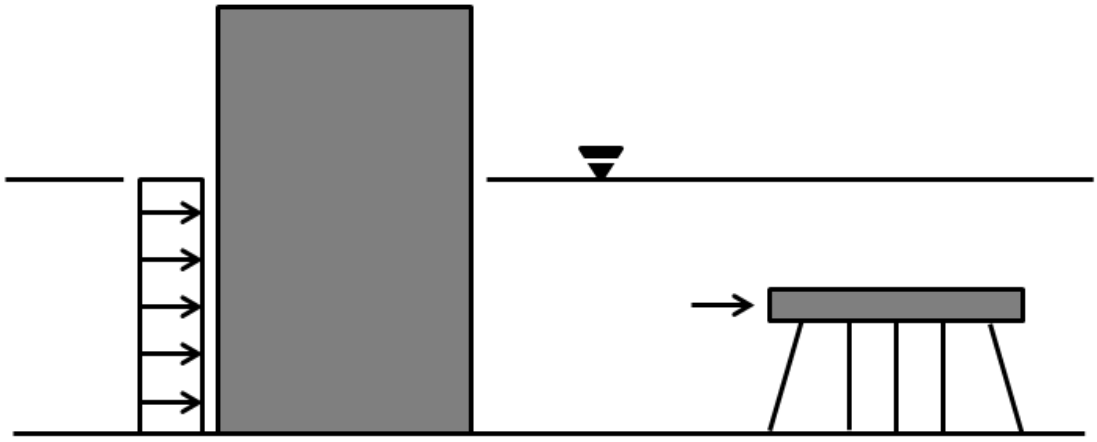

Figure 4-2: Effect of Structure Orientation on Force Equations

These differing reference elevations will also affect the estimated flow parameters, flow velocity and maximum momentum flux, from the FEMA P646 recommendations. These estimation equations were introduced in Subsections 3.4.2 to 3.4.3 and depend on the location of the structure (h_s), the design runup elevation (R), and or the reference ground elevation (z) at the base of the structure. Because a bridge superstructure is raised above the ground, the elevation at its base will not be equal to that of the ground elevation at the location of the structure and therefore the FEMA P646 recommendations will underestimate both the flow velocity and the maximum momentum flux. Figure 4-3 shows that when using the definition of z provided by the FEMA P646 recommendations the equation assumes the bridge will be further inland than it is due to the ratio of elevations used in Equation 3-6 and Figure 3-6.

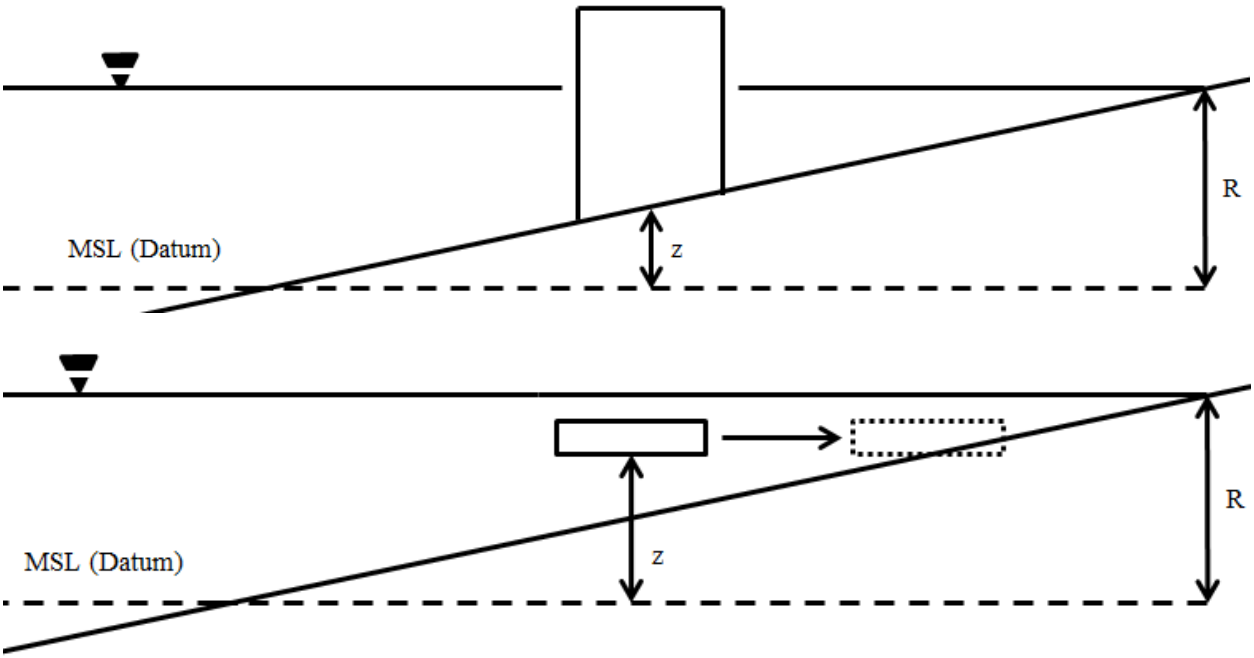

Figure 4-3: Effect of Structural Orientation on the FEMA P646 Recommendations Estimates of Flow Parameters

Therefore the ground elevation at the structure's location, not at the base of the structure, will be used when estimating the flow parameters with the FEMA P646 recommendations for the bridge superstructures in the case studies in Chapter 5. Unlike the FEMA P646 method for obtaining flow parameters the ASCE 7-16 draft method, the EGL method, is not based on the structure's ground elevation but the design runup elevation and inundation limit and therefore the determined flow parameters will not be affected as they were above for the FEMA P646 recommendations.

4.2 Differences in Geometry

The geometric differences between the two structure types will also influence how the tsunami force equations introduced in Table 3-1 should be applied. The largest effect is to the uplift equations introduced by the ASCE 7-16 draft. For example, one of the uplift equations was formulated based on an experiment with a slab connected to a wall, and it was based on the horizontal flow velocity. Using the horizontal flow velocity for determining the uplift force for a bridge superstructure would be unnecessarily conservative due to the water's ability to flow freely underneath it, assuming no significant debris damming or other obstructions. Therefore with no obstructions blocking flow under a bridge superstructure the minimum uplift force of 20 psf or the uplift force based on the grade at the site (if greater than 10 degrees) introduced by

ASCE 7-16 draft should be used. On the other hand the FEMA P646 recommendations use the vertical component of the flow velocity and are therefore applicable to bridge superstructures.

Certain bridge superstructure geometric types can allow for a scenario that is similar to the case of a wall redirecting horizontal flow velocity into an overlaying slab. For example, if protruding sidewalks are present on the bridge superstructure, they may block flow that would be otherwise be redirected around the face of the bridge perpendicular to the flow. This blocking will increase the uplift force that the bridge will experience due to the increased pressure under the protruding sidewalks from the redirected fluid flow. Additionally, guard rails could significantly increase the cross sectional area of the bridge perpendicular to the flow and could therefore increase the hydrodynamic forces. This effect might be reduced by the appropriate selection of geometry for a bridge superstructure, which could greatly decrease the fluid-induced forces on a bridge.

4.3 Local Channeling

The local topography and bathymetry near any structure will affect the local flow parameters for that structure. This effect is recognized in draft ASCE 7-16 proposal, which requires site-specific analyses in situations where the "onland flow fields are expected to vary significantly in the direction parallel to the shoreline due to longshore variability of topography."

Buildings and bridges can experience channeling due to surrounding structures and topography/bathymetry, however bridges typically span over natural channels (rivers) and therefore can experience concentrated channeling effects. From observations and corresponding numerical simulations done by Murakami et al. (2012), simulating bridge damage from the Tōhoku Tsunami (2011), they found an approximate increase in a tsunami wave height from 2.2 m to 5.5 m as it moved through the gradually narrowing mouth of a channel. Channeling effects can be important for bridges, and should be considered when determining the local tsunami flow parameters.

Chapter 5 Research Recommendations

A number of research methodologies have been developed to predict tsunami and wave (storm surge) forces. The Honolulu Building Code and the FEMA P646 recommendations refer to a book by Dames & Moore (1980), which details the design and construction standards for residential construction in tsunami-prone areas in Hawaii. Similarly, the tsunami force equations presented in the FEMA P646 document were influenced by the work done by Yeh et al. (2005), which explored the development of design guidelines for vertical tsunami evacuation structures.

Douglass et al. (2006) investigated the susceptibility of highway bridges to wave action brought on by large storm surges. Additionally, Yeh (2007) investigated the applicability of the tsunami force equations developed at that time. Building on the work done by Douglass and Yeh, FEMA introduced the P646 recommendations for the design of vertical evacuation structures.

Yim et al. (2011) extended the work done by these three previous documents from equations designed for buildings and waves to tsunami equations designed specifically for bridge superstructures. Yim investigated the susceptibility of bridges around the Siletz Bay area in Oregon. In their study, numerical models of four bridges were constructed to estimate tsunami forces for a variety of Cascadia Fault rupture scenarios. These results were then compared to the forces determined from tsunami force equations proposed by a number of other documents. Based on their results, they recommended an approach for determining tsunami forces on deck-girder bridge superstructures.

The following sections will discuss the wave force recommendations by Douglass et al. (2006), and the tsunami force recommendations developed by Yeh (2007) and Yim et al. (2011).

5.1 Douglass et al. (2006): "A Method for Estimating Wave Forces on Bridge Decks"

Douglas et al. (2006) provide guidance for determining specific bridge damage mechanisms during a large storm event and for determining how large these forces actually might be on a bridge deck. To this end a new method for estimating wave loads on a bridge decks was developed. Load factors and combinations were not provided; instead, it was recommended to use a factor of safety equal to 2. In addition it was assumed that the load is applied through the centroid of the bridge, which might not be accurate for wave-induced forces. As well, this approach is not based on differentiating between the drag and inertial forces and was designed to be applied for conditions where storm surge elevations are near the same height of the bridge superstructure. Section 5.4 will provide a brief discussion on the equations that are a part of this new method. To help explain some of the variables used, Figure 5-1 is provided:

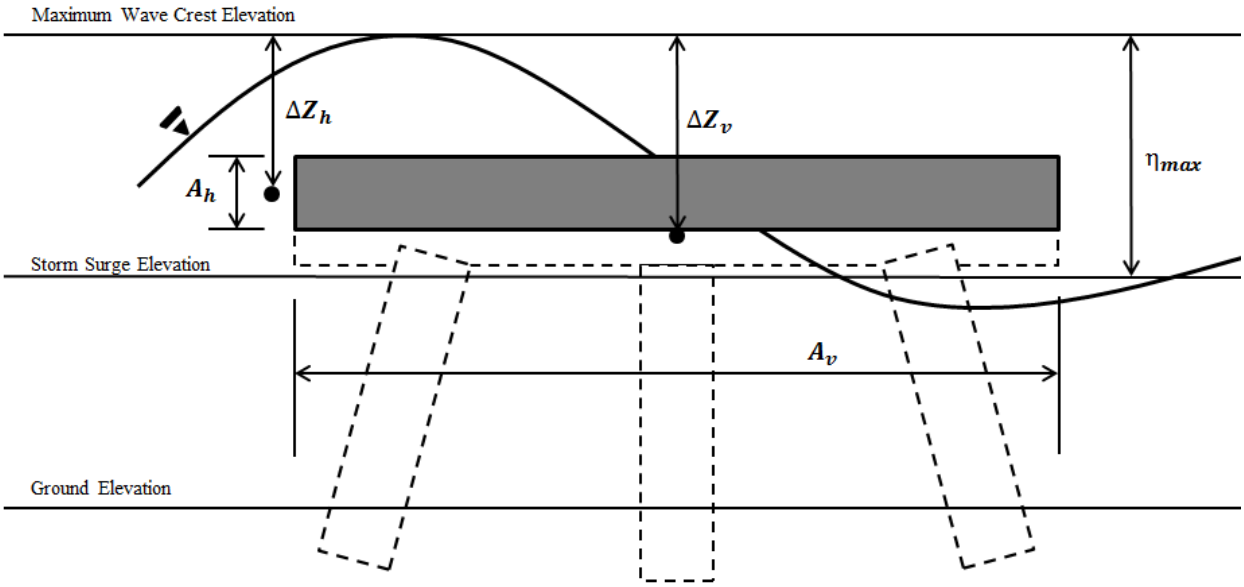

Figure 5-1: Variable used in the Recommended Fluid Force Equations (adapted from Douglass et al. (2006))

In Figure 5-1 the A_h and A_v terms represent the horizontal and vertical cross-sectional areas of the bridge superstructure, respectfully. The fluid depth terms, Z_h and Z_v, represent the fluid depth with respect to the centroid of the horizontal and underside of the bride deck cross-sectional areas. Finally the η_{max} term represents the highest estimated wave height from the average storm surge elevation. An estimation equation for the highest estimated wave height is provided by Douglass, but it is not repeated here, because it is unrelated to tsunamis.

5.2 Yeh (2007): "Design Tsunami Forces for Onshore Structures"

Yeh reviewed and evaluated the existing design codes and recommendations for structures threatened by tsunamis. Most of the previous codes and recommendations are based off of work done by Dames & Moore (1980). From this review a selection of the current tsunami force equations was made for determining forces on buildings located in onshore areas where tsunami inundation maps are available. It should be noted that the FEMA P646 recommendation referenced the work done by Yeh (i.e., the maximum momentum flux estimate (Equation 3-6) was initially introduced by Yeh). Yeh reviewed all of the forces described in Section 3.1 except the uplift force and made recommendations for the hydrodynamic, debris impact, and surge forces while introducing the hydrostatic and buoyancy equations without making any recommendations for them.

From the analysis of all of the available force equations for predicting tsunami loads, it was determined that there are no equations that adequately predict debris impact forces. For the impulse-momentum approach, like the approach used in the Honolulu Building Code, it was determined that there is a significant uncertainty in the determination of the impact duration of the debris (Δt). Additionally, it was determined that there are significant uncertainties in the determination of the Δx parameter that is used in the work-energy approach. Finally, the determination of effective stiffness in the Haehnel and Daly equation (used for debris impact in FEMA P646) is difficult, because it likely is a function of x and t during the impact. In regard to the flow velocity carrying the debris, Yeh recommended the use of Figure 3-6 that was introduced in the FEMA P646 recommendations. The ASCE 7-16 draft uses multiple methods for determining debris impact forces for varying debris types, these methods are also influenced by determining the above debris and impact characteristics.

The same hydrodynamic force that was used in the FEMA P646 recommendations was also recommended by Yeh, where the momentum flux should be maximized. Yeh also recommended the use of Equation 3-6 in the determination of the maximum momentum flux in the absence of detailed computer model. In regards to the surge force Yeh mentioned that only bores moving over already inundated areas would cause noticeable inertia forces on the structure and that this surge force would be approximately 50% greater than the hydrodynamic force (identical to FEMA P646). The surge force introduced by the Honolulu Building Code are also stated to be hard to employ do to the difficulty in estimating the surge height, and is overly conservative if the runup elevation is used as the surge height.

Yeh did not introduce any new tsunami force prediction equations. Instead, he selected the above equations that should be employed when determining what forces a structure would experience during a tsunami event. Therefore, no new equations will be introduced for Yeh. It should be noted that the FEMA P646 was based, in part, on the work done by Yeh and is why a large majority of the equations selected by Yeh for estimating tsunami forces are also present in the FEMA P646 recommendations.

5.3 Yim et al. (2011): "Development of a Guideline for Estimating Tsunami Forces on Bridge Superstructures"

The purpose of the Yim et al. (2011) document was to develop a guideline for estimating tsunami induced forces on deck-girder bridge superstructures along the Oregon Coast. Four bridges were selected from the Siletz Bay area and numerically modeled to determine the tsunami forces caused by separate Cascadia Fault rupture scenarios. These numerical results were then compared to tsunami force equations from a selection of the documents to develop a simplified method for estimating tsunami forces on deck-girder bridge superstructures. Due to the limited data, load factors are not provided and further research will be needed to verify the

recommended values of coefficients. To apply the simplified method for determining tsunami forces on bridge superstructures, the maximum tsunami runup elevation and corresponding inundation depth, tsunami flow velocity, and the maximum momentum flux need to be known at the structure. Figure 5-2 is provided for additional guidance in determining variables.

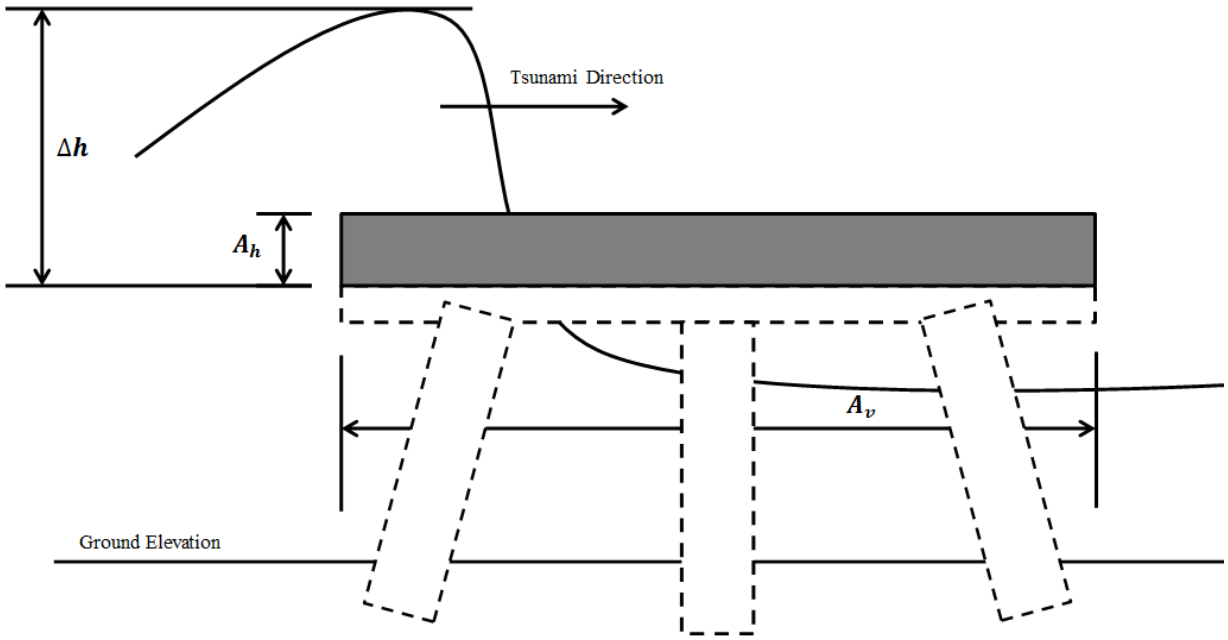

Figure 5-2: Variable used in the Recommended Fluid Force Equations (adapted from Yim et al. (2011))

The area terms are identical to the ones described in Figure 5-1, but the fluid depth term is not identical and is instead defined as the depth from the bottom of the deck to the maximum tsunami depth. The fluid-induced force equations provided by this document, along with those introduced by Douglass, will be introduced in the following section.

5.4 Research Force Equations

Table 5-1 contains the fluid induced force equations for the Douglass et al. (2006) and Yim et al. (2011) research documents.

Table 5-1: Fluid-Induced Force Equations

Force	Douglass et al. (2006)		Yim et al. (2011)	
Hydrostatic	$F_h = [1 + c_r(N-1)]c_{h-va}F_h^*$	$F_h^* = \rho g(\Delta z_h)A_h$	$F_h = \big(1 + C_r(N-1)\big)C_h F_h^*$	$F_h^* = \rho_s g(\Delta h_{max})A_h$
Buoyancy	N/A**		N/A**	
Hydrodynamic	N/A*		$F_d = \frac{1}{2} C_d \rho_s b(\Delta h u^2)_{max}$	
Uplift	$F_u = c_{v-va}F_v^*$	$F_v^* = \rho g(\Delta z_v)A_v$	$F_u = \big[\rho_s g(\Delta h_{max}) + 0.5\rho_s u_{x,max}^2\big]A_v$	
Impulsive/Surge	$F_h = \{[1 + c_r(N-1)]c_{h-va} + c_{h-im}\}F_h^*$	$F_u = \{c_{v-va} + c_{v-im}\}F_v^*$	N/A*	
Debris Impact	N/A*		N/A*	
Debris Damming	N/A*		N/A*	
Additional Forces	N/A*		N/A*	

* Force equation not provided by code
** Buoyancy is included in uplift equation

Table 5-2: Research Equations Nomenclature

Symbol	Dimension	Definition
A_h	L^2	Cross-sectional area perpendicular to flow
A_v	L^2	Cross-sectional area parallel to flow
b	L	Breadth of structural component
C_d	--	Drag coefficient
C_h	--	Horizontal "varying" load coefficient
c_{h-im}	--	Horizontal "impact" load coefficient (recommended as 6.0)
c_{h-va}	--	Horizontal "varying" load coefficient (recommended as 1.0)
C_r	--	Internal girder pressure reduction coefficient (recommended as 0.4)
c_{v-im}	--	Vertical "impact" load coefficient (recommended as 3.0)
c_{v-va}	--	Vertical "varying" load coefficient (recommended as 1.0)
F_d	MLT^{-2}	Hydrodynamic force
F_h	MLT^{-2}	Hydrostatic force
F_h^*	MLT^{-2}	Reference hydrostatic force
F_u	MLT^{-2}	Uplift force
F_v^*	MLT^{-2}	Reference uplift force
g	LT^{-2}	Gravitational constant
Δh_{max}	L	Maximum depth from bottom of deck to tsunami height
$(\Delta hu^2)_{max}$	L^3T^{-2}	Maximum momentum flux
N	--	Number of girders supporting the bridge deck
u	LT^{-1}	Horizontal fluid velocity
u_x	LT^{-1}	Adjusted horizontal fluid velocity
Δz_h	L	Difference between the elevation of the crest of the maximum wave and the elevation of the centroid of A_h
Δz_v	L	Difference between the elevation of the crest of the maximum wave and the elevation of the underside of the bridge deck
ρ	ML^{-3}	Fluid density
ρ_s	ML^{-3}	Fluid density with sediment

Both the Douglass and the Yim documents formulated their equations for a deck-girder type bridge with "N" girders. This bridge geometry type differs from that of slab and or box section bridges due to the influence of trapped air between the girders that can be compressed and increase the forces experienced by the bridge superstructure (Douglass et al., 2006). The largest difference in force estimation between these two documents is due to the fact that the Douglass document's equations are formulated based on storm-surge-induced wave impacts, whereas the Yim document's equations are based on tsunami induced forces. With the period of storm surge wave impacts being much smaller than that of a tsunami, Douglass introduced multiple "varying" load coefficients (see Table 5-2) which need to be modified for a conservative design. Finally both of these documents would likely be very conservative if the structure becomes completely submerged due to the selection of their respective depth terms.

From the previously mentioned three research advances in adapting fluid loading to bridge superstructures, the Douglass document applies to wave induced loading while Yim applies to tsunami loading. The wave induced force equations introduced by Douglass do not consider the flow velocity or hydrodynamic forces. Again, the equations provided by this document were in

regard to a storm surge near the elevation of the bridge deck so that the waves accompanying the surge would just impact the deck. Therefore not considering the flow velocity or hydrodynamic forces is an adequate assumption. These assumptions are not adequate for determining the fluid induced forces on a bridge superstructure due to a tsunami. During a tsunami the water line rises very quickly and can completely submerge a bridge superstructure. With the flow velocities being much larger than that of a storm surge and the possibility of complete submergence, both the flow velocities and hydrodynamic forces need to be considered.

With the consideration of tsunami induced forces on bridge superstructures, Yim does take into account the flow velocity and hydrodynamic forces. The inclusion of the flow velocities and hydrodynamic forces is what separates wave induced forces from tsunami induced forces. Additionally, Yim takes the hydrodynamic force calculation further by determining a time dependent drag coefficient from a numerical model of one of the bridges that was studied, as seen in Figure 5-3.

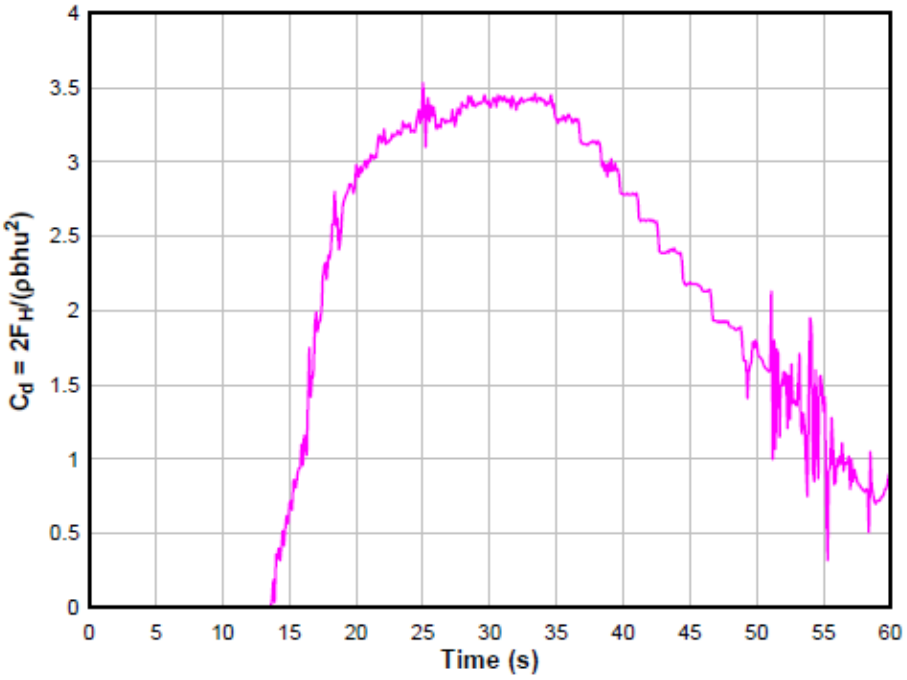

Figure 5-3: Empirical Drag Coefficient for Spencer Creek bridge (obtained from Yim et al. 2011)

It should be noted that a maximum drag coefficient of 3.5, based off of the horizontal forces experienced by the bridge, was determined. Recall that a drag coefficient of this magnitude is larger than any of the drag coefficients supplied in the three previous codes and recommendations. Additionally, this may not lead to an under prediction of the drag force determined from these codes and recommendations due to their inherent conservatism but is worth taking note of. Table 5-2 lists the nomenclature from the research documents.

Chapter 6 Case Studies

The forces that were discussed in chapters 4 and 5 are influenced by the types of bridge geometries, construction methods and material types used in practice. Different cross section geometries will lead to different amounts of displaced water and surface areas influencing the magnitude of fluid and or debris induced forces on the bridge. For example:

- It has been shown that guard rail systems can increase both the horizontal and vertical tsunami forces by up to 20% and 15%, respectfully (Yim et al 2011). Box section geometries can lead to larger buoyancy effects due to the larger volumes of water they can displace and their relatively low weight-to-volume ratio. Box sections also have larger surface areas when compared to deck-girder bridges, further increasing the hydrodynamic forces.
- Research has shown that deck-girder bridges typically experience lower forces than box sections by displacing less water and dissipating vertical fluid forces when air trapped between the girders is compressed (Boon-intra, 2010).
- Compared to a concrete bridge, a steel bridge is lighter and therefore, provides less weight to resist uplift forces. On the other hand, the steel bridge displaces less water, so it would have lower buoyancy forces to resist.

6.1 Description of Selected Bridges

In Chapter 2 it was determined that the most common bridge material type and geometries in the nominal inundation zone for the five considered states was reinforced concrete and deck-girder/slab type bridges, respectively. Based on these findings, two bridges were selected from the nominal inundation zones, one in Washington (Wreck Creek Bridge) and one in Oregon (Schooner Creek Bridge). For the purposes of this case study both bridge superstructures will be examined at the Wreck Creek location at the same deck elevation (216 inches above mean sea level).

Three methods for determining the design flow parameters will be examined with a set of design parameters being selected from one of the three methods. These three methods are:

- Output from a numerical model obtained from post-doctoral work done by Grady Lemoine through the use of the open source program OpenFOAM® (denoted from this point forward as the “OpenFOAM” model).
- Inundation map for the Wreck Creek location (Walsh et al. 2000).

- Analytical solutions and assumptions supplied by the codes and recommendations for determining flow parameters.

The calculation of the forces for the Wreck Creek Bridge case study was conducted using Matlab™ based on the codes and recommendations above, the given geometries for the bridge superstructure, and the selected design tsunami flow parameters. The determined design forces from the codes and recommendations were also applied to an Abaqus™ model for the Wreck Creek Bridge case study, and reaction forces were determined for critical areas. For the Wreck Creek Bridge case study the hydrodynamic, buoyancy, uplift and surge forces will be determined based on both the design codes and recommendations and the current research advances.

Appendix B contains sample calculations pertaining to the determination of the design tsunami forces and flow parameters for the Wreck Creek Bridge.

Specific forces for the Schooner Creek Bridge will not be determined. Instead, only significant differences between the two bridges will be discussed in Section 6.3.

6.1.1 **Wreck Creek Bridge**

In Washington State, a reinforced concrete slab bridge designated as the Wreck Creek Bridge was selected; the location of the bridge along with an elevation view can be seen in Figures 6-1 and 6-2 obtained from Google Earth™ and the Washington State Department of transportation (WSDOT), respectively.

Figure 6-1: Wreck Creek Bridge: 47° 17’ 4.54”N, 124° 14’ 1.51”W (Google Earth™)

Figure 6-2: Wreck Creek Bridge (WSDOT, 2003)

Wreck Creek Bridge is located along the coast of the Pacific Ocean in Washington State and supports a two-lane highway, State Route 109. The bridge was constructed in 1957, and the superstructure consists of three slabs making up 4 spans, the largest spanning 11.6 m (38 feet). Each span is supported either by abutments or bents supported by multiple wood piles.

The design of this bridge is similar to those of some other bridges in the Washington State coastal areas. The key dimensions of the bridge are as follows:

- Deck width of 9.1 m (30 feet)
- Total length of 41.8 m (137 feet)
- Slab depth of 35.6 cm (14 inches)
- Deck elevation of 5.5 m (216 inches), measured from mean sea level (MSL) to the top of the road surface

The Wreck Creek Bridge sustained minor damage in the 1964 Alaskan earthquake and subsequent tsunami (Walsh et al. 2000). A similar reinforced concrete slab bridge (Joe Creek Bridge) near the Wreck Creek Bridge along State Route 109 sustained critical damage. The damage to the Joe Creek Bridge is shown in Figure 6-3.

Figure 6-3: Joe Creek Bridge Damage from 1964 Alaskan Earthquake and Subsequent Tsunami (reprinted from TsuInfo Alert, [February, 2014])

Since the Wreck Creek Bridge is a slab bridge, and assuming that it would be inundated quickly, hydrostatic forces will not be considered for this bridge (except for the initial bore impact).

6.1.2 **Schooner Creek Bridge**

A deck-girder bridge in Oregon, designated as the Schooner Creek Bridge, was also selected and can be seen in figures 6-4 and 6-5 obtained from Google Earth™.

Figure 6-4: Siletz Bay and Schooner Creek Bridge: 44° 55’ 32.55”N, 124° 0’49.87”W (Google Earth™)

Figure 6-5: Schooner Creek Bridge 44° 55' 32.55" N, 124° 0' 49.87" W (Google Earth°)

The Schooner Creek Bridge, in the Siletz bay area in Oregon, supports Highway 101 along the Pacific coast. The bridge was constructed in 1945 and is made up of three deck-girder sections supported by 4 girders each, with the largest spanning 70 feet. Each span is supported either by abutments or capbeams supported by multiple reinforced concrete piers with varying levels of fixity. The key dimensions of the bridge are as follows:

- Deck width of 10.4 m (34 feet)
- Total length of 57 m (186.7 feet)
- Slab depth of 17.8 cm (7 inches)
- Deck elevation at mid-span equal to 10.6 m (417.25 inches), measured from MSL to the top of the road surface

6.2 Flow Parameters

This section compares the flow parameters determined from the numerical model, an inundation map, and the provided equations from the three design documents (Sections 3.4 to 3.6). The numerical model did not attempt to model the actual flow characteristics for the case-study bridges. Instead the nominal flow parameters are used to serve as input to the various design methodologies. These design flow parameters (Subsection 6.2.6) will be used to determine the fluid induced forces on the Wreck Creek Bridge in Section 6.3.

6.2.1 **Numerical Model Description**

The output from the OpenFOAM model was used to determine a set of tsunami depths and velocities. The model was not specifically based on the Wreck Creek geographical area or any Cascadia Fault rupture scenarios. The model simulated the tsunami wave basin at the Oregon State University in Corvallis, and was used to obtain nominal flow parameters for a tsunami bore. This strategy allowed for the selection of flow parameters from any location in the tsunami's path allowing for the full submergence of each of the bridge superstructures. Figure 6-6 provides a sketch of the model domain.

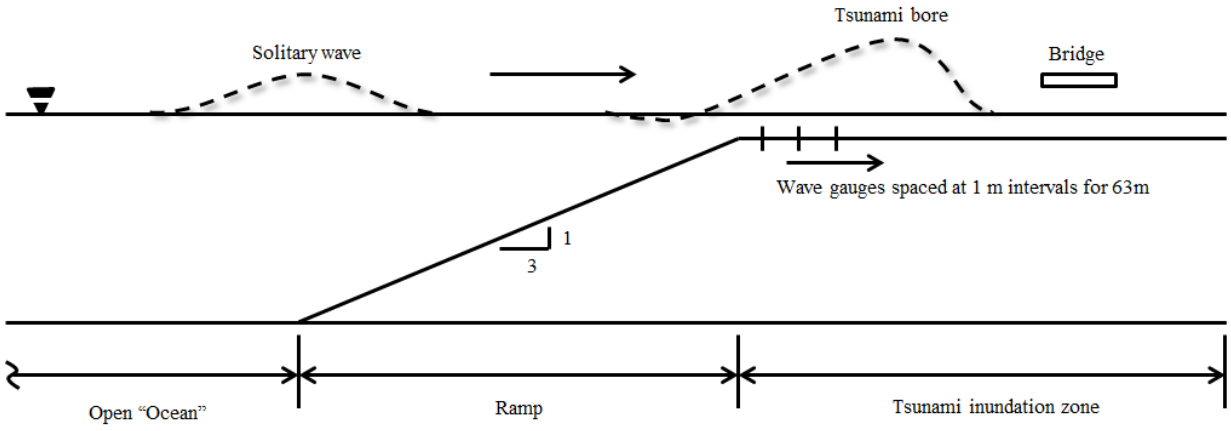

Figure 6-6: Schematic of the OpenFOAM™ Model

Initially a solitary wave is formed in the far left portion of the model domain, and when the ramp begins to influence the wave (representing "near" shore bathymetry), a bore is formed in the tsunami inundation zone portion of the model domain. Along this inundation zone portion of the numerical model, there are wave gauges spaced at 1m intervals for 63m that recorded the flow parameters over time. Each wave gauge location records the flow parameters at the center of the cells vertically from its position (i.e., each wave gauge location stores data from a vertical cross-sectional cut through the domain).

In the model, the centroid of the bridge superstructure was positioned at a wave gauge (recorder) located 40 meters from the top of the ramp (wave gauge 40). This location was selected to best represent a tsunami bore. The flow parameters from the model were scaled up by a scale factor to represent a tsunami bore at full scale. This scale factor was determined by dividing the top of the bridge deck elevation (5.5 m, 216 in. above mean sea level) by that of the model bridge deck elevation (0.99 m, 39 in. above the elevation at the top of the ramp).

6.2.2 Inundation Elevation at Structure

The inundation elevation is a key parameter in the determination of the forces induced by a tsunami. Figure 6-7 shows:

- The time history of scaled inundation elevations at the structure during the entire model duration at the centroid of the model superstructure. The maximum value for this history corresponded to a scaled up inundation elevation of 6.3 m for the prototype.
- The same time history of inundation, with an additional 30% increase required by the FEMA P646 recommendations (assuming the inundation elevation is equal to the runup elevation).

- The EGL methods inundation elevation at the structure's location (assuming again that the inundation elevation was equal to the runup elevation) (Section B.3), assuming Manning's Roughness Coefficient of 0.03, and assuming that the beach slope could be determined from Google Earth™.

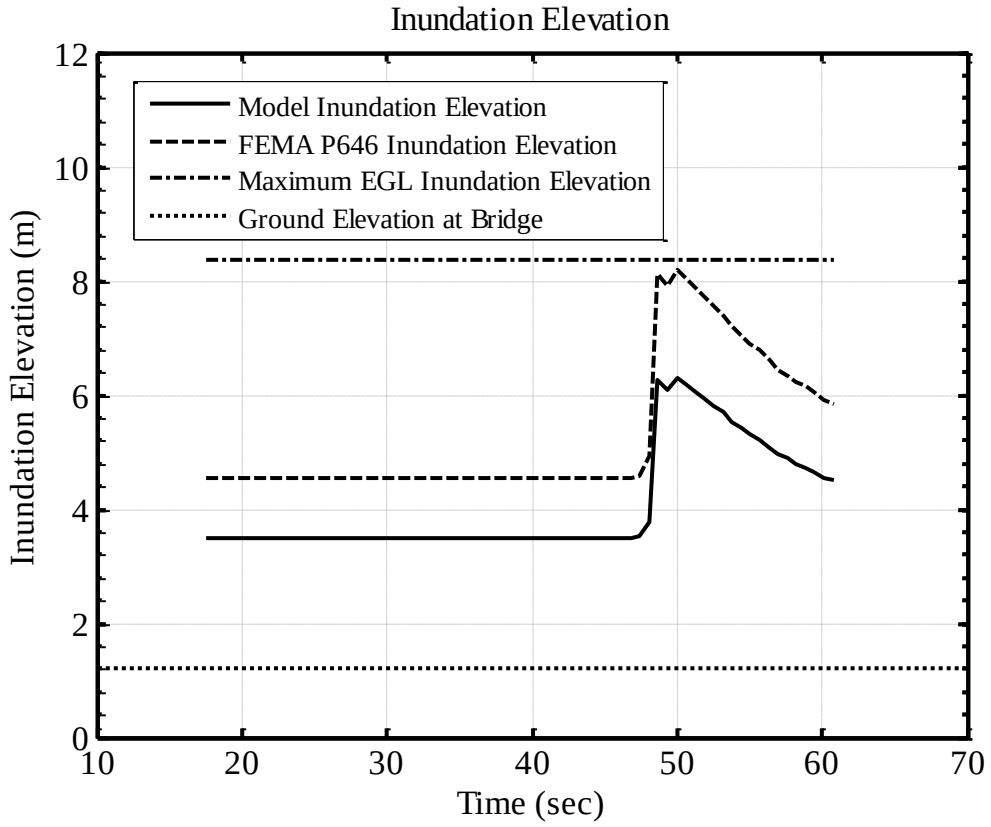

Figure 6-7: Inundation Elevation Time History at the Structure's Location

The maximum inundation elevation at the structure's location estimated with the EGL method is a single value (8.4 m) at the structure's location. By combining this maximum value with the normalized curve in Figure 3-10, the draft ASCE 7-16 proposal does allow the estimation of an inundation time history. However, for Washington State, the predominant tsunami period (T_{su}) ranges from 30 to 40 minutes. In contrast, for both the numerical model and FEMA P646 (based on numerical model output), the length of the solitary wave is much shorter, because the numerical model was developed to simulate an experiment in a tsunami wave flume.

The peaks of the inundation elevations for both the numerical model and the FEMA P646 estimates are not smooth due to the air entrainment of the bore and the time steps not being small enough to capture enough data points in that region. When designing for tsunami forces, preferably the maximum inundation elevation at the site would be obtained from either an inundation map or a detailed numerical model.

Alternately, a time history of inundation elevation from an inundation map for the Wreck Creek area for two Cascadia Subduction zone events are shown in Figure 6-8. It should be noted that these time history of inundation elevations was made for the use of emergency management and not site-specific planning.

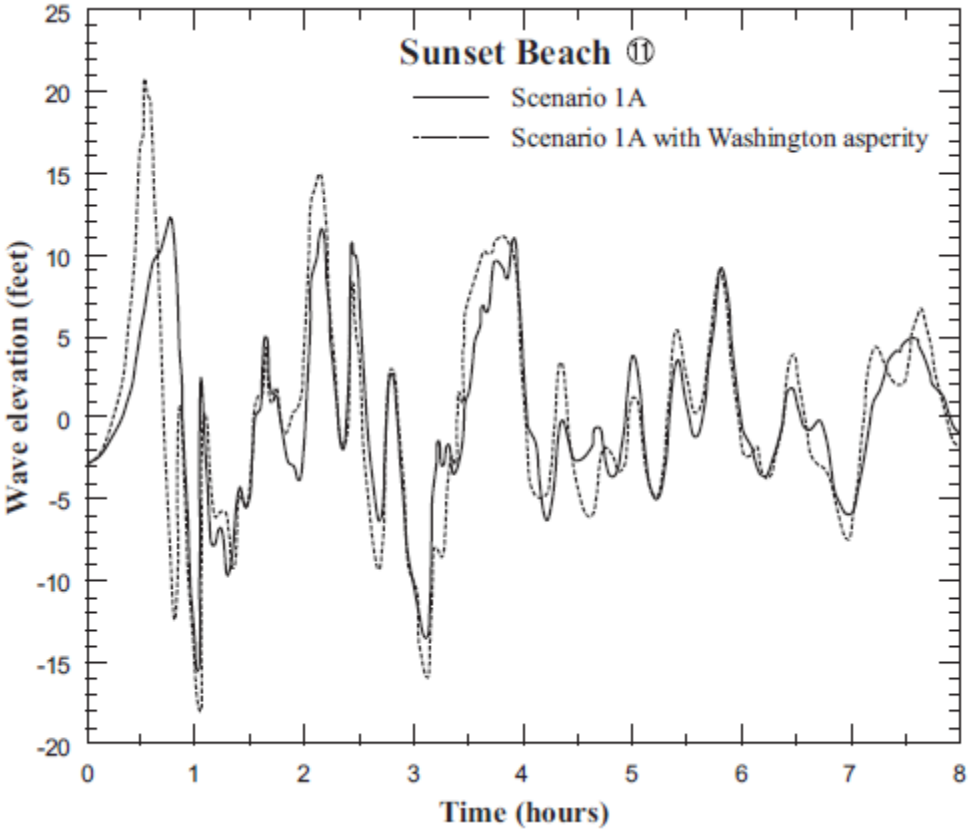

Figure 6-8: Wave Elevation at Wreck Creek Location (Walsh et al. 2000)

The maximum inundation elevation from the inundation history (Fig. 6-8) is 6.4 m (21 ft), which is similar to the maximum inundation elevation obtained from the numerical model, which was 6.3 m. This similarity suggests that the inundation elevation in the numerical model is similar (when scaled up) to that which a designer might consider for the Wreck Creek Bridge.

For the following case studies the maximum inundation elevation determined by the numerical model method will be used as the maximum design inundation elevation at the structure's location and the maximum runup elevation.

6.2.3 **Horizontal Flow Velocity**

The flow velocities for a maximum inundation elevation of 6.3 m were determined using several methods. For the model bore with a maximum inundation elevation of 6.3 m, both the maximum vertical and horizontal flow velocities at the centroid of the bridge cross-sectional were obtained from the numerical model. In practice, these values at the site could also be obtained by the designer through the use of provided equations in the codes and recommendations.

Figure 6-9 shows the time history of the horizontal flow velocity obtained from the numerical model in addition to the three methods introduced in Sections 3.3 to 3.5 for estimating the horizontal velocity from the three considered documents (Honolulu Code, FEMA P646, and ASCE 7-16 draft). The Honolulu Building Code's horizontal flow velocity estimates are based on the design inundation depth from the numerical model (flow velocity is equal to inundation depth at structure). In contrast, the estimated horizontal flow velocity estimated with FEMA P646 is based on Figure 3-6 from Subsection 3.4.2, and the required 30% increase in runup elevation and the runup elevation from the numerical model (refer to Appendix B Section B.3 for sample calculations).

Finally, the ASCE 7-16 draft supplies the EGL method, which also estimates the flow velocity at the structure's location from the Froude number based on the determined inundation depth at the structure. It should also be noted that the EGL method and the Honolulu Code assume a uniform distribution of flow velocity over the depth of the flow and that the EGL method estimates a single flow velocity at the structure's location and is therefore depicted as a straight line in Figure 6-9.

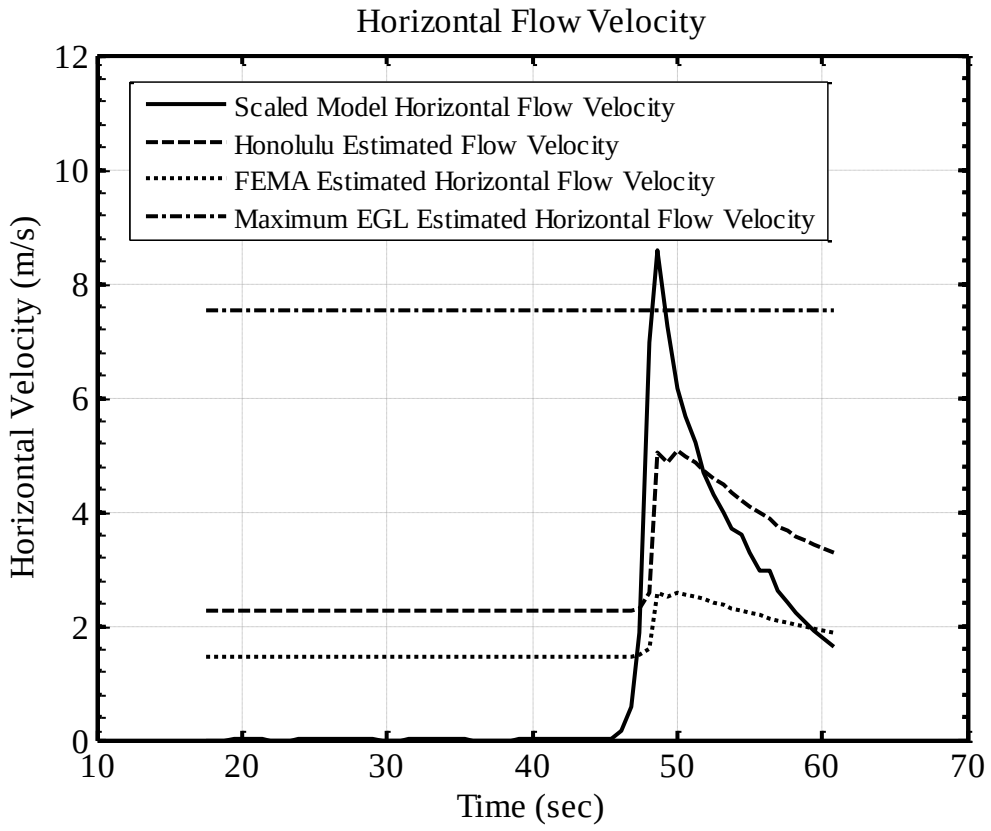

Figure 6-9: Horizontal Flow Velocity at the Centroid of the Bridge Cross-Section

Figure 6-9 lead to the following conclusions:

- For a maximum inundation elevation of 6.3 m, the numerical model estimated the largest horizontal flow velocity (8.6 m/s).
- The maximum estimate form the Honolulu Building Code equation is 41% less than that of the numerical model.
- Despite the fact that the FEMA P46 estimates include a runup factor of 1.3, the FEMA estimates are 70% less than the numerical results.
- The maximum estimate from ASCE 7-16 draft methodology is only 13% less than the numerical model estimates. It is surprising that the velocity estimates would be so close, since the numerical model considered a wave flume, not a long-period tsunami.

FEMA P646's horizontal flow estimate is based on the structure's location in terms of the ground elevation for a given local inundation depth. Employing Figure 3-6 leads to the use of the limit curve due to the value of η being greater than 0.12. From this limit curve one can see that the velocity is limited to the range of 0 m/s when the maximum runup elevation is reached to 4.1

m/s on the shoreline for the bridges elevation (see Appendix B). This range of horizontal flow velocities is quite small, and leads to the conclusion that the calculation of η may be inaccurate for bridge superstructures.

The FEMA P646 recommendation also estimates the horizontal flow velocity based on a uniformly sloping beach, with no lateral change in topography and no friction, whereas in the numerical model the local ground elevation is constant, with the wave moving over already inundated land. As a result, the two situations are different and result in different velocity estimates. In fact, if Figure 3-6 is employed for the bridge being at the shoreline and close to the ground a velocity of approximately 11.1 m/s is obtained. This shows that the elevations and distances from the shoreline greatly affect the flow velocity and that because the model has a constant slope in the inundation zone these affects are not accounted for. Even though, the use of the model is purely for a demonstration of one of the methods available to determine flow parameters.

The estimation of the horizontal flow velocity at the structure by the EGL method is closer to what was estimated by the numerical model. Again this method, like FEMA P646, also takes into account the topography of the area. The EGL method estimates a horizontal flow velocity that is similar to the numerical model due to the grade being small at the site. Additionally, the EGL method takes into account the surface roughness of the ground over the inundation area through the use of the Manning's coefficient. This is important because during the inundation in the numerical model the bore moved over already inundated land and therefore was not affected as much by the roughness of the surface it was traveling over.

Table 6-1 shows the estimated maximum horizontal flow velocities for the FEMA P646 recommendations, the Honolulu Building Code, the numerical model, and the ASCE 7-16 draft.

Table 6-1: Estimated Maximum Horizontal Flow Velocities

Source Obtained From	Estimated Maximum Horizontal Flow Velocity (m/s)
Numerical Model	8.6
Honolulu Building Code	5.1
FEMA P646	2.6
ASCE 7-16 Draft	7.5

It should be noted that in a real design situation, with a numerical model representative of the design location, the numerical model results are required by the FEMA P646 recommendations to not be less than 80% of the analytical results. A similar requirement is made by the ASCE 7-16 draft when using a numerical model during a site specific analysis (PTHA). The design flow velocity determined from a numerical model for urban environments may not be less than 100% of that determined from the EGL method, and the design flow velocity determined form a numerical model for other terrain may not be less than 80% of that determined from the EGL

method. For the purpose of this study the horizontal velocity determined from the numerical model will be used as the design horizontal velocity.

6.2.4 **Vertical Flow Velocity**

The vertical flow velocity from the numerical model at the bridge elevation along with the FEMA P646 estimate can be seen in Figure 6-10.

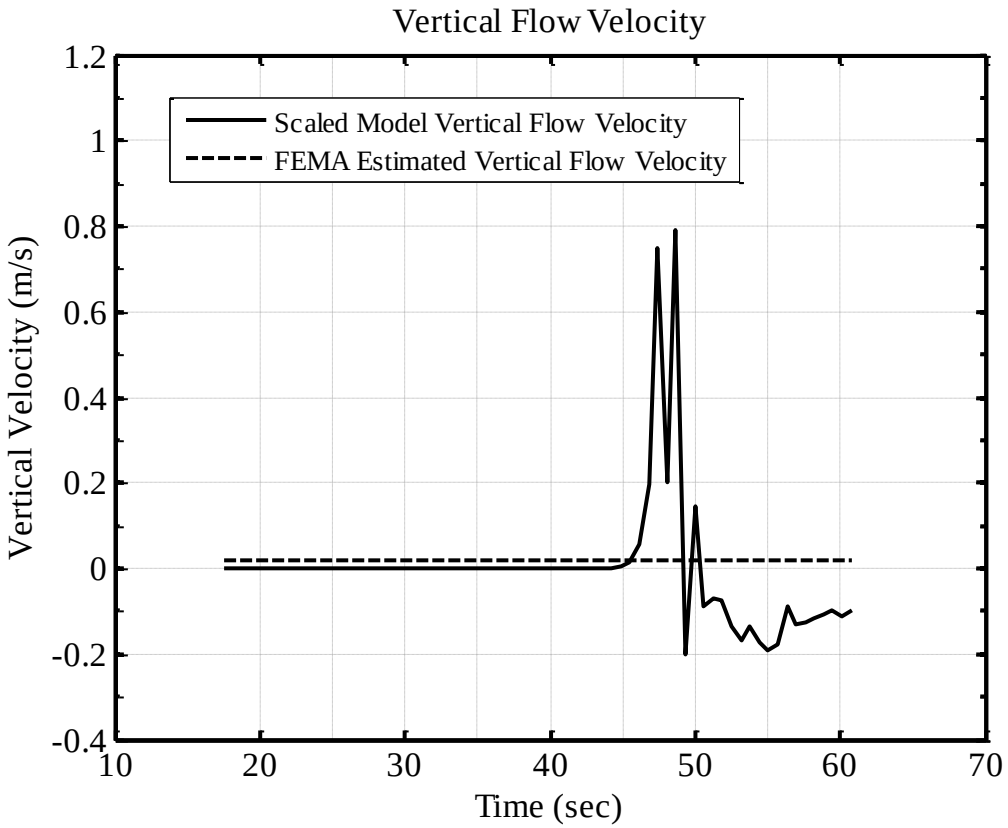

Figure 6-10: Vertical Flow Velocity at the Centroid of the Bridge Cross-Section

The vertical flow velocity determined from the numerical model at the bridge elevation is much smaller than the horizontal flow velocity determined from the numerical model, and does contain negative velocities. Again the estimate from the FEMA P646 recommendations is less than that of the model and can be attributed to what was discussed for the horizontal flow estimate above. A vertical flow velocity estimate from the ASCE 7-16 draft is not supplied due to the recommended uplift being the minimum value (957.6 Pa or 20 psf) due to the slope at the site being less than ten degrees. Therefore, the vertical flow velocity is not required for the uplift force equation provided by the ASCE 7-16 draft. Additionally, the Honolulu Code does not

supply a vertical flow velocity estimate due to none of its supplied force equations requiring a vertical flow velocity.

6.2.5 **Momentum Flux**

Another flow parameter that is needed is the momentum flux at the bridge location, with FEMA P646 requiring this value to be maximized. The maximum momentum flux determined from Equation 3-6 and the numerical model along with the regular momentum flux from the numerical model and the ASCE 7-16 draft can be seen in Figure 6-11

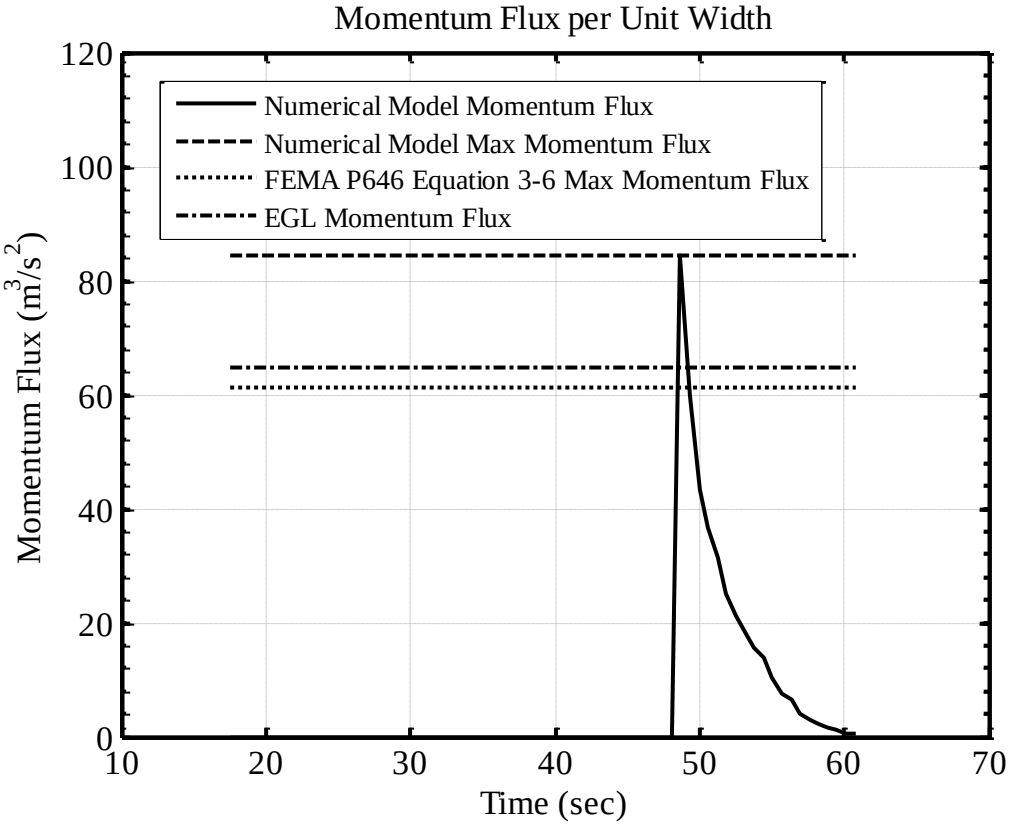

Figure 6-11: Momentum Flux per Unit Width

It should be noted that it is possible for the maximum water depth and velocity to not occur at the same time, as they do for the numerical model for this study. Both the FEMA P646 and ASCE 7-16 draft estimations for the momentum flux underestimate the momentum flux determined from the numerical model. This difference for the FEMA P646 stems back to how maximum momentum flux estimation equation is based on one-dimensional nonlinear shallow-water theory for a uniformly sloping beach, with no lateral topographical variation and no friction. In fact, if a ground elevation of zero is used for Equation 3-6 a maximum momentum flux of approximately

82.4 m^3/s^2 is determined which is similar to that of the numerical model. The ASCE 7-16 draft's estimate is also less than the numerical model's estimate due again to the reasons discussed for the horizontal flow velocity. Section B.3 in Appendix B contains a sample calculation for both the FEMA P646 and ASCE 7-16 drafts estimate for the momentum flux.

6.2.6 **Flow Parameters Used in Case Studies**

Special care needs to be taken when determining the design flow parameters for the specific situation and location for a structure's design in regard to tsunami forces. Future codes and recommendations that require tsunami forces to be considered for structures will need to also have specific guidelines for determining all of these flow parameters, especially for bridge superstructures that are both horizontal and located off of the ground. The ASCE 7-16 draft, even though it is still in the draft stages, introduces and discusses the methods for determining flow parameters in an in depth and intelligent manner.

For the two case studies (Sections 6.3 and 6.4) the estimated flow parameters determined from the OpenFOAM® model will be considered as the design flow parameters to determine the maximum design tsunami forces. These design flow parameters can be seen in Table 6-2.

Table 6-2: Maximum Design Flow Parameters

Flow Parameter	Design Value
Maximum Design Inundation Elevation	6.3 m
Design Horizontal Flow Velocity	8.6 m/s
Design Vertical Flow Velocity	0.79 m/s
Design Momentum Flux	84.3 m^3/s^s
Maximum Design Momentum Flux	84.3 m^3/s^s

For each case study the effects of varying the inundation depth from the ground elevation at the structure to the design inundation elevation (6.3 m) will be explored. This range corresponds to a range of inundation depths from 0.0 to 5.3 m. The three approximations for horizontal flow velocity provided by the Honolulu Code, FEMA P646, and the ASCE 7-16 draft will be used to estimate the horizontal flow velocity. These approximations can be seen in Figure 6-12.

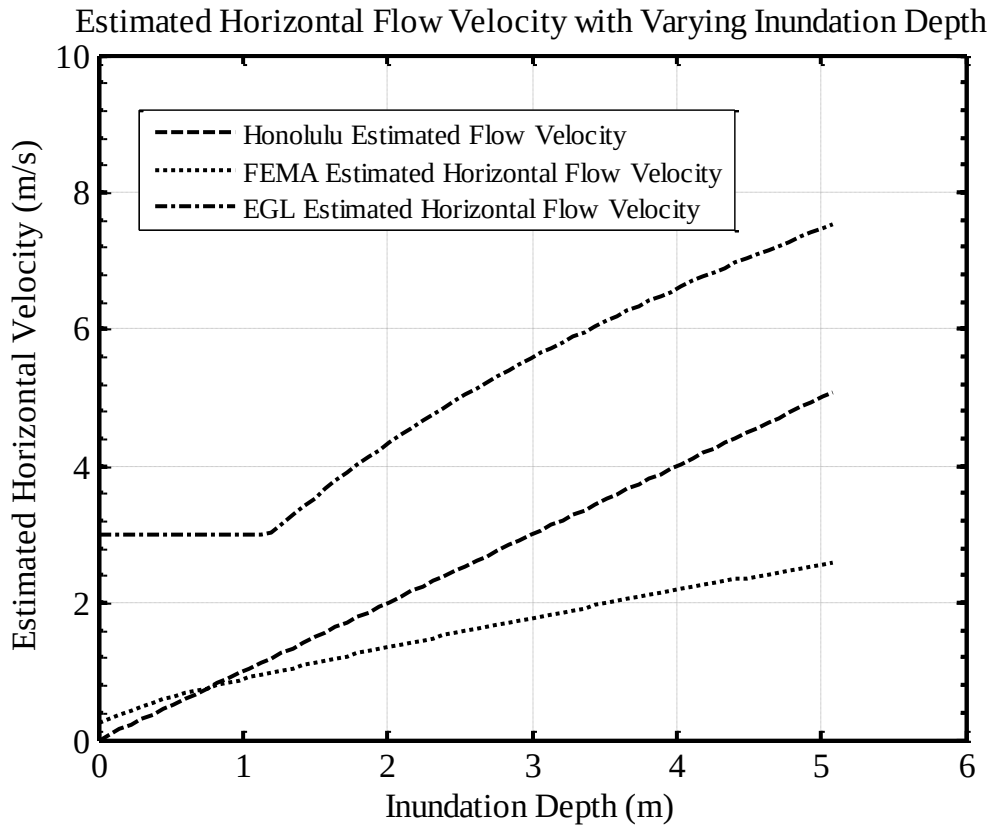

Figure 6-12: Horizontal Flow Velocity Estimates

FEMA P646's horizontal flow velocity estimate is shifted up from zero due to the required 30% increase in runup elevation. Additionally, the horizontal flow velocity estimated by the EGL method is also shifted up from zero due to the requirement by the ASCE 7-16 draft that the minimum horizontal flow velocity must be 3 m/s. The design loads calculated using the three horizontal flow velocity estimates (for a variety of inundation depths) will be compared to each other. Sample calculations for determining all of the flow parameters for the design methods can be found in Appendix B Section B.3.

6.3 Tsunami Forces for Wreck Creek Bridge

The following sections discuss the fluid-induced forces on the Wreck Creek Bridge superstructure, as determined from the design codes and recommendations (this section) and the current research advances (Section 6.4). Specified buoyancy, hydrodynamic drag, hydrodynamic uplift, and hydrodynamic surge forces are compared.

It should be noted that during the design phase, the designer will need to apply the required load and force combinations along with load cases and any other requirements put forth by the code

or recommendation. For the purpose of this case study, the fluid-induced forces and plots are supplied for the purpose of discussing how varying inundation depths and velocities affect each component of the calculated fluid-induced forces (tables 3-1 and 5-1). For this reason, load cases and load combinations are not considered in this study.

The dimensions needed for determining the tsunami-induced forces and a set of sample calculations for all of the considered documents for the Wreck Creek Bridge are supplied in Appendix B, Section B.1. Additionally, the final design forces for all five codes, recommendations, and research equations can be found in Table 6-3 in Subsection 6.3.3.

6.3.1 **Design Code and Recommendation Tsunami Forces**

This section compares the calculated fluid-induced forces among the three codes and recommendations for the Wreck Creek Bridge.

Buoyancy Force

All three of the design codes and recommendations (FEMA P646, Honolulu Code, and the ASCE 7-16 draft) provide equations (Table 3-1) for determining the buoyancy force on a structure. Figure 6-13 shows the variation of these buoyancy forces for the Wreck Creek Bridge while varying the inundation depth up to the design inundation elevation (6.3 m) selected in Section 6.1. The FEMA P646 buoyancy force reflects the required 30% increase in the runup elevation.

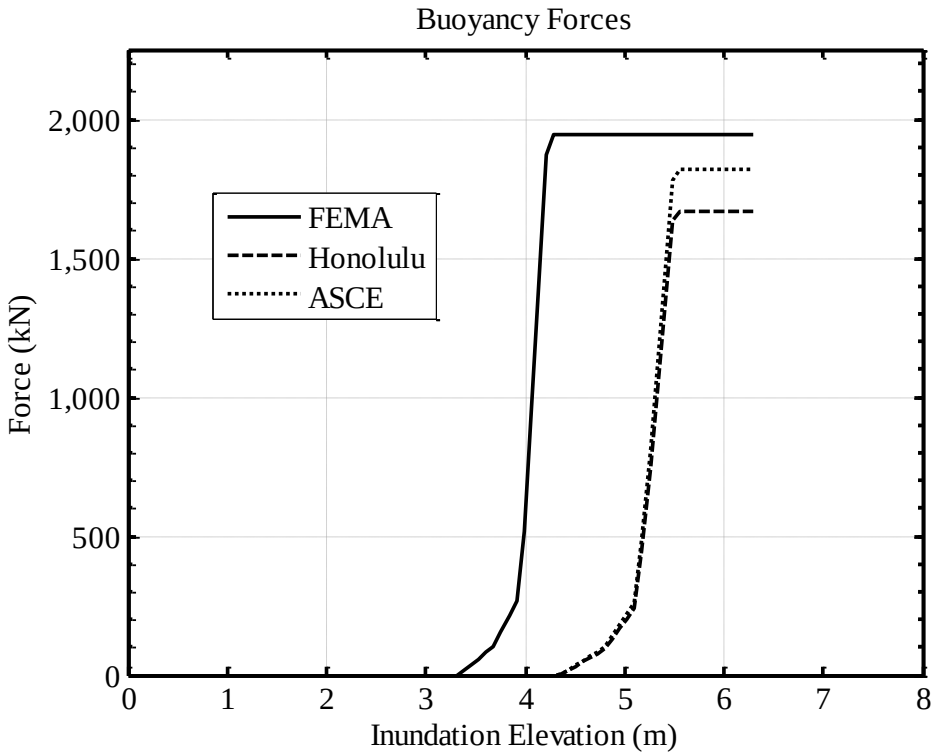

Figure 6-13: Wreck Creek Bridge Buoyancy Force (varying inundation depth)

The 30% increase in the runup elevation required by the FEMA P646 recommendations leads to the Wreck Creek Bridge becoming fully submerged at a smaller inundation depth than the submergence depth resulting from application of the Honolulu Building Code and the ASCE 7-16 draft. As expected, the rate of increase of force with depth depends only on the volume displaced by the superstructure and the assumed fluid density. Once the superstructure is fully submerged, the buoyancy force is constant.

The difference in the selected fluid densities (or specific weights) leads to slight differences in the design buoyancy forces. The FEMA P646 recommendation estimates a maximum buoyancy force of 1,946 kN (at an inundation depth of 6.3 m), which is approximately 14% higher than that of the Honolulu Building Code value (1,670 kN) and 6.6% higher than that of ASCE 7-16 draft value (1,818 kN). Compared to the total weight of the Wreck Creek Bridge superstructure, 3,894 kN, the design buoyancy force alone will not be large enough to lift the superstructure from the substructure. The design buoyancy force estimated by FEMA P646 does only leave a residual dead weight of 50% for the Wreck Creek Bridge superstructure when it is fully submerged.

Hydrodynamic Drag Force

Figures 6-14 to 6-16 show the influence of changing the inundation depth up to the design inundation elevation, while the horizontal velocity is estimated by FEMA P646, the Honolulu Code, and the ASCE 7-16 draft, respectively. An importance factor of 1.0 was assumed for determining the hydrodynamic drag force for the ASCE 7-16 draft.

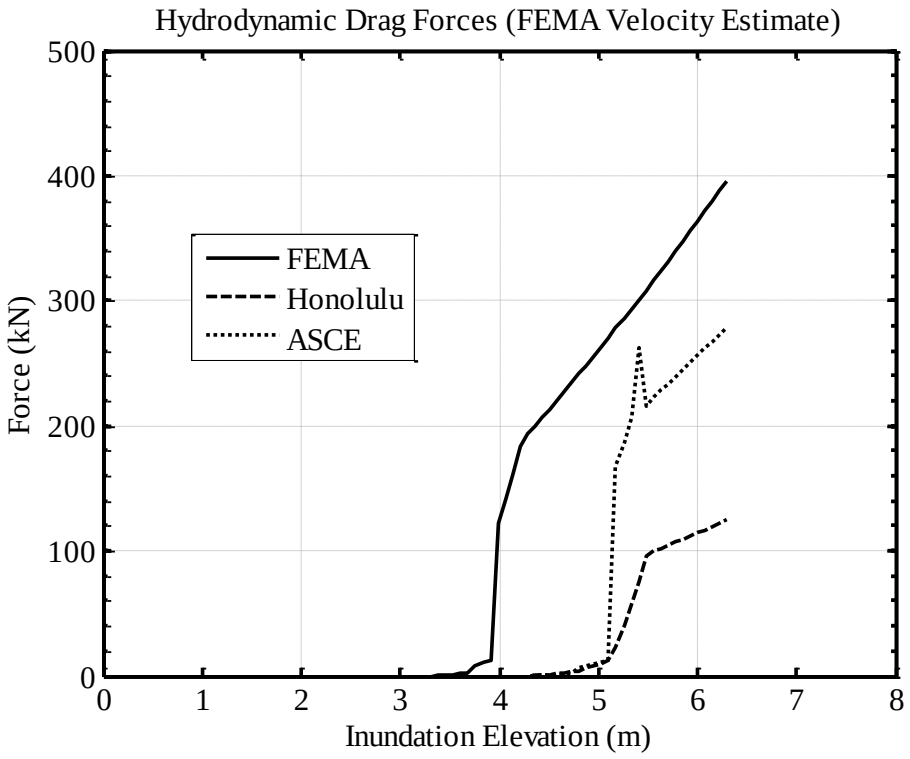

Figure 6-14: Hydrodynamic Forces with FEMA Velocity Estimate

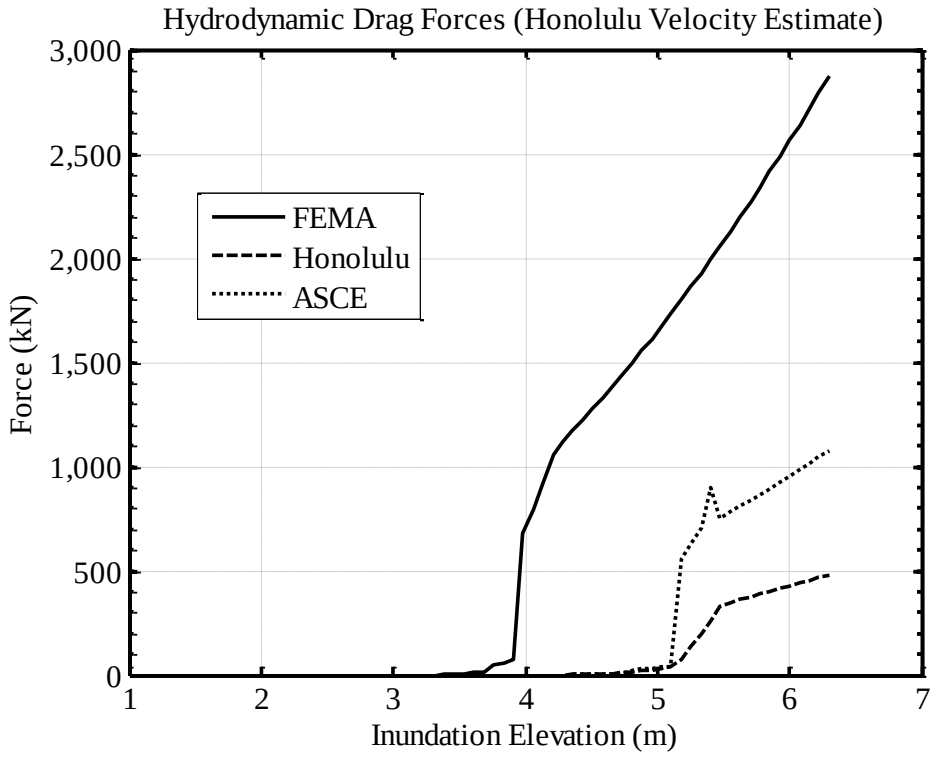

Figure 6-15: Hydrodynamic Forces with Honolulu Code Velocity Estimate

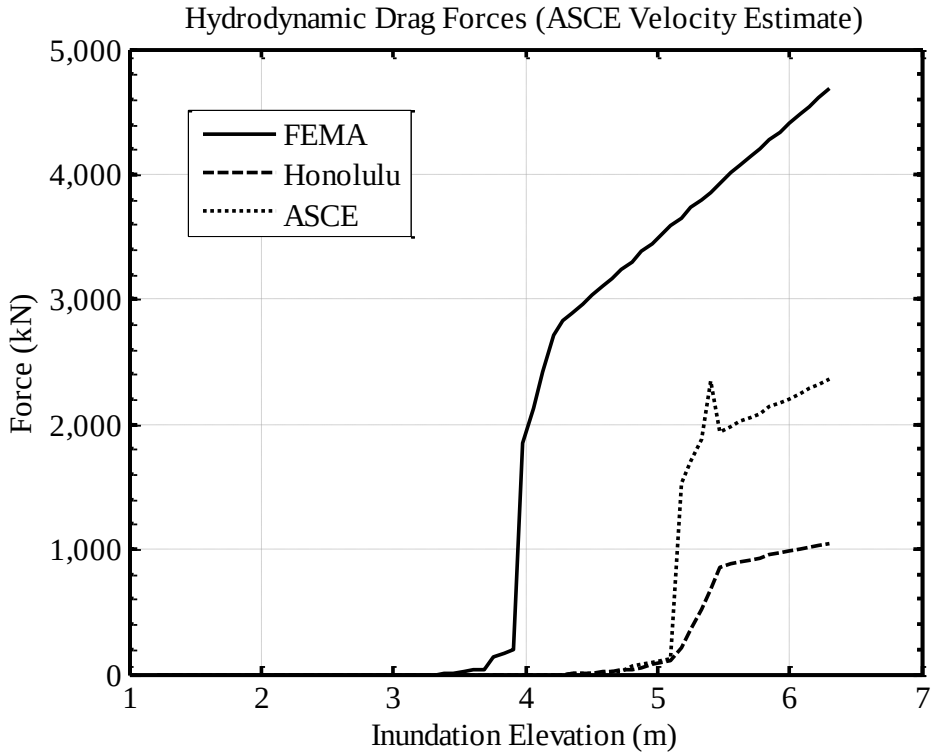

Figure 6-16: Hydrodynamic Forces with ASCE Velocity Estimate

The curves for each code and recommendation in Figures 6-14 to 6-16 have similar shapes but varying magnitudes. The variations among the three figures are due solely to the variations in the estimated horizontal flow velocities between FEMA P646, the Honolulu Code, and the ASCE 7-16 draft. These differences in magnitudes are large, and therefore the estimation of the design horizontal flow velocity is critical. For example, the ASCE 7-16 draft estimate for the design hydrodynamic force varies from approximately 279 kN for the FEMA P646 horizontal flow velocity estimates to approximately 2,357 kN for the ASCE 7-16 drafts horizontal flow velocity estimates (8.4 times larger). This large difference in the design hydrodynamic force estimates is also evident for both the Honolulu Code and the FEMA P646 code and will be evident again for the design hydrodynamic surge forces for all three documents.

Even for the same design velocity, there are also other significant variations among the methodologies. With the 30% increase in the runup elevation, the bridge superstructure begins to be submerged sooner for FEMA P646, leading to the FEMA P646 curve being shifted to the left. This increased runup elevation also leads to increased estimated flow velocities due to all of the flow velocity estimation equations being dependent on the runup elevation. This increased flow velocity then leads to larger estimated hydrodynamic drag forces. In adapting these recommendations for bridges, it would be necessary to determine the circumstances under which it would be necessary to apply the factor 30% increase. Presumably, the application of this factor would depend on the importance of the bridge.

The ASCE 7-16 draft uses both a variable drag coefficient (Subsection 3.5.4) and a smaller value for the fluid density when compared with the FEMA P646 recommendations. In fact, at the design inundation elevation of 6.3 m the ASCE 7-16 draft is using a drag coefficient of 1.5 while both the FEMA P646 recommendation and the Honolulu Building Code are using drag coefficients of 2.0. This switch in drag coefficients is denoted by the "spike" in the ASCE 7-16 drafts curve.

These factors lead to design hydrodynamic drag force for the ASCE 7-16 draft being much less than that of the FEMA P646 recommendations. Even if the ASCE draft importance factor (I_{tsu}) is increased to 1.3, the calculated forces will still be less than that of those estimated by FEMA P646.

The Honolulu Building Code estimates the smallest design hydrodynamic drag forces, in part because it does not take into account sediment accumulation for the fluid density value. More importantly, the Honolulu Code estimates the drag based on the wetted area, whereas the drag force for the other two methodologies is based on the total structure depth and width. For rectangular cross-sections, the two areas would be the same, but for non-rectangular sections, the wetted area is less.

Hydrodynamic Surge Force

Figures 6-17 to 6-19 show the influence of changing the inundation depth up to the design inundation elevation (6.3 m), while the horizontal velocity is estimated by FEMA P646, the Honolulu Code, and the ASCE 7-16 draft recomendations. As mention in the previous section, the main differences among the figures result from differences in the assumed fluid velocities. The 30% increase in runup elevation again leads to the FEMA estimate being shifted to the left in the figures.

The three figures are another example of the importance of estimating the flow parameters properly. For example, the FEMA P646 estimate for the design surge force varies from approximately 600 kN for the FEMA P646 horizontal flow velocity estimate to approximately 7,000 kN for the ASCE 7-16 drafts horizontal flow velocity estimate (11.6 times larger). Again, like the hydrodynamic force estimates, this difference is not only evident for the FEMA P646 surge force estimate but also for both the Honolulu Code and the ASCE 7-16 draft estimates for the design surge force. Finally, if the importance factor is increased to 1.3 for the ASCE 7-16 draft its estimated surge force will be closer, but still less than, that determined from FEMA P646.

The Honolulu Building Code's surge force methodology differs based on whether height of the structure is below or above 3 times the bore height (Subsection 3.6.4). This provision was not developed for bridges, so the interpretation of it is ambiguous, because it is not clear whether the provision should be based on the elevation of the deck or the deck depth. The height of the Wreck Creek Bridge is well below three times the bore height, so its surge force is calculated based on the summation of the hydrodynamic drag and hydrostatic force equations. On the other hand both the FEMA P646 and the ASCE 7-16 draft equations for the surge force are simply the hydrodynamic force equation multiplied by a factor of 1.5 (assuming the closure coefficient to be 1.0).

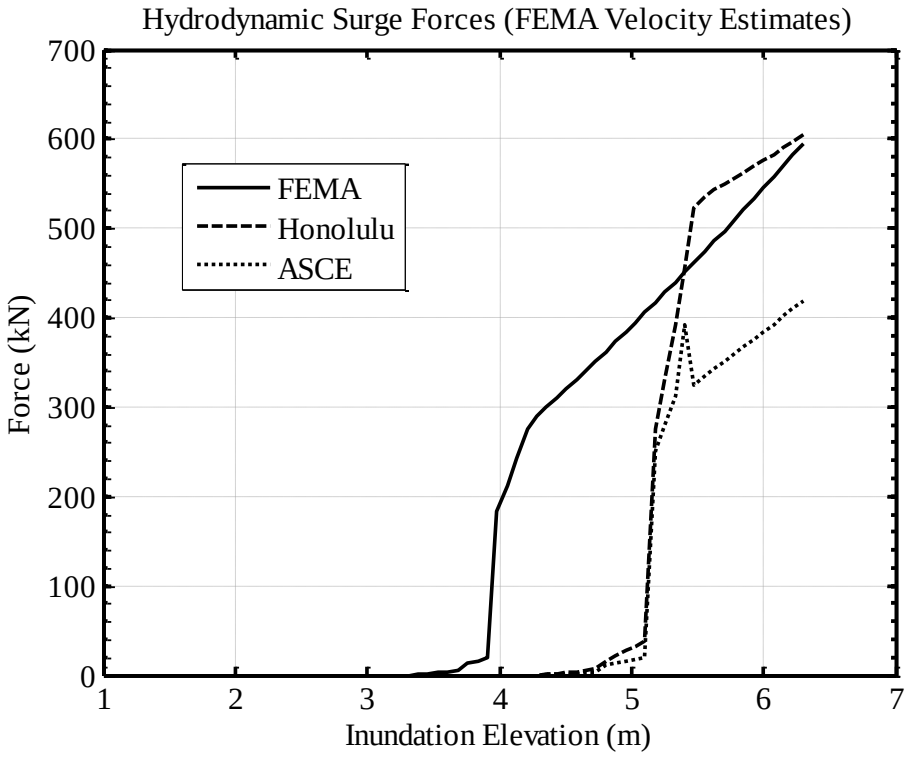

Figure 6-17: Surge Forces with FEMA Velocity Estimates

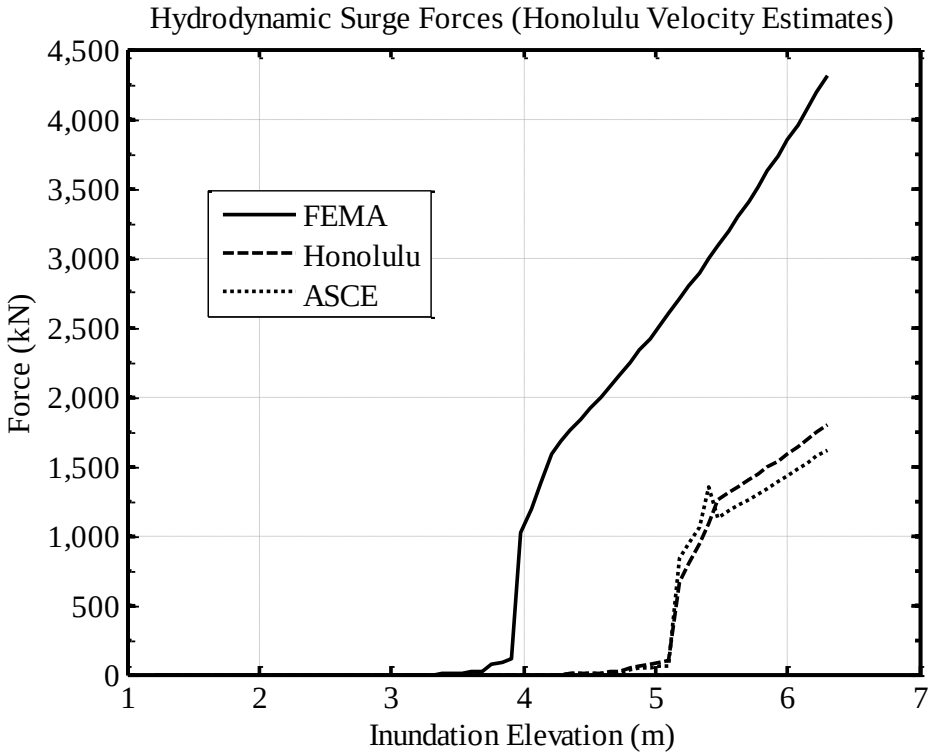

Figure 6-18: Surge Forces with Honolulu Code Velocity Estimates

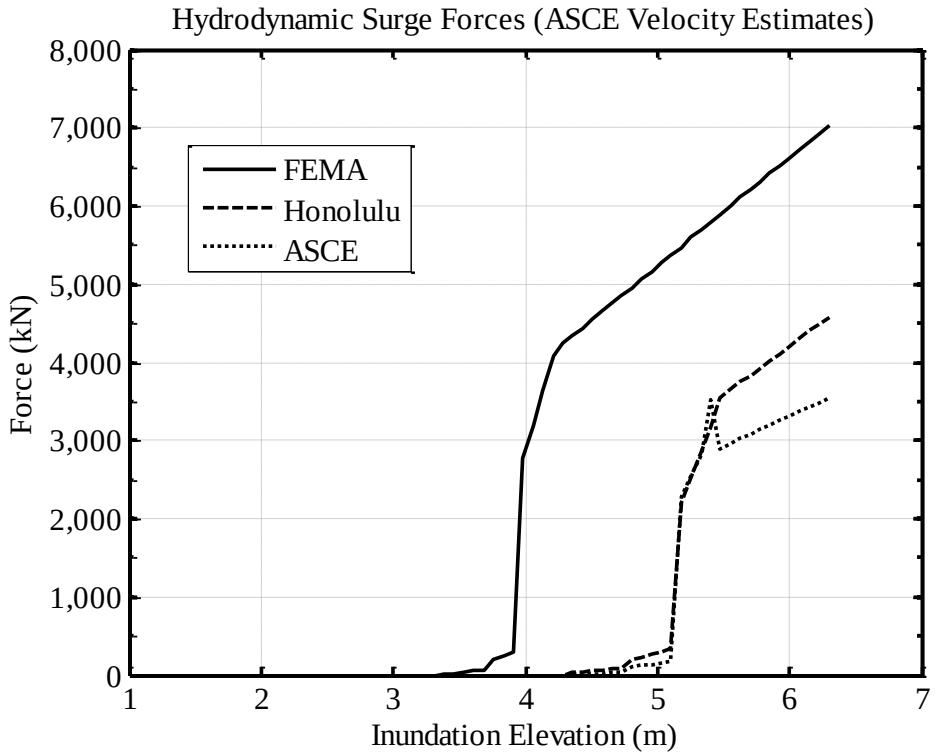

Figure 6-19: Surge Forces with ASCE Velocity Estimates

Hydrodynamic Uplift Force

Uplift force equations are provided by both FEMA P646 and the ASCE 7-16 draft provisions. The Honolulu Code does not provide a methodology for estimating the hydrodynamic uplift force.

Figure 6-20 depicts the influence of changing the inundation depth up to the design inundation elevation of 6.3 m for both the FEMA P646 and the ASCE 7-16 draft methodologies. The ground slope at the Wreck Creek Bridge location is less than ten degrees. For this reason the vertical component of velocity is small, regardless of the methodology used to estimate the horizontal velocity (FEMA P646 estimates approximately 0 kN). The ASCE 7-16 drafts methodology for the uplift force requires a minimum pressure along the underside of the bridge of 958 Pa (20 psf).

For this configuration, the ASCE 7-16 draft estimates the largest uplift force (378 kN) which is only 30% of the buoyancy force.

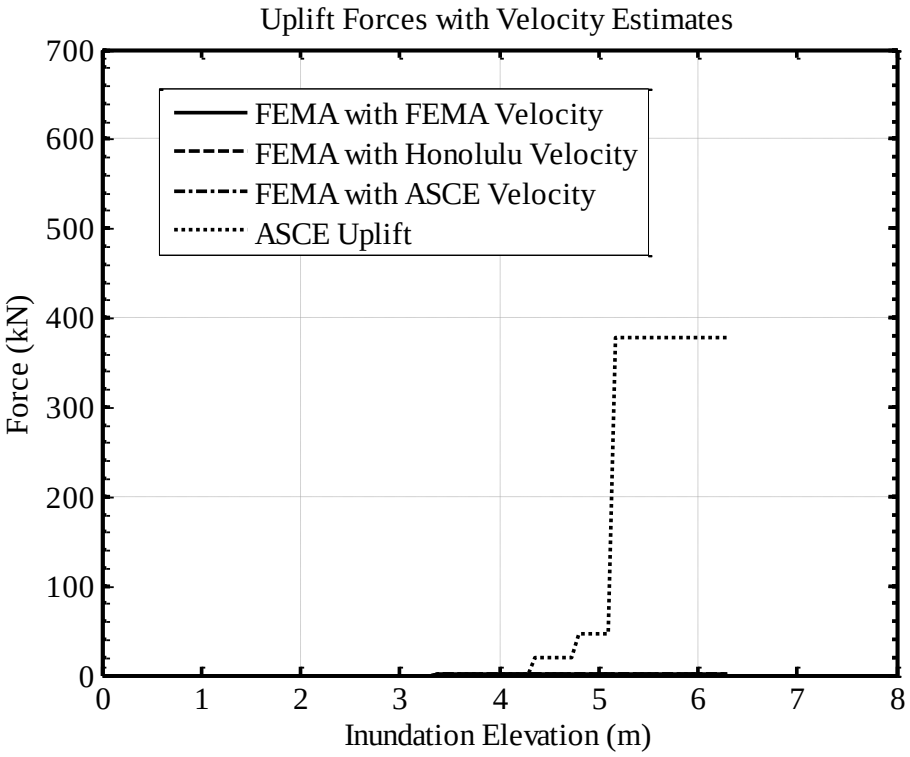

Figure 6-20: Uplift Forces

6.3.2 **Current Research Tsunami Forces**

Hydrodynamic Drag Force

Only Yim introduces a hydrodynamic drag force equation, and it is identical to the one introduced by FEMA P646 (but without the factor of 1.3 on runup), leading to identical hydrodynamic drag force estimate. Figure 6-23 shows the effect on the hydrodynamic drag when varying the inundation depth up to the design inundation elevation of 6.3 m.

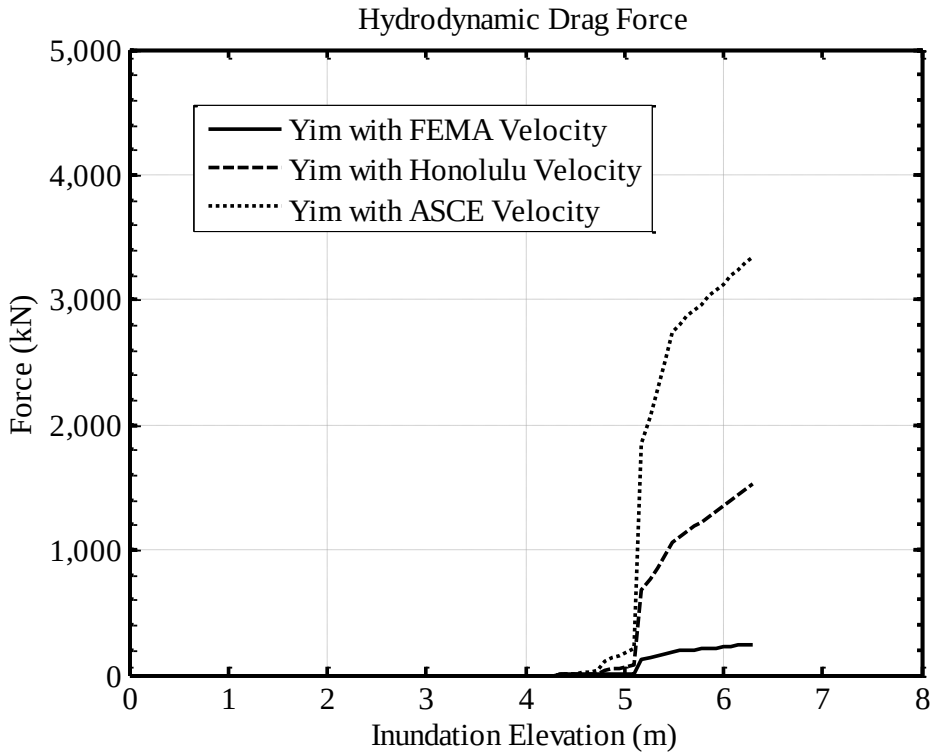

Figure 6-21: Wreck Creek Bridge Hydrodynamic Forces for Research Advances (varying inundation depth)

Hydrodynamic Surge Force

Douglass also introduces a surge force based on the hydrostatic force and can be seen in Figure 6-24. As the Wreck Creek Bridge is submerged both the area perpendicular to the flow and the flow depth, measured from the centroid of the area perpendicular to the flow, begin to increase leading to the exponential force gain. Once the bridge is fully submerged the area term is constant as the flow depth continuous to increase leading to the linear portion of the curve.

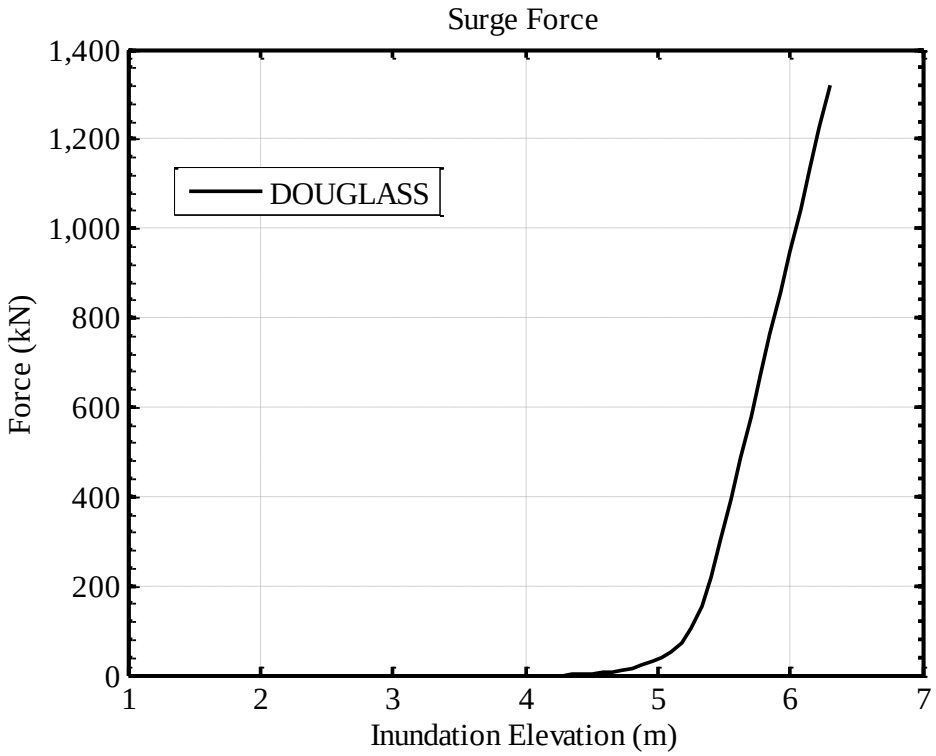

Figure 6-22: Wreck Creek Bridge Hydrodynamic Forces for Research Advances (varying inundation depth)

Hydrodynamic Uplift Force

Both Yim et al. (2011) and Douglass et al. (2006) incorporate the buoyancy force calculation within their uplift force calculations, where Yim's uplift force also includes a hydrodynamic force consideration. Figure 6-23 shows the uplift forces while varying the inundation depth up to the design inundation elevation of 6.3 m. The uplift forces predicted by these two research documents are orders of magnitude larger than those calculated in Subsection 6.3.1.

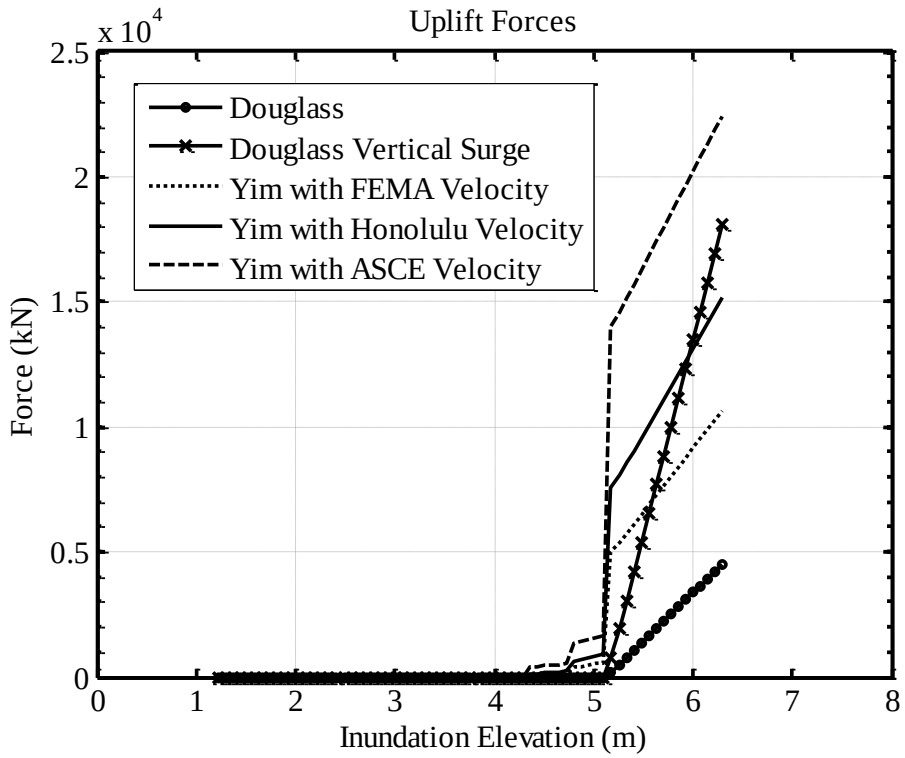

Figure 6-23: Wreck Creek Bridge Uplift Forces for Research

As the inundation depth increases above the top of the bridge superstructure the buoyancy continues to increase for both methodologies. This trend is implausible because, once the bridge is fully submerged, the buoyancy will remain constant. The buoyancy increases with inundation depth due to the definition used for the water depth term in both of the research documents. Yim's uplift prediction also takes into account horizontal flow velocity, further increasing the predicted uplift force. The changes in slope in the Yim predictions are solely due to the increase in area parallel to the flow as the inundation depth increases. Once the bottom area of Wreck Creek Bridge becomes fully inundated (at approximately 5.1 m) the slope remains constant due to the entire underside of the bridge being submerged. Additionally, the variations among the Yim uplift force estimations are due to the different flow velocities assumed by each of the methods.

As was discussed in Section 5.1, the Douglass's equations were formulated for wave action occurring near the elevation of the road surface, whereas for this study the water elevation is above the road surface at the design inundation elevation. Consequently, the Douglass equations are being applied outside of the range for which they were designed. In addition, the Douglass equations were designed for wave impacts not tsunamis. Additionally, the two estimates for the uplift force by Douglass vary in slope due to the larger "impact" coefficient used for the vertical surge uplift equation.

Hydrodynamic Surge Force

Douglass also introduces a surge force based on the hydrostatic force and can be seen in Figure 6-24. As the Wreck Creek Bridge is submerged both the area perpendicular to the flow and the flow depth, measured from the centroid of the area perpendicular to the flow, begin to increase leading to the exponential force gain. Once the bridge is fully submerged the area term is constant as the flow depth continuous to increase leading to the linear portion of the curve above.

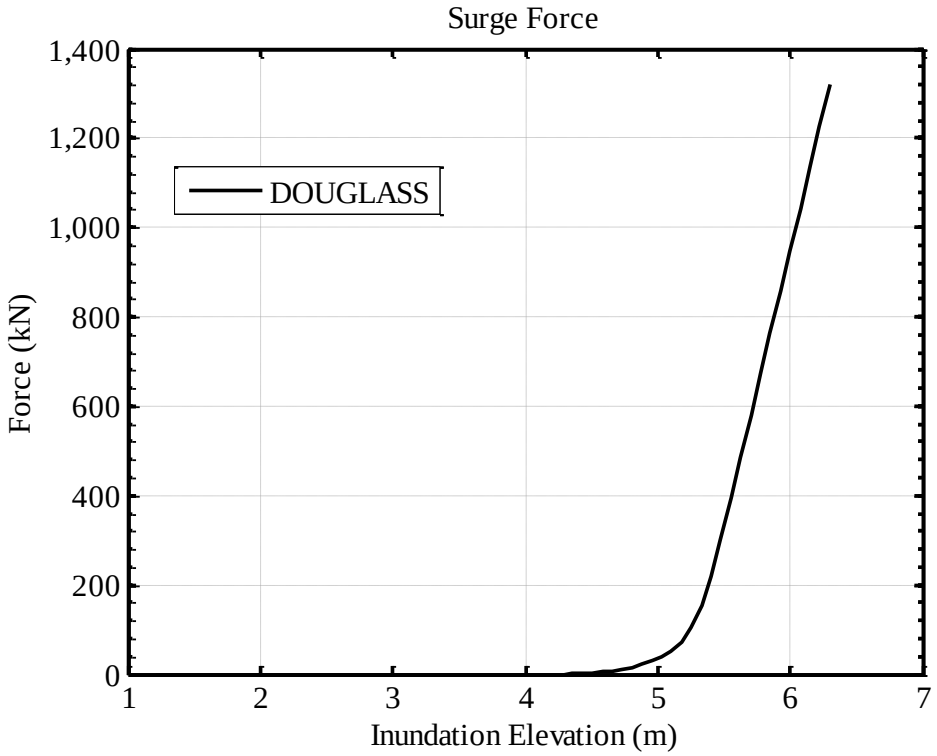

Figure 6-24: Wreck Creek Bridge Hydrodynamic Forces for Research Advances (varying inundation depth)

6.3.3 **Summary of Computed Tsunami Forces**

The effect of changing the inundation depth and the estimated horizontal flow velocity was examined for the buoyancy, hydrodynamic drag, hydrodynamic surge and hydrodynamic uplift forces in the above subsections. Table 6-3 provides the final design forces for an inundation depth of 6.3 m (for each of the codes, recommendations, and research documents).

Table 6-3: Summary of Design Forces

Code, Recommendation or Research	Buoyancy Force (kN)	Hydrodynamic Force (kN)	Surge Force (kN)	Uplift Force (kN)
Table 6-2 Design Flow Parameters				
Honolulu Building Code	1,670	1,372	7,227	N/A***
FEMA P646	1,946	4,361	6,541	443
ASCE	1,818	3,073	4,610	378
"Douglass"	N/A***	N/A***	1,320	4,519* / 18,075**
"Yim"	N/A***	4,356	N/A***	26,500
Horizontal Flow Velocity Estimated by FEMA P646				
Honolulu Building Code	1,670	125	605	N/A***
FEMA P646	1,946	396	594	0.03
ASCE	1,818	279	419	378
"Douglass"	N/A***	N/A***	1,320	4,519* / 18,075**
"Yim"	N/A***	396	N/A***	10,657
Horizontal Flow Velocity Estimated by Honolulu Code				
Honolulu Building Code	1,670	481	1,798	N/A***
FEMA P646	1,946	2,875	4,382	0.2
ASCE	1,818	1,076	1,614	378
"Douglass"	N/A***	N/A***	1,320	4,519* / 18,075**
"Yim"	N/A***	1,526	N/A***	15,177
Horizontal Flow Velocity Estimated by ASCE 7-16 Draft				
Honolulu Building Code	1,670	1,052	4,581	N/A***
FEMA P646	1,946	4,685	7,027	0.21
ASCE	1,818	2,357	3,535	378
"Douglass"	N/A***	N/A***	1,320	4,519* / 18,075**
"Yim"	N/A***	3,341	N/A***	22,438

* Represents "Douglass" uplift not considering surge impact
** Represents "Douglass" uplift considering surge impact
*** Equation was not provided by the given code, recommendation or document

At the design inundation elevation the numerical model estimated a flow velocity of 8.6 m/s, the EGL method from the ASCE 7-16 draft estimated 7.5 m/s, the Honolulu Code estimated 5.1 m/s, and FEMA P646, including 30% increase in runup elevation, estimated 2.6 m/s. These large variations in the calculated flow velocity led to large variations among the estimated hydrodynamic tsunami forces, including the hydrodynamic drag, hydrodynamic surge, and hydrodynamic uplift forces. In contrast, the buoyancy force calculation is not influenced by the flow velocity and therefore the three sets of buoyancy forces were much similar.

For a given flow velocity, FEMA P646 and Yim estimated the largest hydrodynamic drag forces because their drag coefficients are larger than the one used by ASCE 7-16 draft. Their fluid densities are greater than the one used for the Honolulu Building Code. The smaller estimate of

the flow velocity by FEMA P646 also led to smaller force estimates for both the surge and uplift forces.

The estimates of the surge force were closer together for each of the documents at the lower flow velocities (Fig. 6-17) than at higher velocity (Fig. 6-18). The surge force estimates depend on the square of the velocity and the selected drag coefficient for the ASCE 7-16 draft and FEMA P646. Because the drag coefficient is less for ASCE 7-16 draft, and because Douglass does not take into account flow velocity, these two documents estimate a smaller surge force than the Honolulu Code and the FEMA P646 document. Additionally, the Honolulu Code also includes the hydrostatic force from when the bore first comes into contact with the structure further increasing the surge force estimate.

For each of the cases shown in Table 6-3, the differences among the uplift forces in each flow velocity case were extreme (i.e. for the design flow parameters the uplift varied from 378 kN to 26,500kN). This is due to the definition of depth for both Douglass and Yim leading to increasing buoyancy forces once the bridge is already submerged. Additionally, Yim uses the horizontal flow velocity instead of the vertical flow velocity, as FEMA P646 does, when calculating the hydrodynamic component of the uplift force. Uplift forces of this magnitude are large enough to lift the Wreck Creek bridge superstructure from its substructure (Figure 6-28).

6.3.4 **Reaction Forces at Supports**

An abutment and capbeam are located at each end of the Wreck Creek Bridge superstructure, with three more capbeams positioned between the two ends of the bridge. Each end and intermediate capbeam is supported by a pile group of 8 piles resulting in a total of 5 pile groups. The reactions at each of the five supports (2 abutments and 3 intermediate supports) are difficult to estimate, because the details of these supports are unknown.

If the deck is nearly rigid compared to the stiffness of the supports, then the reactions of at the supports would be proportional to their horizontal or vertical stiffness, depending on the direction of the tsunami load. For example:

- If the pile groups all have the same stiffness, then each support would have the same reaction.
- If the abutments are much stiffer than the intermediate supports (because of differing solid conditions), then each abutment would resist approximately one half of the applied horizontal and vertical loads.
- If the abutments are much more flexible than the intermediate supports, then each intermediate would resist approximately one third of the applied horizontal and vertical loads.

To consider a fourth scenario, the design forces determined from the design flow parameters (Table 6-2) were applied to an Abaqus™ model of the Wreck Creek Bridge superstructure. The reaction forces were estimated along each of the capbeams due to the vertical hydrodynamic forces, horizontal hydrodynamic forces, and the surge forces. The resultant forces at each of the pile group locations for the Wreck Creek Bridge superstructure were determined from the model shown in Figure 6-25. In the model, all of the supports were fixed against horizontal and vertical displacements and rotations.

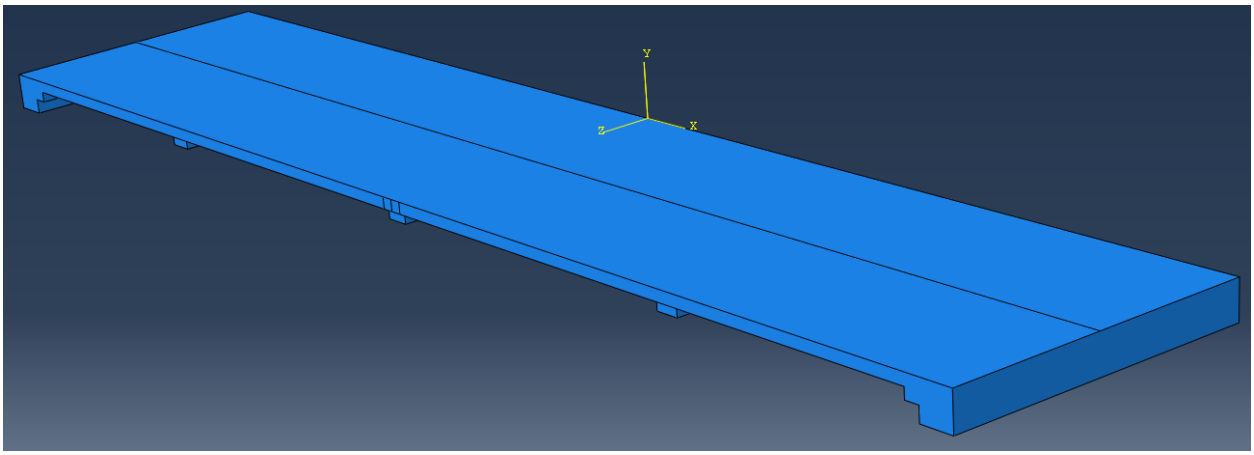

Figure 6-25: Wreck Creek Bridge Superstructure Abaqus™ Model

In the analysis, the tsunami was assumed to be coming from a direction perpendicular to the span (parallel to the z axis). The actual connection details are unknown, so for simplicity, it was assumed that the abutments are rigidly connected to the ground and therefore all six of the abutment degrees of freedom were fixed. Additionally, all six degrees of freedom were fixed at the top of the pile. Figures 6-26 and 6-27 are provided to show these boundary conditions and pile group locations respectively for the model.

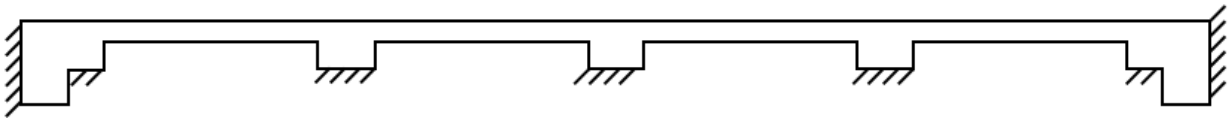

Figure 6-26: Boundary Condition Locations

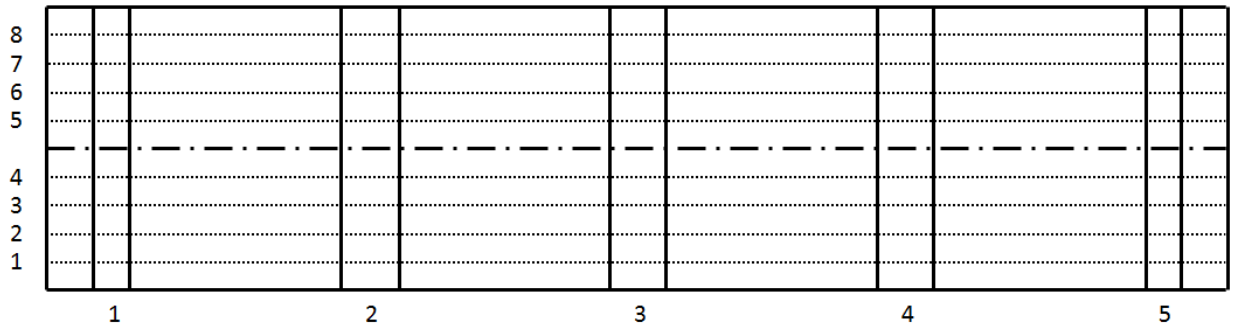

Figure 6-27: Capbeam and Pile Locations for the Wreck Creek Bridge

The model was made up of deformable ten node tetrahedral elements with elastic material properties representing concrete, where the concrete strength used was 1.5 times larger than that noted on the plans for the Wreck Creek Bridge (Appendix C, 1320 psi) to account for curing time and overstrength provided by the contractor.

Vertical Reactions

A uniform pressure was applied on the underside of the superstructure to represent the design uplift force for each of the codes, recommendations, and documents. The surge and hydrodynamic drag forces were applied in a similar manner but over the side of the superstructure. In Figure 6-28 the buoyancy force is combined with the uplift force for the FEMA P646 document, the Honolulu Building Code, and the ASCE 7-16 draft (the buoyancy force is included in the uplift equations for both Yim et al. 2011 and Douglass et al. 2006).

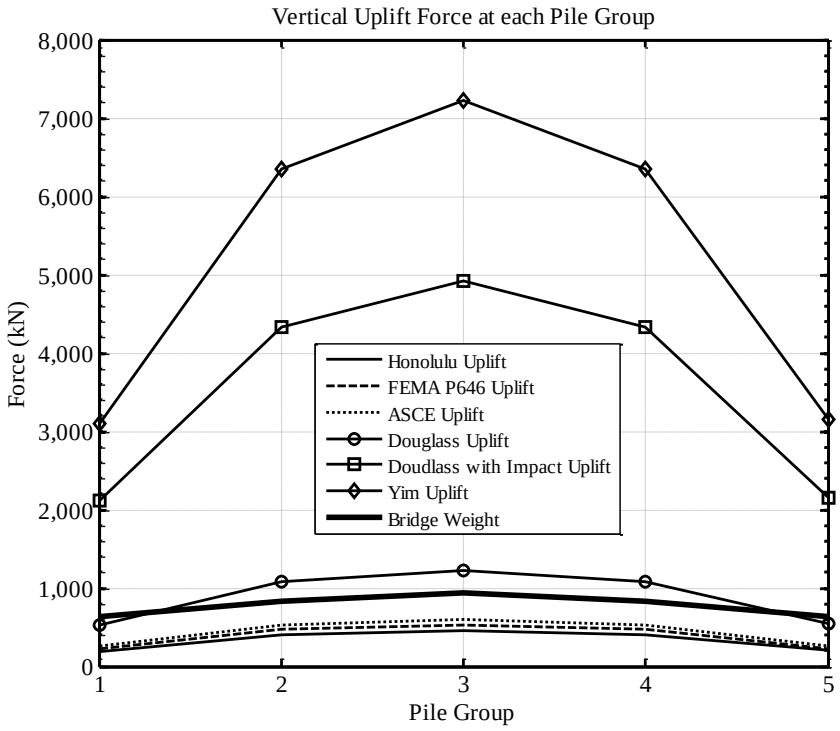

Figure 6-28: Wreck Creek Bridge Pile Groups Uplift Reactions

The research documents (Douglass and Yim) estimate design uplift forces that greatly exceed the weight of the Wreck Creek Bridge Superstructure (3,894 kN). These high uplift forces can be attributed to how both of these documents calculate the water depth for their respective force equations. Additionally, Yim uses the much faster horizontal flow velocity (not the vertical flow velocity) when calculating the uplift force. On the other hand, FEMA P646, the Honolulu Code, and the ASCE 7-16 draft estimate uplift forces that are relatively close together. It should be noted that both the Douglass and Yim documents are specific towards deck-girder bridge superstructures and not buildings as FEMA P646, the Honolulu Code, and the ASCE 7-16 draft are.

Horizontal Reactions

Both the surge and hydrodynamic drag forces act in Figures 6-29 and 6-30 respectively. The larger the horizontal force acting on the superstructure is, the easier it will be for the superstructure to be lifted from the substructure. This is due to both the surge force and hydrodynamic forces not actually acting normal to the superstructures cross-sectional area perpendicular to the flow due to local topography and the front of the bore not being exactly parallel to the bridges cross-sectional area perpendicular to the flow. Additionally, the

hydrodynamic force will act in addition to the uplift force, if the hydrodynamic force is not normal to the bridges area perpendicular to the flow it may add to the uplift.

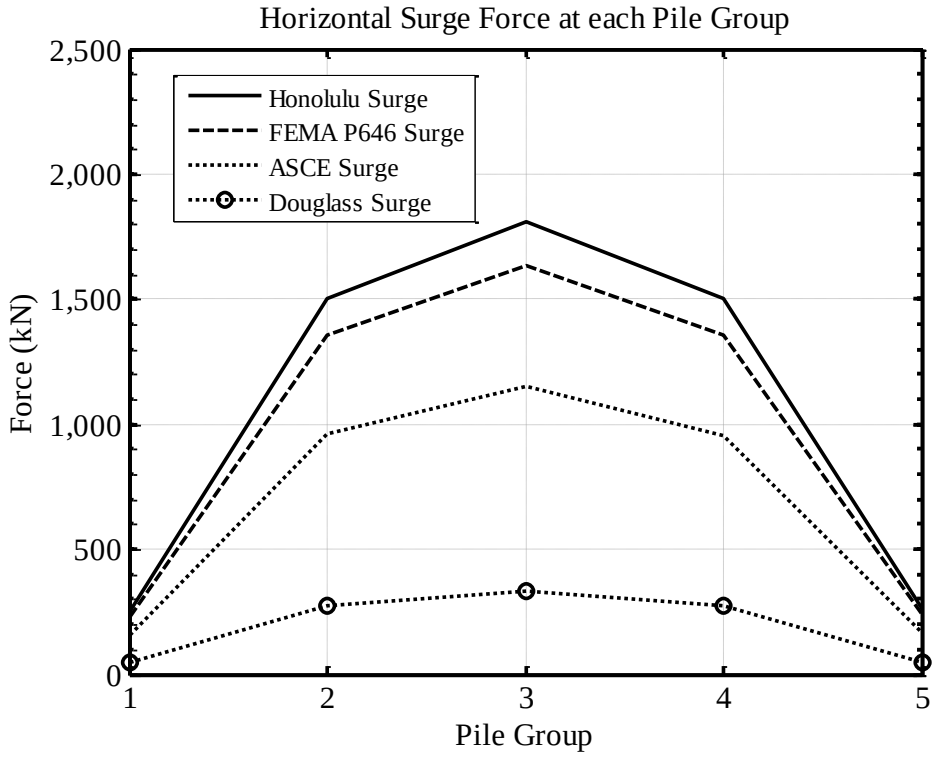

Figure 6-29: Wreck Creek Bridge Pile Groups Horizontal Surge Reactions

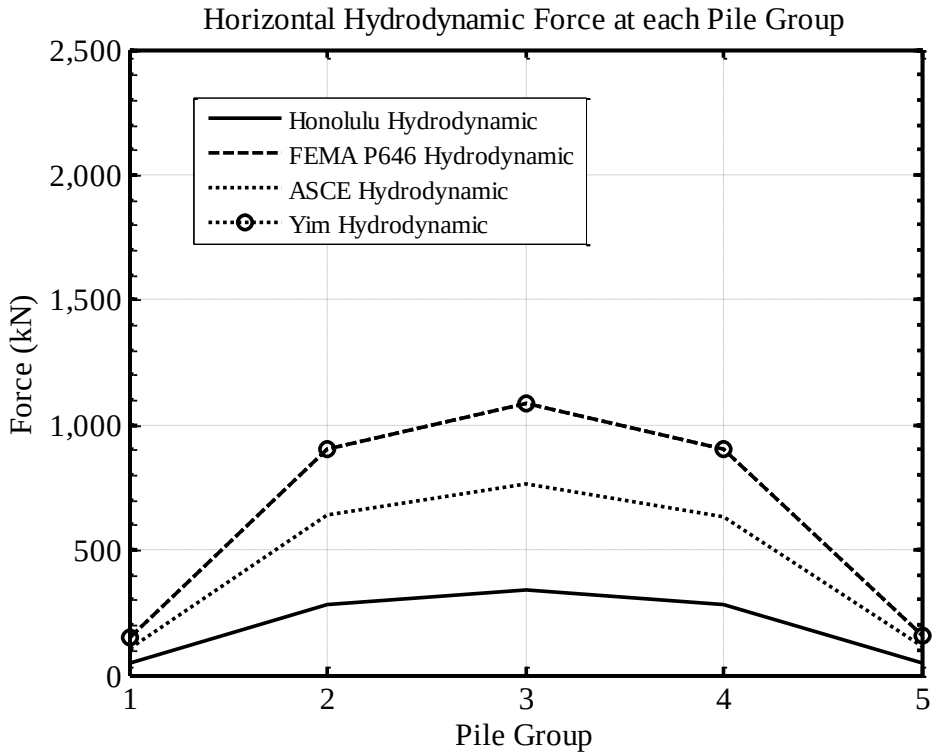

Figure 6-30: Wreck Creek Bridge Pile Groups Horizontal Hydrodynamic Reactions

6.4 Tsunami Forces for Schooner Creek Bridge

The Schooner Creek Bridge is much longer than the Wreck Creek Bridge (134 ft vs 286 ft), and it is constructed with a deck-girder geometry instead of a slab geometry. The longer spans and depths will increase the surface areas and result in larger forces. This section discusses the differences in the fluid-induced forces that the Schooner Creek Bridge will experience, compared with the forces experienced by the Wreck Creek Bridge for identical flow parameters. Each of the types of fluid-induced forces will be discussed in this section.

Buoyancy Force

The calculation methodology for the buoyancy force for the Schooner Creek Bridge is identical to that of the Wreck Creek Bridge. Because the Schooner Creek Bridge will displace a larger volume of water than the Wreck Creek Bridge, its calculated buoyancy force would be much larger than that of the Wreck Creek Bridge. Additionally, with the use of the deck-girder type geometry it is possible for air to be trapped between the girders which will further affect the buoyancy forces.

Hydrostatic Force

Hydrostatic forces were negligible for the Wreck Creek Bridge, because the deck was thin, and because it was assumed that the entire bridge superstructure (unlike a building) would be

submerged rapidly. For the Schooner Creek Bridge, unbalanced hydrostatic forces would need to be taken into account, because air might be trapped between the girders. These forces would act perpendicularly to the girders in areas of differing pressure (e.g., if one side of a girder is submerged but the other side is only partially submerged).

Hydrodynamic Drag Force

The larger surface areas of the Schooner Creek Bridge will lead to larger hydrodynamic drag forces than those for the Wreck Creek Bridge. Unlike the constant cross-sectional area perpendicular to the flow direction that the Wreck Creek Bridge has, the Schooner Creek Bridges cross-sectional area changes due to the addition of the girders. These abrupt changes in cross-sectional area will lead to the Schooner Creek Bridge experiencing larger amounts of drag in the flow. It is unlikely that the drag coefficients that are provided for building geometries would be appropriate for bridge geometries, such as those that include bridge girders.

Hydrodynamic Uplift Force

The application of the uplift force equations provided by both the Honolulu Code and the FEMA P646 methodologies is identical for both of the bridge superstructures. However, the Schooner Creek Bridge will experience larger hydrodynamic uplift due to its increased surface area compared to the Wreck Creek Bridge.

Additionally, the Schooner Creek Bridge has a protruding sidewalk structure. This type of geometry can amplify the uplift forces due to the redirection of the flow upwards and into the bottom of the protruding sidewalk, as seen in Figure 6-31.

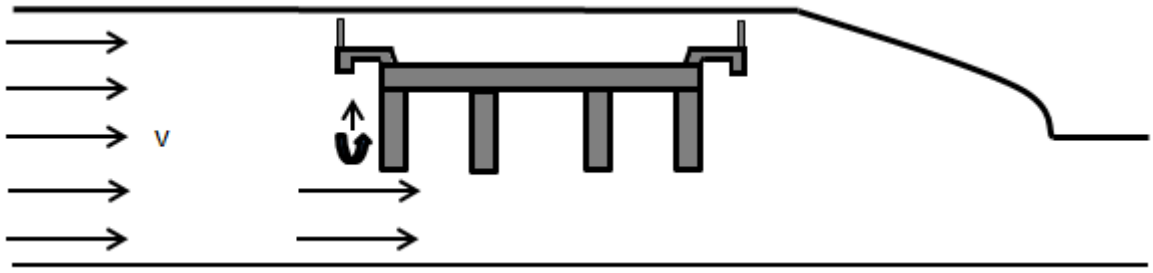

Figure 6-31: Influence of Protruding Sidewalk on Horizontal Flow Velocity

This type of geometry is taken into account in the uplift force equations provided by the ASCE 7-16 draft, but because the ASCE 7-16 draft is for buildings, the force it estimates will be conservative. This approach would be conservative, because the bridge girders do not extend all the way to the ground, and therefore all of the flow will not be trapped and directed up or down

as it would for building walls and slabs (Figure 3-9). The ASCE 7-16 draft recommends a uniform pressure of 350 psf (16.76 kPa) within a certain distance from the slab-to-wall connection (sidewalk connection in the case of the Schooner Creek Bridge). This pressure can then be reduced based on the inundation height and or openings that will allow the reduction of pressure.

Hydrodynamic Surge Force

As was the case for the other forces, the Schooner Creek Bridge will experience a larger surge force due to the increased area of the bridge. Otherwise the determination of the surge forces will be identical between the two bridge superstructures.

Summary

Engineers will need to take into account the effects of different bridge superstructure geometries when designing a bridge in a tsunami prone area. In summary, the four main differences between two bridges would be:

- The Schooner Creek Bridge has a much larger area parallel and perpendicular to the flow, so the calculated forces would be correspondingly higher.
- The deck-girder geometry would likely have a higher drag coefficient than the slab geometry. For example, Yim determined the drag coefficient during a simulation of a deck-girder bridge based on the magnitude of the horizontal (parallel to flow direction) force the bridge was experiencing. A plot of the drag coefficient during the duration of the simulation can be seen in Figure 6-32. During Yim's simulation the drag coefficient reaches a maximum value of 3.5, this is larger than any of the supplied drag coefficients from either the Honolulu Building Code, FEMA P646, or the ASCE 7-16 draft.
- The possibility of air becoming trapped between the girders would increase the buoyancy and unbalanced hydrostatic forces.
- The extended sidewalk for the Schooner Creek bridge will increase the uplift forces due to the redirection of the flow.

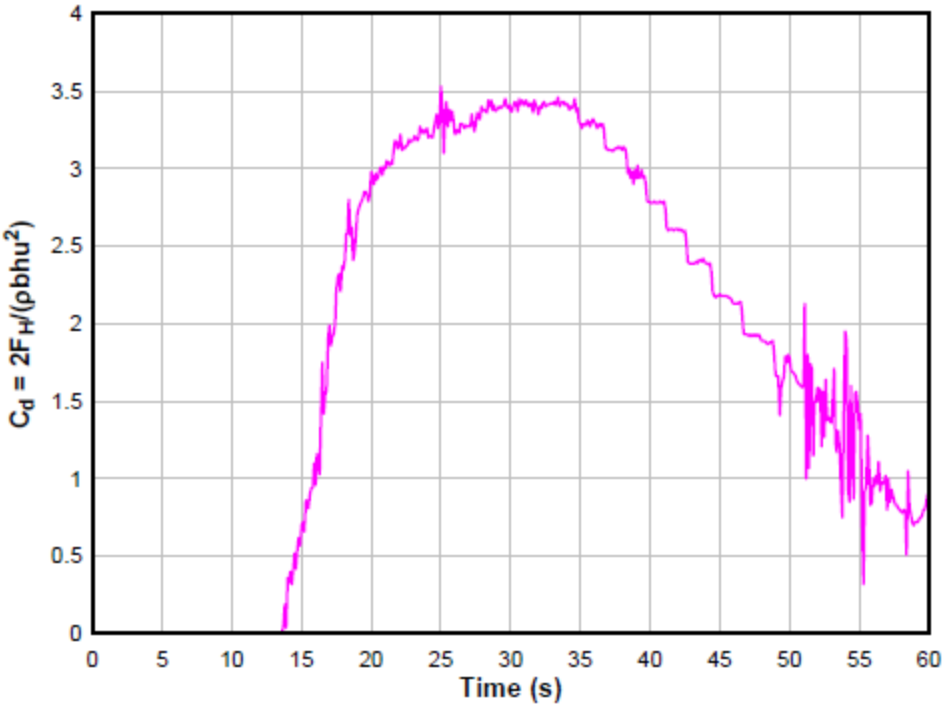

Figure 6-32: Drag Coefficient for Spencer Creek Bridge (Yim et al. 2011)

Chapter 7 Conclusions

Recent events in the U.S., such as Hurricane Katrina, have shown how susceptible the transportation systems are to storm surges caused by hurricanes or tropical storms. The loss of critical transportation infrastructure in coastal areas has delayed emergency services, evacuation, and recovery efforts for extended periods of time.

The pacific region of the United States, including the states of Alaska, Washington, Oregon, California and Hawaii, as well as several U.S. territories, are susceptible to being struck by major tsunamis. The failure of critical bridges during a tsunami event would also have severe consequences.

7.1 Current Codes and Recommendations

Currently there are no mandatory nationwide tsunami design codes. However, there are three methodologies for determining tsunami-induced forces for buildings:

1. Honolulu Building Code: Chapter 16 Article 11 "Regulations Within Flood Districts and Development Adjacent to Drainage Facilities"

2. FEMA P646: "Guidelines for Design of Structures for Vertical Evacuation from Tsunamis"

3. ASCE 7 Standards Committee Drafts No. I to XI to Revise the 2010 Edition of ASCE/SEI 7 (ASCE 7-16 Draft): "Chapter 6: Tsunami Loads and Effects". When adopted by local jurisdictions, this chapter will be the first nationwide mandatory tsunami design code.

Variations in the estimated flow parameters at the structure's location are a key difference among the methodologies (Chapter 3). In addition, there are many differences in the definitions of variables and the types of forces considered (Table 7-1)

Table 7-1: Tsunami Forces Considered by each Document

Considered Forces	Honolulu Code	FEMA P646	ASCE 7-16 Draft
Hydrostatic	YES	YES	YES
Buoyancy	YES	YES	YES
Hydrodynamic	YES	YES	YES
Uplift		YES	YES
Surge	YES	YES	YES
Debris Impact	YES	YES	YES
Debris Damming		YES	YES
Additional Forces		YES	YES

7.2 Application to Bridges

As was discussed in Chapter 4, there are a number of changes that would need to be implemented to adequately apply the building based tsunami-induced force equations to bridge superstructures. The three key differences are the elevation of the base of the structure, the structural geometry and the likelihood of channeling.

Unlike buildings, bridge superstructures are elevated above the ground, which can lead to much larger uplift forces due to varying flow velocities along the top and bottom of the bridge superstructure. The elevation difference will also influence the flow parameter approximation equations provided by FEMA P646 (dependent on ground elevation). Additionally, the definitions of the variables provided to calculate tsunami-induced forces will need to take into account this elevation difference.

The multiple geometric differences between buildings and bridges will also need to be taken into account when determining tsunami-induced forces on bridge superstructures. In the current documents the drag coefficient is either constant (FEMA P646), based on a select number of simple shapes (the Honolulu Code), or depends on the width-to-inundation depth ratio (ASCE 7-16 Draft). These drag coefficient may not be appropriate for many bridge geometries. Whereas a typical building is rectangular in elevation, a bridge superstructure can have a variety of geometries and configurations, depending on its purpose, location, and material. Abrupt changes in geometry can also lead to increased drag on a bridge superstructure. To address these challenges, it may be necessary to conduct a number of site-specific analyses on bridge superstructures to determine a set of drag coefficients for bridge superstructures.

In addition, the high likelihood of flow channeling for bridges will also need to be taken into account when determining tsunami-induced flow parameters and forces on bridge superstructures.

7.3 Case Studies

In Chapter 2, it was determined that concrete is by far the most widely used material type in the nominal inundation zones. The three most widely used geometries were tee-beam, deck-girder and slab type geometries (tables 2-3 to 2-7). For this reason, concrete slab and deck-girder bridge geometries were selected along the Pacific Ocean coastline to be examined in the case studies (Chapter 6).

The case studies illustrated the importance of determining location specific and conservative tsunami flow parameters. The flow parameters determined from the three codes and recommendations varied greatly. The methods for determining flow parameters described by the ASCE 7-16 draft (Section 3.5) appear to be significantly improved over the previously developed methods.

These case studies also suggested that varying fluid parameters (e.g., density and velocity) could have a large effect on the predicted tsunami-induced fluid forces. Additionally, it was discussed how differences in the structural geometry between the two bridge superstructures (slab or deck-girder) could influence the determined tsunami-induced forces, calculated under identical flow parameters.

7.4 Future Work

In the future, researchers should conduct experiments to calibrate force methodologies for common bridge geometries and construction methods. These tests should be accompanied by extensive numerical modeling to extend the experimental results to a much wider range of scenarios.

The states of Alaska, Washington, Oregon, California, and Hawaii are prone to large tsunamis. If measures are taken to adequately design or retrofit bridge superstructures, it is more likely that the transportation infrastructure along the coastline will be available to support response, evacuation and recovery efforts.

References

Aglipay, M.R.I., Keshab, S., Kyokawa, H., and Konagai K., "Bridges washed away by tsunami in Minamisanriku, Miyagi Prefecture in the March 11th 2011 Great Japan Earthquake", Seisan kenky$\bar{u}$, 63 (6), p. 723-727, 2011.

Akiyama, M., Frangopol, D.M., Arai, M., and Koshimura, S., "Probabilistic assessment of structural performance of bridges under tsunami hazard", *ASCE Structures Congress*, 2012.

American Association of State Highway and Transportation Officials (AASHTO), (2012), AASHTO LRFD Bridge Design Specifications, Section 3.8, 6th edition, Washington D.C.

Anderson, J.D., "Fundamentals of Aerodynamics", 6th edition, McGraw-Hill, Avenue of the Americas, New York, 2011.

Atwater, B.F., Satoko, M.R., Kenji, S., Yoshinobu, T., Kazue, U., and Yamaguchi, D.K., "The orphan tsunami of 1700: Japanese clues to a parent earthquake in North America", US Geological Survey, 2005.

Boon-intra, S. and Yim, S.C., "Development of a Guideline for Estimating Tsunami Forces on bridge Superstructures", November 30, 2010.

California State Department of Transportation, "Tsunami Hazard Guidelines", Memo to Designers 20-13, January 2010.

Carrier, G. F., Wu, T. T., and Yeh, H. (2003). "Tsunami runup and drawdown on a plane beach." J. *Fluid Mech.*, 62, pp. 97-109.

Chock, G., "ASCE 7 development of tsunami structural design provisions for the U.S.", presentation, retrieved May 24, 2013 from http://nees.org/resources/6277/supportingdocs

Chock, G., Chair of the ASCE 7 Tsunami Loads and Effects Subcommittee, "ASCE 7 Standards Committee Proposals No. I to XI to Revise the 2010 Edition of ASCE/SEI 7, retrieved March 27, 2014 from Chock, G.

Chock, G., Robertson, I., Kriebel, D., Francis, M., Nistor, I., "Tōhoku, Japan, Earthquake and Tsunami of 2011: Performance of Structures under Tsunami Loads", American Society of Civil Engineers (ASCE), Reston, Virgina, 2013.

Chock, G., Robertson, I., and Riggs, H.R., "Tsunami structural design provisions for a new update of building codes and performance-based engineering", *Solutions to Coastal Disasters*, pp. 423-435, 2011.

City & County of Honolulu (1980), Honolulu Flood Ordinance 16 Section 11, Regulations Within Flood Hazard Districts.

Cuomo, G., Shimosako, K., and Takahashi, S., "Wave-in-deck loads on coastal bridges and the role of air", *Coastal Engineering*, 56, pp. 793-809, 2009.

Douglass, S.L., Chen, Q., Olsen, J.M., Edge, B.L., and Brown, D., "Wave forces on bridge decks", U.S. Department of Transportation Federal Highway Administration, Office of Bridge Technology Washington D.C.

FEMA P646, Guidelines for Design of Structures for Vertical Evacuation from Tsunamis, Federal Emergency Management Agency, Washington, DC, 2008.

Haehnel, R.B., and Daly, S.F., 2002, "Maximum Impact Force of Woody Debris on Floodplain Structures", Technical Report ERDC/CRREL TR-02-2, U.S. Army Corps of Engineers. Springfield, Virginia.

Kajitani, Y., Change, S.E., and Tatano, H., "Economic impacts of the 2011 Tōhoku-Oki earthquake and tsunami", Earthquake Spectra, 29 (s1), pp. S457-S478, 2013.

Kosa, K., "Damage analysis of bridges affected by tsunami due to Great East Japan Earthquake", Proceedings of the International Symposium on Engineering Lessons Learned from the 2011 Great East Japan Earthquake, pp. 1386-1397, 2012.

Murakami, K., Sakamoto, Y., and Nonaka, T., "Analytical investigation of slab bridge damages caused by tsunami flow", Coastal Engineering Proceedings, 1 (33), 2012.

National Bridge Inventory Database, U.S. Department of Transportation: Federal Highway Administration, from: www.fhwa.dot.gov.

National Oceanic and Atmospheric Administration, "The Tsunami Story", from: www.tsunami.noaa.gov.

Peregrine, D. H., and Williams, S. M., "Swash overtopping a truncated plane beach", J. *Fluid Mech*., 440, pp. 391-399, 2001.

Rabinovich, A. B., Thomson, R. E., Kulikov, E. A., Bornhold, B. D., and Fine, I. V., "The landslide-generated tsunami of November 3, 1994 in Skagway Harbor, Alaska: A case study", 1999.

Ramsden, J.D., "Tsuanmis: Forces on a vertical wall caused by long waves, bores, and surges on a dry bed", Report No.KH-R-54, W. M. Keck Laboratory, California Institute of Technology, Pasadena, Calif., 251 pp, 1993.

Robertson, I.N., Riggs, H.R., Yim, S.C.S., and Young, Y.L., "Lessons from Hurricane Katrina storm surge on bridges and buildings", Journal of Waterway, Port, Coastal and Ocean Engienering, 133, pp. 463-483, 2007.

Robertson et, I.N., Yim, S.C., and Tran, T., "Case study of concrete bridge subjected to hurricane storm surge and wave action", *Solutions to Coastal Disasters,* 2011.

Shen, M. C., and Meyer, R. E. (1963). "Climb of a bore on a beach. Part 3. Run-up" J. *Fluid Mech.,* 16, pp. 113-125.

U.S. Department of Commerce, National Oceanic and Atmospheric Administration (NOAA), "Floods: the Awesome Power", March 2005.

Walsh, T., Caruthers, C., Heinitz, A., Myers III, E., Baptista, A., Erdakos, G., and Kamphaus, R., "Tsunami Hazard Map of the Southers Washington Coast: Modeled Tsunami Inundation from a Cascadia Subduction Zone Earthquake", prepared for the Washington State Department of natural Resources, October 2000.

Yeh, H., Robertson, I., and Preuss, J., "Development of design guidelines for structures that serve as tsunami vertical evacuation sites", Report 2005-4, Washington State Department of Natural Resources, November 2005.

Yeh, H., "Maximum Fluid Forces in the Tsunami Runup Zone", Journal of Waterway, port, Coastal, and ocean Engineering © ASCE, November/December 2006.

Yeh, H., "Design tsunami forces for onshore structures", Journal of Disaster Research, 2 (6), pp. 531-536, 2007.

Yim, S.C., "Modeling and simulation of tsunami and storm surge hydrodynamic loads on coastal bridge structures", 2005.

Yim, S.C., Boon-intra, S., Nimmala, S.B., Winston, H.M., Azadbakht, M., and Kwok, F.C., "Development of a guideline for estimating tsunami forces on bridge superstructures", Final Report SR 500-340 for Oregon Department of Transportation, October 2011.

Appendix A ArcMap™

The mapping program ArcMap™ was used to analyze the NBI database to find the locations of bridges in the coastal counties or boroughs. Initially, a world topographic map layer was established along with a geographical coordinate system, which will be discussed below. The distortions of this topographic map increase as you move away from the equator due to the map projection used. These distortions occur because the earth is a sphere or spheroid and therefore to be able to look at it on a two-dimensional map the three-dimensional spheroid must be transformed or projected. Distortions in the shape, area or distance arise from the fact that a sphere cannot be flattened. In the case of the selected topographic map the projection that was used is a Mercator Auxiliary Sphere, which uses a cylindrical type projection (ArcGIS Help 10.1). The cylinder will be tangent to the globe along one line and distortions increase as you move away from this line, as shown in Figure A-1.

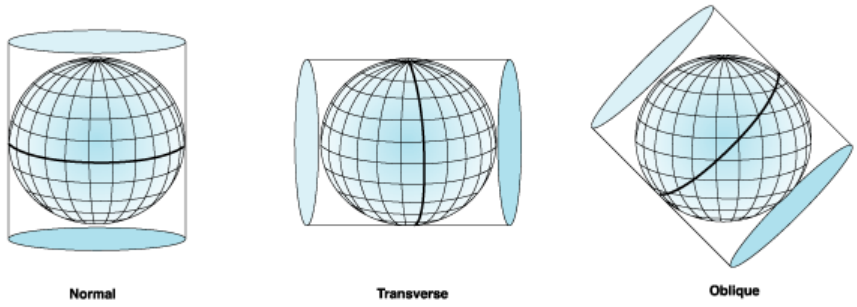

Figure A-1: Cylindrical Type Projection (ArcGIS Resource Center)

Typically the normal cylindrical projection is used for Mercator projections, which leads to the best accuracy along the equator and increasing distortions as you move towards the poles. These distortions were not of great concern because the bridge locations were dependent on a geographic coordinate system, unlike the topographic map which was also based on a map projection. A section of the topographic map layer that was added can be seen in Figure A-2.

Figure A-2: World Topographic Map

As can easily be seen in Figure A-2, Alaska's shape is distorted relative to its true size. This arises from map projection as discussed above. Again the bridge location data was based only on a geographic coordinate system and was not projected and therefore should not be distorted to the extent that Alaska is.

The NBI information was then imported into ArcMap™ as a spreadsheet for each state and converted into a format ArcMap™ could recognize. With this data in a table format it was then displayed as X and Y coordinates based on the coordinate data for each bridge and created as a layer. This layer was then modified through geoprocessing tools and map editing tools so that only the bridge locations in the five states were displayed. Figure A-3 shows an example of the corresponding bridge locations in Washington and Oregon, where the bridges outside of the coastal regions have not yet been eliminated from the map.

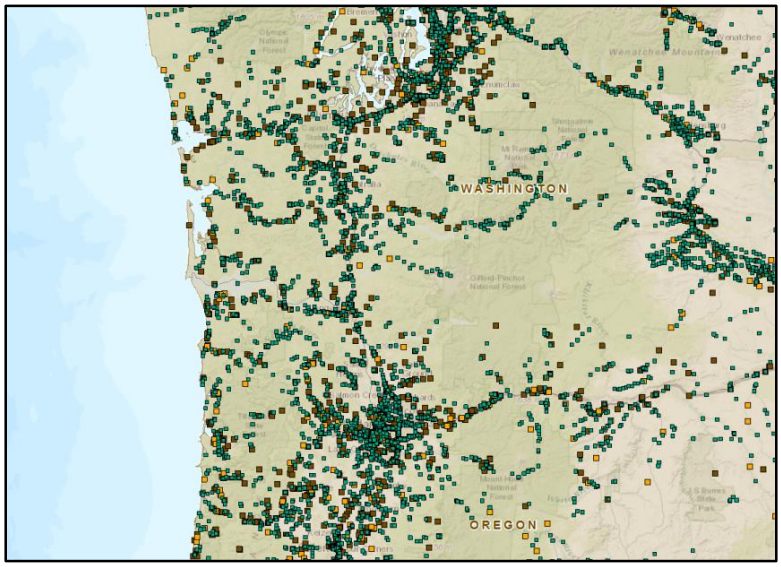

Figure A-3: Bridge Locations in states of Washington and Oregon

Following the addition of the NBI map layer, a coastal outline layer was imported and can be seen in Figure A-4 for Washington.

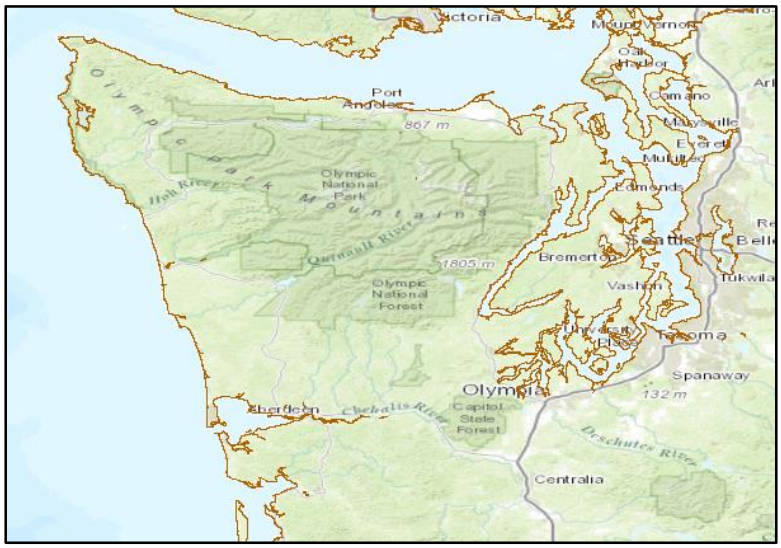

Figure A-4: Olympic Peninsula Coastline (Washington State)

The coastline layers extend down the entire west coast of the continental United States along with the entire coastlines of Alaska and Hawaii. Like the topographic map these coastline outlines can also have distortions. After establishing the position of the coastline, a one-mile

offset around the coastline layer was created by using the geoprocessing command "Buffer". The one-mile buffer was chosen to help counteract the distortions that may be present in the coastline outline and therefore allow for a representative sample of bridges in the five state's respective coastal regions. Once the buffer had been established the bridges that were outside of the buffer were eliminated by specifying that every point outside of the buffer should be eliminated. This was done state by state so that there would be separate tables of bridge information for each state. The remaining bridges were then within the nominal inundation zone. An example of the bridges of interest along the coast of Washington can be seen in Figure A-5. It should be noted that the bridges within the Puget Sound will not be considered due to the relatively large uncertainty in predicting tsunami inundations in that region.

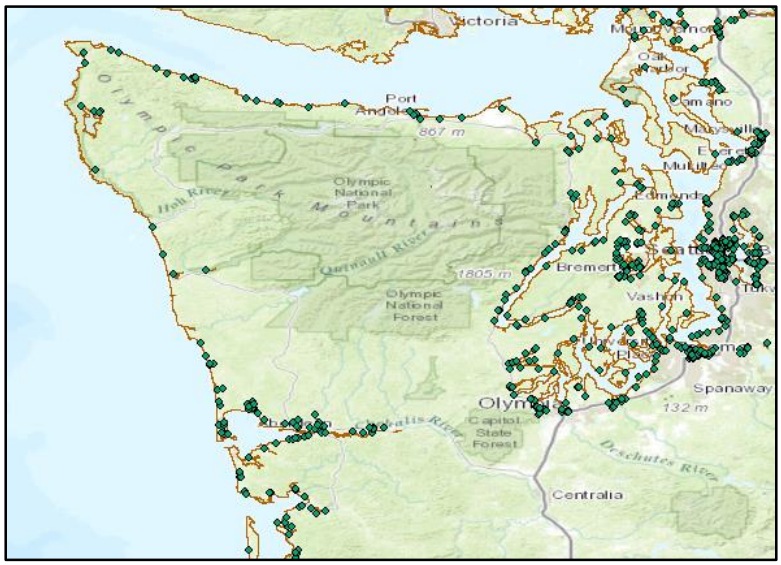

Figure A-5: Olympic Peninsula Coastline Bridges (Washington State)

A count of the bridges within the nominal inundation zone was important to help distinguish what the most likely material and structure types were in each state. From this information, basic tsunami force analysis could be performed based on the types of bridges in the nominal inundation zone. From the analysis it was discovered that the largest percentage of bridge types along the five states respective coast lines were prestressed reinforced concrete slab type bridges for Washington and Oregon, continuous reinforced concrete girder type bridges for California, continuous reinforced concrete tee beam bridges for Hawaii and steel girder bridge types for Alaska.

It is important to note that each map layer that was added needed to have identical geographic coordinate systems to limit any alignment errors that may exist. The geographical coordinate system that was used for this analysis was the World Geodetic System (WGS) 1984.

All of the layers had identical coordinate systems; however, this does not mean that errors do not exist. The topographic map was also dependent on the projection it used, and because ArcMap™ does corrections instantaneously (corrects data to fit the first map imported) this may have distorted the coastal outlines and bridge locations. To make sure this did not take place, the coastal outlines and bridge locations were imported into the program OpenJUMP™ which does not do corrections instantaneously and places the data based only on the coordinates of the data. The positions of the coastline outlines and bridge locations were then verified and it was determined that their positions were adequate in ArcMap™. Figure A-6 shows this verification of the coastline outlines and coastal bridge locations in the OpenJUMP™ program. The extent of the data East to West was -117 to -179 degrees and North to South was 62 to 19 degrees, which is what you would expect based on the true coordinates of these locations on the earth.

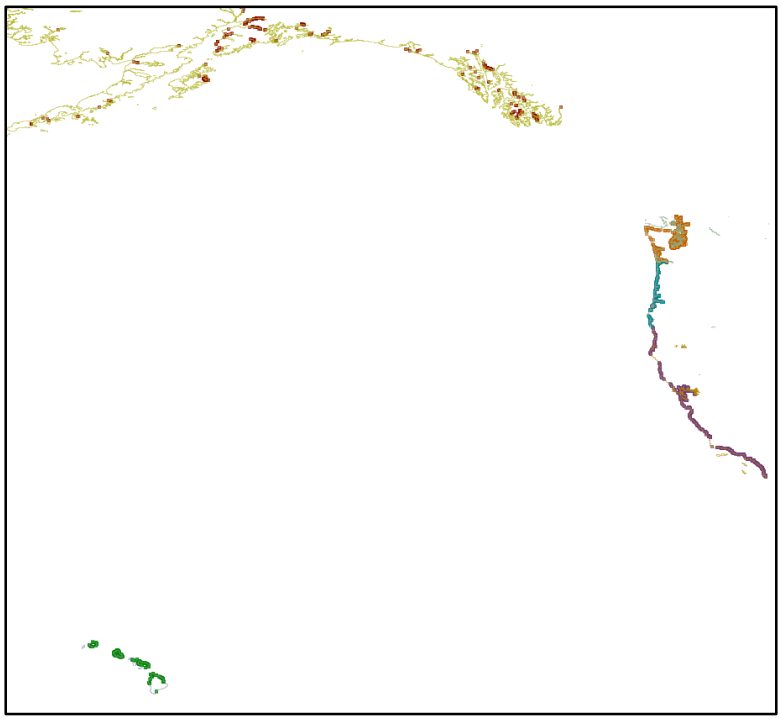

Figure A-6: OpenJUMP™ Position Verification

All of the bridges that were determined to be within the nominal inundation zone of one mile from the coastline may actually not experience tsunami forces. The NBI data did not include the elevation of the bridges and therefore there will be some that are well above the elevation that a design tsunami inundation could reach. The statistics determined from this study should still be representative of the types of bridges along the coastlines of the five states that were examined.

Appendix B Case Study Sample Calculations

Tables B-1 and B-2 show the design flow parameters along with the design forces determined from these design flow parameters respectively. The values from Table B-1 will be used in the following sample calculation section (Section B.1) for the Wreck Creek Bridge superstructure. Additionally, sample calculations for the flow parameter estimates by both the FEMA P646 recommendations and the ASCE 7-16 draft are provided in Section B.2.

Table B-1: Design Flow Parameters

Flow Parameter	Design Value
Maximum Design Inundation Depth	6.3 m (8.2 m for FEMA P646)
Design Horizontal Flow Velocity	8.6 m/s
Design Vertical Flow Velocity	0.79 m/s
Design Momentum Flux	84.26 m^3/s^2
Maximum Design Momentum Flux	84.26 m^3/s^2

Table B-2: Design Forces

Codes, Recommendations or Research	Buoyancy Force (kN)	Hydrodynamic Force (kN)	Surge Force (kN)	Uplift Force (kN)
Honolulu Building Code	1,670	1,372	7,174	N/A***
FEMA P646	1,946	4,361	6,541	2,387
"Chock"	1,913	3,216	3,216	N/A***
"Douglass"	N/A***	N/A***	1,312	4,519* / 18,075**
"Yim"	N/A***	4,356	N/A***	26,468

* Represents "Douglass" uplift not considering surge impact
** Represents "Douglass" uplift considering surge impact
*** Equation was not provided by the given code, recommendation or document

B.1 Wreck Creek Bridge Sample Calculations:

This section of Appendix B contains the sample calculations for each of the methods used to determine the tsunami forces on the Wreck Creek Bridge superstructure. The forces determined in this section are identical to that of those shown in Table 6-3, displayed in Subsection 6.3.3. Tables B-2 and B-3 show general dimensions for the Wreck Creek Bridge superstructure that will be used for each of the methods for calculating the tsunami forces.

Table B-3: General Bridge Dimensions

Dimension	Value
Elevation at top of deck	5.49 m
Elevation at bottom of deck	5.13 m
Elevation at lowest point of cross-section	4.34 m
Length	43.13 m
Width	9.14 m

Table B-4: Bridge Dimensions for Force Calculations at Design Inundation Depth

Variable	Description	Value
V	Volume of bridge submerged	165.264 m^3
b	Width of bridge submerged	43.13 m
A_n	Projected are normal to flow	18.07 m^2
A_f	Horizontal projected area	394.37 m^2

Each of the methods used to determine the tsunami forces on Wreck Creek Bridge superstructure will be conducted separately below. Any error between that of the tsunami forces determined from Matlab and the hand calculations, below, is simply due to rounding.

Honolulu Building Code

Hydrostatic Force

$$F_h = \frac{1}{2}\rho b g \left\{h + \frac{u^2}{2g}\right\}^2$$

Due to the assumption of rapid inundation, full submergence, and no water tight areas hydrostatic forces do not influence the Wreck Creek Bridge superstructure (except for bore impacts).

Buoyancy Force

$$F_b = \rho g V$$

Where the fluid density is assumed to be equal to 1,030 kg/m^3 for the Honolulu Building Code:

$$F_b = \frac{1}{1000} * 1{,}030\ \frac{kg}{m^3} * 9.81\ \frac{m}{s^2} * 165.264\ m^3 \cong \mathbf{1{,}670\ kN}$$

Hydrodynamic Force

$$F_d = \frac{1}{2}\rho C_d A_n u^2$$

Where the drag coefficient is assumed to be 2.0 for the Honolulu Building Code:

$$F_d = \frac{1}{1000} * \frac{1}{2} * 1{,}030\ \frac{kg}{m^3} * 2.0 * 18.07\ m^2 * \left(8.6\frac{m}{s}\right)^2 \cong \mathbf{1{,}376\ kN}$$

Uplift Force

This equation is not provided by the Honolulu Building Code and should be assumed to be due to buoyancy alone.

Surge Force

$$F_{bore} = 4.5\rho g h_b^2$$

Because the Wreck Creek Bridge superstructure has a height less than three times the surge height, a combination of the hydrostatic and hydrodynamic forces is used to determine the surge force. During the initial impact of the surge there will be hydrostatic force acting on the Wreck Creek Bridge superstructure.

$$F_{bore} = \frac{1}{2}\rho b g \left\{h + \frac{u^2}{2g}\right\}^2 + \frac{1}{2}\rho C_d A_n u^2$$

Because the superstructure does not start at the ground the hydrostatic portion of the above equation needs to be modified to correctly represent the hydrostatic force.

$$F_{bore} = \rho b g h^2 + \frac{1}{2}\rho b g \left\{h + \frac{u^2}{2g}\right\}^2 + \frac{1}{2}\rho C_d A_n u^2$$

$$h = 5.49\ m - 4.34\ m = 1.15\ m$$

$$F_{bore} = \left(1{,}030\ \frac{kg}{m^3} * 43.13\ m * 9.81\frac{m}{s^2} * (1.15\ m)^2 + \frac{1}{2} * 1{,}030\ \frac{kg}{m^3} * 43.13\ m * 9.81\frac{m}{s^2} \cdots \right.$$
$$\left. * \left\{ 1.15\ m + \frac{\left(8.6\frac{m}{s}\right)^2}{2 * 9.81\frac{m}{s^2}} \right\}^2 + \frac{1}{2} * 1{,}030\ \frac{kg}{m^3} * 2.0 * 18.07\ m^2 * \left(8.6\frac{m}{s}\right)^2 \right) \cdots$$
$$* \frac{1}{1000} \cong \mathbf{7{,}227\ kN}$$

FEMA P646

Hydrostatic Force

$$F_h = p_c A_w = \frac{1}{2}\rho_s g b h_{max}^2$$

Due to the assumption of rapid inundation, full submergence, and no water tight areas hydrostatic forces do not influence the Wreck Creek Bridge superstructure.

Buoyancy Force

Where the fluid density is assumed to be equal to 1,200 kg/m^3 for FEMA P646:

$$F_b = \frac{1}{1000} * 1200\ \frac{kg}{m^3} * 9.81\ \frac{m}{s^2} * 165.264\ m^3 \cong \mathbf{1,946\ kN}$$

Hydrodynamic Force

$$F_d = \frac{1}{2}\rho_s C_d b (hu^2)_{max}$$

Where the drag coefficient is assumed to be 2.0 for FEMA P646:

$$F_d = \frac{1}{1000} * \frac{1}{2} * 1{,}200\ \frac{kg}{m^3} * 2.0 * 43.13\ m * \left(84.26 \frac{m^3}{s^2}\right) \cong \mathbf{4,361\ kN}$$

Uplift Force:

$$F_u = \frac{1}{2} C_u \rho_s A_f u_v^2$$

$$F_u = \left(\frac{1}{2} * 3.0 * 1{,}200\ \frac{kg}{m^3} * 394.37\ \text{m}^2 * \left(0.79 \frac{m}{s}\right)^2\right) * \frac{1}{1000} \cong \mathbf{443\ kN}$$

Surge Force

$$F_{bore} = 1.5 * F_d$$

$$F_{bore} = 1.5 * 4{,}361\ kN \cong \mathbf{6,541\ kN}$$

ASCE 7 – 16 Draft Proposal

Hydrostatic Force

$$F_h = \frac{1}{2}\gamma_s b h_{max}^2 = \frac{1}{2}\rho_s g b h_{max}^2$$

Due to the assumption of rapid inundation, full submergence, and no water tight areas hydrostatic forces do not influence the Wreck Creek Bridge superstructure.

Buoyancy Force

$$F_b = \gamma_s V_w = \rho_s g V$$

Where the fluid density is assumed to be equal to 1,128 kg/m^3 for ASCE 7-16 draft proposal:

$$F_b = \frac{1}{1000} * 1128\ \frac{kg}{m^3} * 9.81\ \frac{m}{s^2} * 165.264\ m^3 \cong \mathbf{1,828\ kN}$$

Hydrodynamic Force

$$F_d = F_{dx} = \frac{1}{2}\rho_s I_{tsu} C_d C_{cx} b(hu^2)$$

Where the drag coefficient is assumed to be 1.5 for ASCE 7-16 draft proposal at the design inundation depth:

$$F_d = \frac{1}{1000} * \frac{1}{2} * 1{,}128\ \frac{kg}{m^3} * 1.0 * 1.5 * 1.0 * 43.13\ m * \left(84.26 \frac{m^3}{s^2}\right) \cong \mathbf{3,075\ kN}$$

Uplift Force

$$P_u = 1.5 I_{tsu} \rho_s u_v^2$$

Or for the case of the Wreck Creek location with the small grade:

$$P_u = 20\ psf$$

$$P_u = 20\ psf = 957.6 \frac{N}{m^2} * 394.37\ m^2 * \frac{1}{1000} = \mathbf{377.6\ kN}$$

If buoyancy is included the new uplift force will be approximately $\mathbf{2,205.6\ kN}$

Surge Force

$$F_{bore} = F_w = \frac{3}{4}\rho_s I_{tsu} C_d b(h_e u^2)$$

$$F_{bore} = F_w = \frac{3}{4} * 1{,}128\ \frac{kg}{m^3} * 1.0 * 1.5 * 43.13\ m * \left(84.26 \frac{m^3}{s^2}\right) * \frac{1}{1000} = \mathbf{4{,}611.7\ kN}$$

Douglass

Hydrostatic Force

$$F_h = [1 + c_r(N-1)]c_{h-va}F_h^* \qquad F_h^* = \rho g(\Delta z_h)A_h$$

Due to the assumption of rapid inundation, full submergence, and no water tight areas hydrostatic forces do not influence the Wreck Creek Bridge superstructure (except for bore impacts).

Buoyancy Force

Buoyancy is not directly provided by Douglass, but is included in the uplift equation. Additionally, the buoyancy force increases as the depth increases even when the bridge is fully submerged. This increase in the buoyancy force is fundamentally incorrect, once the bridge superstructure is fully submerged buoyancy will be constant. Keep in mind, Douglass's equations are for waves that are just striking the bottom of a deck-girder bridge and may not apply to this situation.

Hydrodynamic Force

Again Douglass's equations are for waves that are just striking the bottom of a deck-girder bridge and therefore do not take into account flow velocities and thus hydrodynamic forces are not considered.

Uplift Force

$$F_u = c_{v-va}F_v^* \qquad F_v^* = \rho g(\Delta z_v)A_v$$

Where the fluid density is assumed to be equal to 1,000 kg/m^3 and c_{v-va} = 1.0:

$$\Delta z_v = design\ runup\ elevation - elevation\ of\ bottom\ of\ bridge\ deck$$

$$\Delta z_v = 6.3\ m - 5.13\ m = 1.17\ m$$

$$F_u = 1.0 * \left(1000\ \frac{kg}{m^3} * 9.81 \frac{m}{s^2} * 1.17\ m * \ 394.37\ \text{m}^2\right) * \frac{1}{1000} \cong \mathbf{4{,}526\ kN}$$

Including vertical surge:

$$F_u = \{c_{v-va} + c_{v-im}\}F_v^*$$

Where c_{v-im} = 3.0:

$$F_u = \{1.0 + 3.0\} * \left(1000\ \frac{kg}{m^3} * 9.81 \frac{m}{s^2} * 1.17\ m *\ 394.37\ \text{m}^2\right) * \frac{1}{1000} \cong \mathbf{18,106\ kN}$$

Surge Force

$$F_h = \{[1 + c_r(N-1)]c_{h-va} + c_{h-im}\}F_h^* \qquad F_h^* = \rho g(\Delta z_h)A_h$$

Where c_r = 0.4, c_{h-va} = 1.0, c_{h-im} = 6.0, and N = 1:

$$\Delta z_h = design\ runup\ elevation - elevation\ of\ centroid\ of\ wetted\ area\ normal\ to\ flow$$

$$= 6.3\ m - 5.24\ m = 1.06\ m$$

$$F_u = \{[1 + 0.4 * (1-1)] * 1.0 + 6.0\} * \left(1000\ \frac{kg}{m^3} * 9.81 \frac{m}{s^2} * 1.06\ m *\ 18.07\ \text{m}^2\right) * \frac{1}{1000} \cdots$$
$$\cong \mathbf{1,315\ kN}$$

Yim:

Hydrostatic Force

$$F_h = \big(1 + C_r(N-1)\big)C_h F_h^* \qquad F_h^* = \rho_s g(\Delta h_{max})A_h$$

Due to the assumption of rapid inundation, full submergence, and no water tight areas hydrostatic forces do not influence the Wreck Creek Bridge superstructure.

Buoyancy Force

Buoyancy is not directly provided by Yim, but is included in the uplift equation. Additionally, the buoyancy force increases as the depth increases even when the bridge is fully submerged. This increase in the buoyancy force is fundamentally incorrect, once the bridge superstructure is fully submerged buoyancy will be constant.

Hydrodynamic Force

$$F_d = \frac{1}{2} C_d \rho_s b(\Delta h u^2)_{max}$$

Where the fluid density is assumed to be equal to 1,199 kg/m^3 and C_d = 2.0:

$$F_d = \frac{1}{2} * 2.0 * 1199 \frac{kg}{m^3} * 43.13\ m * 84.26 \frac{m^3}{s^2} * \frac{1}{1000} \cong \mathbf{4,357\ kN}$$

Uplift Force

$$F_u = \left[\rho_s g(\Delta h_{max}) + \frac{1}{2}\rho_s u_{x,max}^2\right] A_v$$

$$\Delta h_{max} = Design\ runup\ elevation - bottom\ elevation\ of\ bridge$$

$$\Delta h_{max} = 6.3\ m - 4.34\ m = 1.96\ m$$

$$F_u = \left[1199\frac{kg}{m^3} * 9.81\frac{m}{s^2} * 1.96\ m + \frac{1}{2} * 1199\frac{kg}{m^3} * \left(8.6\frac{m}{s}\right)^2\right] * 394.37\ \text{m}^2 * \frac{1}{1000} \cdots$$
$$\cong \mathbf{26,578\ kN}$$

Surge Force

A surge force equation was not provided by Yim.

B.2 Flow Parameter Estimates by both FEMA P646 and the ASCE 7-16 Draft Proposal:

The horizontal flow velocity was estimated by the Honolulu Building Code, the FEMA P646 recommendations, and the ASCE 7-16 draft proposal in Subsection 6.2.3, this section of Appendix B shows how the flow parameters were estimated by both the FEMA P646 recommendations and the ASCE 7-16 draft proposal (the Honolulu Code estimate is not shown due to the trivial nature of the calculation).

FEMA P646:

To estimate the horizontal flow velocity for the design runup elevation of 8.2 m for FEMA P646 Figure 3-6 and Equation 3-4 were employed.

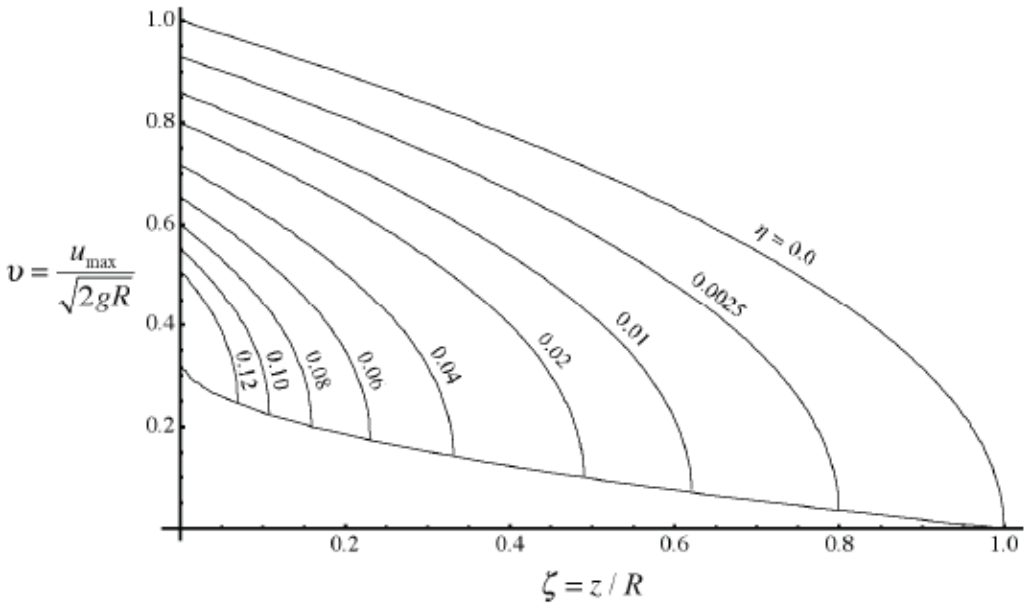

$$\eta = \frac{h_s}{R}$$

Because of the elevations of the bridges being close to the design runup the value of η is much greater than 0.12 (closest η curve to y axis) and the value of ζ being equal to 0.15 the velocities are obtained from the lower limit curve.

$$\eta = \frac{h_s}{R} = \frac{4.34\ m}{8.2\ m} = 0.53$$

$$\zeta = \frac{z}{R} = \frac{1.2\ m}{8.2\ m} = 0.15$$

Applying the ζ value to the above curve leads to the following value for ν:

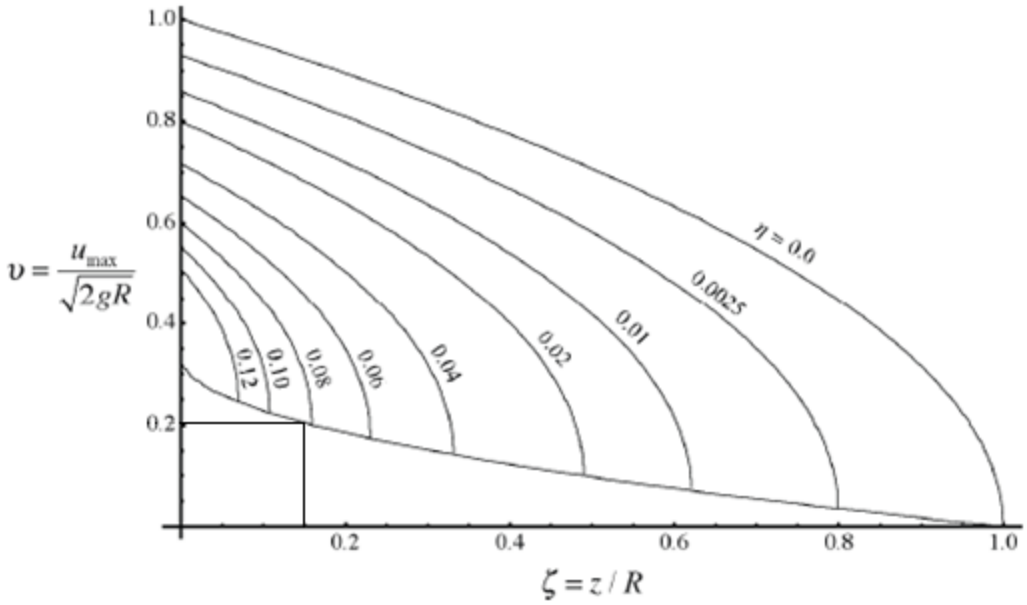

$$\nu \approx 0.205 = \frac{u_{max}}{\sqrt{2 * g * R}} = \frac{u_{max}}{\sqrt{2 * 9.81 \frac{m}{s^2} * 8.2\ m}}$$

therefore,

$$u_{max} \cong \mathbf{2.6}\ \frac{\boldsymbol{m}}{\boldsymbol{s}}$$

This is identical to that shown in Table 6-1.

In Subsection 6.2.5 the maximum momentum flux was also estimated by an equation provided by the FEMA P646 recommendations, the calculation can be seen below.

$$(hu^2)_{max} = gR^2 \left(0.125 - 0.235 \left(\frac{z}{R}\right) + 0.11 \left(\frac{z}{R}\right)^2\right)$$

$$= 9.81\ \frac{m}{s^2} * (8.2\ m)^2 \left(0.125 - 0.235 * \frac{1.2\ m}{8.2\ m} + 0.11 * \left(\frac{1.2\ m}{8.2\ m}\right)^2\right) = \mathbf{61.3}\ \frac{\boldsymbol{m^3}}{\boldsymbol{s^2}}$$

This is identical to the maximum momentum flux seen in Figure 6-11

ASCE 7-16 Draft Proposal:

The Energy Grade Line (EGL) method that was supplied by the ASCE 7-16 draft proposal was used to estimate both the flow depth and the horizontal flow velocity at the Wreck Creek Bridge area for the case studies conducted in Chapter 6. The EGL method is a spatial step method that steps along a topographic transect where the designer determines both the design inundation limit and runup elevation from available inundation limit maps and then steps backwards from the design runup elevation to the shore line determining flow depths and velocities along the way. For the purpose of the case studies the EGL method was conducted in Matlab, two spatial steps will be shown here as an example. Recall from Table 6-2 that the design runup elevation was 6.3 m, to determine the inundation limit the general beach slope was used as the average slope at the site (the inundation limit graph found (Figure 6-8) only contained inundation elevation not an inundation limit). This will lead to a large over estimation in the inundation limit, and in a real design situation the topography at the site needs to be determined.

$$Beach\ Slope = \frac{rise}{run} = \frac{1.23\ m}{535.5\ m} \cong 0.0023$$

$$Inundation\ Limit = \frac{Design\ Runup\ Elevation}{Beach\ Slope} = \frac{6.3\ m}{0.0023} \cong 2{,}743\ m$$

An inundation limit of almost 3 kilometers is due to the use of the very small beach slope, even though the application of the EGL method can still be examined. Now that the topography (beach slope), design inundation limit, and design runup elevation are known the EGL method can be used. For the case of this study the beach slope represents the average ground slope (φ_i) between every point. Five hundred points were evaluated along the topographic transect line to calculate both the flow velocity and depth. Additionally, a Manning's Roughness Coefficient (n) of 0.03 was selected from Table 3-4. To begin a very small inundation depth was used at the design runup elevation ($h_1 = 0.03$ m) and the change in x was calculated, this value can be seen below.

$$dx_i = \frac{Inundation\ Limit}{Number\ of\ Transect\ Points}$$

$$dx_i = \frac{2{,}743\ m}{500} = 5.4856\ m$$

Now with an initial value of the hydraulic head ($E_{g,1}$) of zero at the design runup elevation the required values can be calculated and then one spatial step towards the shoreline may be made.

Step 1 (at design runup elevation)

$$\frac{x_1}{x_R} = \frac{2{,}743\ m}{2{,}743\ m} = 1$$

$$Froude\ Number\ at\ i = F_{r1} = \left(1 - \frac{x_1}{x_R}\right)^{.5} = 0$$

$$Friction\ Slope\ at\ i = s_1 = \frac{g * F_{r1}^2}{\left(\frac{1}{n}\right)^2 * h_1^{1/3}} = 0$$

$$Flow\ Velocity\ at\ i = u_1 = F_{r1} * (g * h_1)^{.5} = 0.0\ \frac{m}{s} = 3.0\frac{m}{s}\ (required\ minumim)$$

$$E_{g,i+1} = E_{g,i} + (\varphi_i + s_i) * dx_i = E_{g,2} = E_{g,1} + (\varphi_1 + s_1) * dx_1$$

$$E_{g,2} = 0 + (0.0023 + 0) * 5.4856\ m \cong 0.0126\ m$$

Step 2 (one step (dx) closer to shoreline)

$$x_2 = x_1 - dx = 2{,}743\ m - 5.4856\ m = 2{,}737.5\ m$$

$$z_2 = x_2 - Beach\ Slope = 2{,}737.5\ m * 0.0023\ m = 6.29\ m$$

$$\frac{x_2}{x_R} = \frac{2{,}737.5\ m}{2{,}743\ m} = 0.998$$

$$Froude\ Number\ at\ i = F_{r2} = \left(1 - \frac{x_2}{x_R}\right)^{.5} \cong 0.04472$$

$$h_2 = \frac{E_{g,2}}{1 + 0.5 * F_{r2}^2} = \frac{0.0126}{1 + 0.5 * 0.04472^2} \cong 0.0126\ m$$

$$Friction\ Slope\ at\ i = s_2 = \frac{g * F_{r2}^2}{\left(\frac{1}{n}\right)^2 * h_2^{1/3}} \cong 0.000076$$

$$Flow\ Velocity\ at\ i = u_2 = F_{r2} * (g * h_2)^{.5} \cong 0.016\ \frac{m}{s} = 3.0\frac{m}{s}\ (required\ minumim)$$

$$E_{g,i+1} = E_{g,i} + (\varphi_i + s_i) * dx_i = E_{g,3} = E_{g,2} + (\varphi_2 + s_2) * dx_2$$

$$E_{g,3} = 0.0126 + (0.0023 + 0.000076) * 5.4856\ m \cong 0.0256\ m$$

Applying the above until the ground elevation at the bridge site was reached (1.22 m) resulted in an inundation elevation of 8.34 m (identical to Figure 6-7) and a horizontal flow velocity of 7.5 m/s (identical to Table 6-1). This same process was used when the inundation depth was varied for the case studies in Chapter 6 to determine the estimated horizontal flow velocities form the ASCE 7-16 draft proposal.

Appendix C WSDOT Plans for Wreck Creek Bridge

FED. ROAD DIV. NO.	STATE	FED. AID PROJ. NO.	FISCAL YEAR	SHEET NO.	TOTAL SHEETS
8	WASH.				

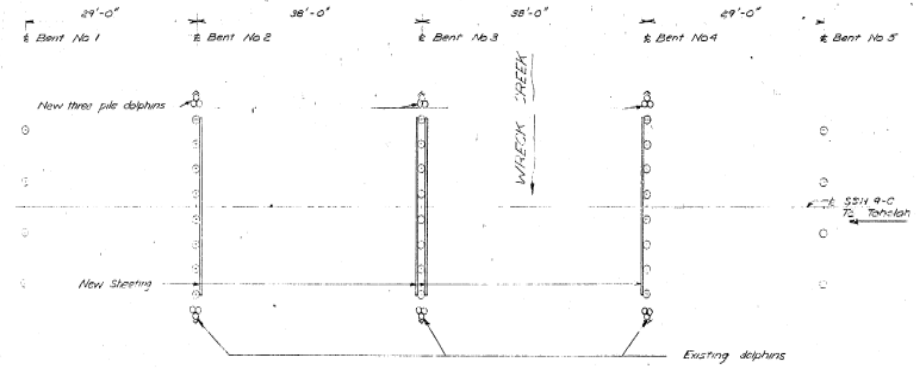

PILING AND SHEETING LAYOUT

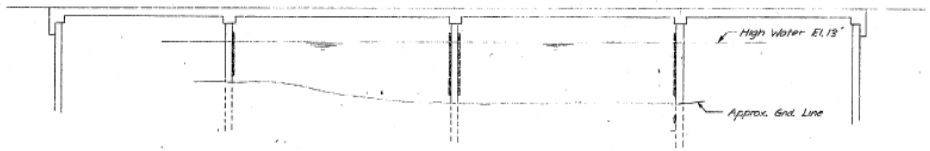

PROFILE

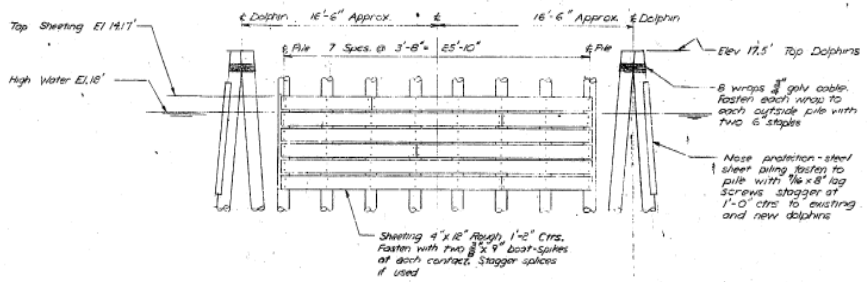

PILING AND SHEETING DETAIL

GENERAL NOTES

All material and work shall be in accordance with the requirments of the State of Washington, Department of Highways Standard Specifications for Road and Bridge Construction dated July 1957.

All piles shall be treated by the Full-Cell Process to provide a minimum retention of fourteen (14) lbs. of creosote oil per cu. ft. of pile. Piles shall be driven to a minimum penetration of 44 feet and to a minimum bearing capacity of fifteen tons.

All timber and lumber shall be pressure treated by the Empty-Cell Process to provide a minimum retention of ten (10) lbs. of creosote oil per cubic foot of timber and shall be "construction" grade

All hardware shall be galvanized in accordance with A.S.T.M. designation A-153.

Estimated length of piles 25' below cut-off

SUMMARY OF QUANTITIES

ITEM NO	ITEM	QUANTITY	UNIT
1	Timber and Lumber (Creosote Treated)	6.8	M.B.M
2	Furnishing Timber Piling (Creosote Treated)	225	lin. ft.
3	Driving Timber Piling First 10 feet	9	Only
4	Driving Timber Piling Over 10 feet	135	lin ft.
5	Sheet Piling - Steel	50	lin. ft.

SECONDARY STATE HIGHWAY 1/C 9-C
WRECK CREEK BRIDGE NO. 9-C/13
GRAYS HARBOR COUNTY

DOLPHIN AND SHEETING CONSTRUCTION

WASHINGTON STATE HIGHWAY COMMISSION
DEPARTMENT OF HIGHWAYS
OLYMPIA WASHINGTON

E.A. COWELL CHAIRMAN

J.M. BLAIR, SR. R.L. MIKALSON
G.D. TAHN EJ VETCHAM

APPROVED Sept. 15, 1961
BRIDGE ENGINEER

SHEET 1 OF 1 SHEETS

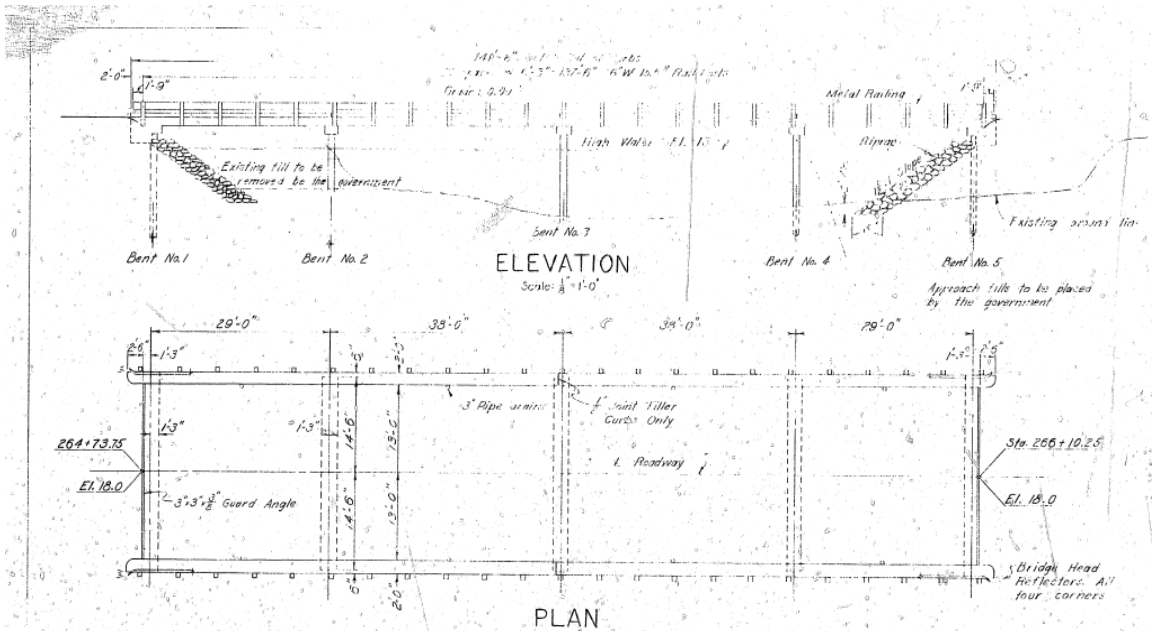

GENERAL NOTES

Specifications: Construction: As listed in the contract Standard Form 23, Revised March 1953.
Design: A.A.S.H.O. Standard Specifications for Highway Bridges, 1953.
Dead Load: Concrete 150 lb. per cu. ft. Paving allowance 25 lb. per sq. ft. of roadway surface.
Live Load: H 15 - S 12 - 44 Loading, Impact 30%.
Unit Stresses: f_c = 1320 p.s.i. f_s = 20,000 p.s.i. n = 10.
Concrete: All concrete shall be Class 'A'. All exposed corners shall be chamfered 3/4" unless otherwise noted.
Finishing Concrete: Both faces of curbs and slab and end faces of caps shall have a "Rubbed" Finish. All other surfaces shall have an "Ordinary" Finish.
Reinforcing Steel: All bars shall be deformed intermediate grade open steel conforming to A.S.T.M. Specification A 15-54 T. All bars shall be supported on "metal chairs". Except as shown all dimensions refer to centers of bars.
Bridge Railing: All items of steel bridge railing shall be galvanized.
Bridge Head Reflectors: Will be furnished by the Contracting Agency. The cost of installation will be included in the contract price for "Bridge Railing".
Piles: Piles shall be coast variety Douglas fir. Piles shall be treated by the full cell process with Creosote Oil preservative. Treatment shall be for use in coastal waters with minimum retention of preservative of 14 lb. per cu. ft. of wood. Estimated required length of pile = 30 ft. Maximum pile load = 22 tons per pile.

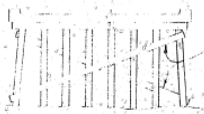

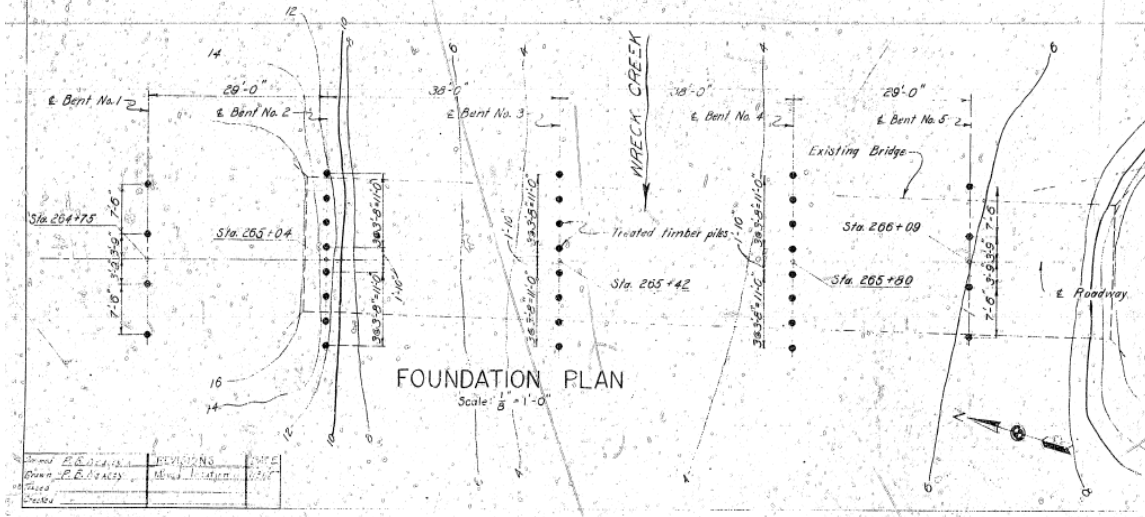

ESTIMATE

Structure Excavation	40 Cu. Yd.
Class A Concrete	213.5 Cu. Yd.
* Reinforcing Steel	64,000 Lb.
Treated Timber Piles, Furnishing	960 Lin. Ft.
Treated Timber Piles, Driving	32 Each
Treated Timber — Creosote	0.6 M.f.b.M.
Railing	282 Lin. Ft.
Removal and Salvage of Existing Bridge	All Req'd.
Loose Riprap	300 Cu. Yd.

* Includes weight of drains and guard angles.

BUREAU OF INDIAN AFFAIRS
WRECK CREEK BRIDGE
QUINAULT INDIAN RESERVATION-WASHINGTON
ROUTE 1-PROJECT Q.I.R.1(5)
SCALE: 1/8"=1'-0" JULY 1957
SHEET 1 OF 1 SHEETS **R8-G-24**

Designed P.E.D.(A.E.)	REVISIONS	DATE
Drawn P.E.D.(A.E.)		
Traced		
Checked		

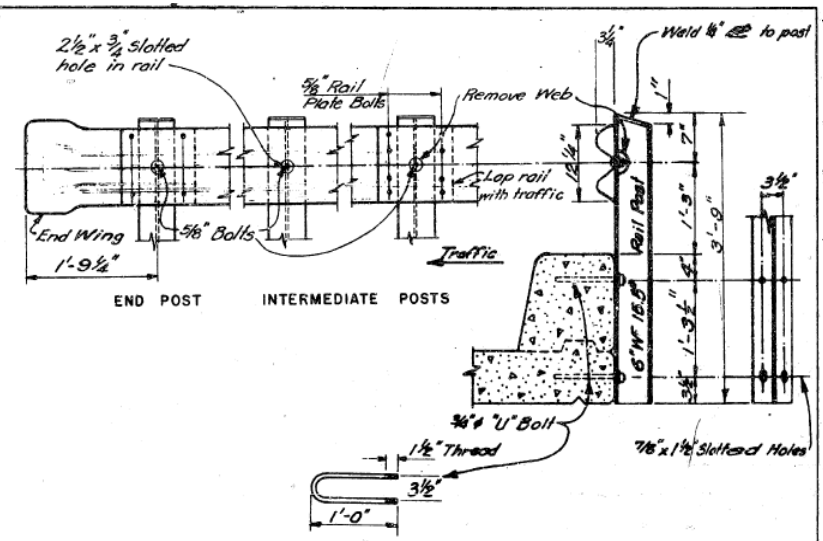

NOTE:-
A TOLERANCE OF 3 PERCENT ON ANY DIMENSION OF RAIL PLATE WILL BE ALLOWED.

Provide shims as required for alignment of rail posts.

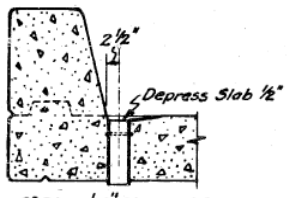

3" Dia. x 1'-0" Standard Iron Pipe. Weld ⅛" wire around pipe before galvanizing.

DRAIN DETAILS
SCALE ¼" = 1'-0"

BEAM GUARD RAIL
SCALE 3/4" = 1'-0"

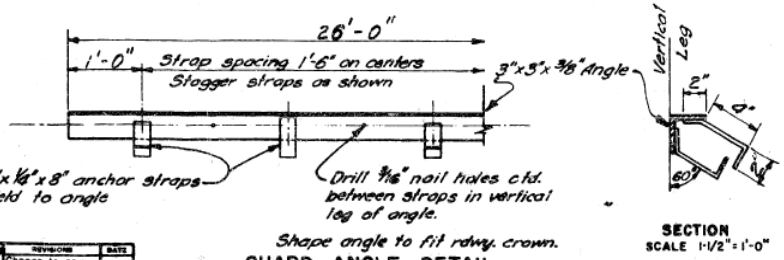

GUARD ANGLE DETAIL
SCALE 1" = 1'-0"

SECTION
SCALE 1-1/2" = 1'-0"

DESIGNED	H. S. Steinbrugge
DRAWN	P. R. Luckgroth
TRACED	M. D. Replogle
CHECKED	Steinbrugge

REVISIONS	DATE
Change to new approved RAIL	2-15-1957

U. S. DEPARTMENT OF COMMERCE
BUREAU OF PUBLIC ROADS
REGION EIGHT PORTLAND, OREGON

STANDARD RAILING, DRAIN AND GUARD ANGLE DETAILS

DATE 14 JUNE 1956 SCALE AS NOTED
SHEET 3 OF 3 SHEETS
R8-G-24